THEORY OF MULTIWAVE MIXING IN TWO- AND THREE-LEVEL MEDIA

by

Sunghyuck An

A Dissertation Submitted to the Faculty of the

DEPARTMENT OF PHYSICS

In Partial Fulfillment of the Requirements
For the Degree of

DOCTOR OF PHILOSOPHY

In the Graduate College

THE UNIVERSITY OF ARIZONA

1988

Order Number 8906373

Theory of multiwave mixing in two- and three-level media

An, Sunghyuck, Ph.D.

The University of Arizona, 1988

U·M·I
300 N. Zeeb Rd.
Ann Arbor, MI 48106

THEORY OF MULTIWAVE MIXING IN TWO- AND THREE-LEVEL MEDIA

by

Sunghyuck An

A Dissertation Submitted to the Faculty of the

DEPARTMENT OF PHYSICS

In Partial Fulfillment of the Requirements
For the Degree of

DOCTOR OF PHILOSOPHY

In the Graduate College

THE UNIVERSITY OF ARIZONA

1988

THE UNIVERSITY OF ARIZONA
GRADUATE COLLEGE

As members of the Final Examination Committee, we certify that we have read the dissertation prepared by SUNGHYUCK AN

entitled THEORY OF MULTIWAVE MIXING IN TWO- AND THREE-LEVEL MEDIA

and recommend that it be accepted as fulfilling the dissertation requirement for the Degree of DOCTOR OF PHILOSOPHY.

Murray Sargent III	18-nov-88
MURRAY SARGENT III	Date
William S. Bickel	Nov 19 1988
WILLIAM S. BICKEL	Date
John O. Kessler	Nov. 18 1988
JOHN O. KESSLER	Date
Robert H. Parmenter	Nov. 18, 1988
ROBERT H. PARMENTER	Date
Robert L. Thews	Nov 18, 1988
ROBERT L. THEWS	Date

Final approval and acceptance of this dissertation is contingent upon the candidate's submission of the final copy of the dissertation to the Graduate College.

I hereby certify that I have read this dissertation prepared under my direction and recommend that it be accepted as fulfilling the dissertation requirement.

Murray Sargent III	22-nov-88
Dissertation Director	Date

STATEMENT BY THE AUTHOR

This dissertation has been submitted in partial fulfillment of requirements for an advanced degree at The University of Arizona and is deposited in the University Library to be made available to borrowers under rules of the Library.

Brief quotations from this dissertation are allowable without special permission, provided that accurate acknowledgement is made. Requests for permission for extended quotation from or reproduction of this manuscript in whole or in part may be granted by the head of the major department or the Dean of the Graduate College when in his or her judgement the proposed use of the material is in the interests of scholarship. In all other instances, however, permission must be obtained from the author.

SIGNED : 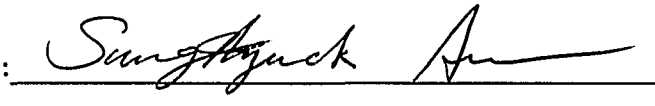

ACKNOWLEDGEMENTS

Above all I thank God for the gift of wisdom, however small, to gain insight into His marvelous works, which has helped me come closer to Him.

I would like to thank my advisor, Prof. Murray Sargent III for his valuable teaching, generosity of ideas, patient guidance, and support, which were indispensible in carrying out this research. I owe a special thanks for the many hours he spent programming making possible all computations and graphs presented in this work. I would also like to thank David Holm and Barbara Capron for their helpful discussions and encouragement during this study.

I would like to thank the other members of my commitee Profs. John Kessler, William Bickle, Robert Parmenter, and Robert Thews for their time in reading the manuscript and for their helpful comments.

Finally I wish to express my deepest appreciation to every member of my family, without whose love and sacrifice none of this would be possible.

TABLE OF CONTENTS

Page

LIST OF ILLUSTRATIONS 7

ABSTRACT 9

1. INTRODUCTION 11

2. SIMPLE SEMICLASSICAL THEORY OF FOUR-WAVE MIXING 16

2-1. Nondegenerate Phase Conjugation Without Pump Spatial Holes 18
2-2. Comparison to Abrams and Lind Degenerate Theory 21

3. EFFECTS OF A SQUEEZED VACUUM ON MULTIWAVE MIXING 25

3-1. Three-Wave Mixing in a Squeezed Vacuum 26
3-2. Four-Wave Mixing in a Squeezed Vacuum 39

4. EFFECTS OF SIDEMODE SATURATION IN ONE-PHOTON TWO-LEVEL MEDIA 44

4-1. Semiclassical Sidemode Saturation 45

4-1-1. Fourier Analysis and Continued Fraction 45
4-1-2. Degenerate Solution 51
4-1-3. Nondegenerate Solution 54

4-2. Quantum Sidemode Saturation 56

4-2-1. Summary of the Second-Order Theory 56
4-2-2. Derivation of the Fourth-Order Theory 59
4-2-3. Reduction to the Semiclassical Theory 67

4-3. Effects of Cavities on the Photon Number Spectrum 69

4-3-1. Second-Order Theory 69
4-3-2. Fourth-Order Theory 72

TABLE OF CONTENTS --- Continued

5. QUANTUM MULTIWAVE MIXING IN TWO-PHOTON THREE-LEVEL MEDIA 76

5-1. Semiclassical Single-Mode Interaction 79
5-2. Quantum Sidemode Interactions 82
5-3. Application to Squeezing 92

6. SUMMARY 96

APPENDIX 100

REFERENCES 109

LIST OF ILLUSTRATIONS

Figure — Page

1. (*a*) and (*b*) Four-wave mixing diagrams occurring in Abrams and Lind degenerate theory. In (*a*) the down-pump (↓) and the signal waves induce a grating. The conjugate wave is created because the up-pump (↑) scatters off this grating into the opposite direction to the signal wave. In (*b*) another grating is induced by the up-pump and the signal waves. (*c*) Phase conjugation without spatial holes. Only one grating is induced. 17

2. Reflectivity R *vs* pump intensity I_2 (*a*) in Abrams and Lind degenerate theory and (*b*) phase conjugation without spatial holes ($I_{2\downarrow} = I_{2\uparrow}$, $\nu_1 = \nu_2$) for various values of $\alpha_0 L$. $\gamma = 1$ and $\omega = \nu_2$. 22

3. Reflectivity R *vs* pump intensity $I_{2\uparrow}$ for various values of the pump intensity $I_{2\downarrow}$. $\alpha_0 L = 10$, $\nu_1 = \nu_2$, $\gamma = 1$, and $\omega = \nu_2$. 23

4. Spectrum of three-wave fields. Waves with frequencies ν_1 and ν_3 are taken to be weak (nonsaturating), while the ν_2 wave is allowed to be arbitrarily intense. 26

5. Real part of α_1 versus pump/probe beat frequency $\Delta = \nu_2 - \nu_1$, for $\Gamma = 2\gamma_+$, $\omega = \nu_2$, $I_2 = 9$, and $\gamma_- = 0$ (the original Mollow spectrum) and 0.92. The phase of the pump field differs from that of the vacuum by $\pi/2$. Note that our frequencies are normalized in units of γ_+, which for a highly squeezed vacuum is a much larger unit than that used by Ritsch and Zoller (1987). 36

6. Real part of α_1 versus Δ for $\omega - \nu_2 = -0.2$ and -3, $\gamma_- = 0.92$, and the other parameters are the same as in Fig. 2. 37

7. Real part of α_1 versus Δ for the phase of pump field $\phi = 0$ and $2\pi/5$, $\gamma_- = 0.92$, and the other parameters are the same as in Fig. 2. 38

8. Real part of χ_1 versus Δ for $\gamma_- = 0.01$ and 0.92, $\phi = \pi/2$, and the other parameters are the same as in Fig. 2. 38

9. Four-wave mixing diagram defining the pump, signal, and conjugate waves. There is another grating induced by the signal and the other pump wave. 40

10. Reflectivity R versus Δ for $\Gamma = 2\gamma_+$, $\omega = \nu_2$, $I_2 = 1$, $L = 4$, $\phi = \pi/2$. $\gamma_- = 0$, 0.46, and 0.92. 42

LIST OF ILLUSTRATIONS --- Continued

11. Reflectivity R versus Δ for $\phi = 0$. The other parameters are the same as in Fig. 7. 42

12. Basic pump-probe saturation spectroscopy configuration. 46

13. Eight-level atom-field energy-level diagram. 60

14. (a) and (b) H′ versus ΔT_1 for $T_2 = 2T_1$ and $I_2 = 50$. 65

15. G′ versus ΔT_1. Same parameters as in Fig. 14. 66

16. F′ versus ΔT_1. Same parameters as in Fig. 14. 66

17. The spectrum of $\langle n_{10} \rangle$ given by Eq. (4.99) versus ΔT_1 for $\beta = 1.0, 0.1, 0.05$, and 0.04. $T_2 = 2T_1$ and $I_2 = 50$. 72

18. The spectrum of $\langle n_1 \rangle$ given by Eq. (4.103) for $\alpha = 0.01$. Other parameters are the same as in Fig. 17. 74

19. The spectrum of $\langle n_1 \rangle$ given by Eq. (4.103) for $\alpha = 0.05$. Other parameters are the same as in Fig. 17. 75

20. The three-level cascade model with a two-photon pump. 78

21. Five-level atom-field energy-level diagram. 84

22. The free space resonance fluorescence spectrum A_1 + c.c. versus Δ' for $I_2 = 0.5$ and 20, $\Delta_2 = 0$, $C = 1$, $\Gamma_a = 1$, $\Gamma_1 = \Gamma_3 = 1$, and $\gamma_1 = \gamma_3 = \gamma_2 = 1$. All frequencies are in units of γ_2. 91

23. Real part of C_3 for $I_2 = 0.5$ and 10. The other parameters are the same as in Fig. 22. 91

24. Variance Δd_1^2 versus $\Delta' = (\omega_{bc} - \nu_2) - \Delta$ for $I_2 = 0.5$ and 150, $C = 100$, and the other parameters are the same as in Fig. 22. 94

25. Variance Δd_1^2 versus I_2 for $C = 100$ and 1000, $\Delta' = 0$, and the other parameters are the same as in Fig. 22. 94

ABSTRACT

This dissertation presents theories of multiwave mixing in two- and three-level media. The first part of the dissertation treats the semiclassical theories in two-level media. Chapter 2 gives the simple semiclassical theory of four-wave mixing when the two pump frequencies differ by more than the reciprocal of the population-difference lifetime. This difference washes out the pump spatial holes as well as one of the two reflection gratings. We compare the results to the degenerate treatment of Abrams and Lind and find significant differences in the reflection coefficient spectra.

Chapter 3 presents the semiclassical theory of multiwave in a squeezed vacuum characterized by unequal in-phase and in-quadrature dipole decay times. For a highly squeezed vacuum, we find sharp resonances in both probe absorption and reflection coefficients, which provide sensitive ways to measure the amount of squeezing in the vacuum.

The second part of the dissertation treats the quantum theories in two- and three-level media. Chapter 4 develops the fourth-order quantum theory of multiwave mixing to describe the effects of sidemode saturation in two-level media. We derive explicit formulas for the fourth-order quantum coefficients and show that the fourth-order quantum theory reproduces the third-order semiclassical coefficient obtained by truncating a continued fraction. We apply the results to cavity problems and find significant differences in the sideband spectra given by the second- and fourth-order treatments, particularly as the sidemode approaches the laser threshold.

The final chapter presents a quantum theory of multiwave mixing in three-level cascades with a two-photon pump. The explicit formulas for the resonance fluo-

rescence spectrum and the quantum combination-tone source term are derived. The theory is applied to the generation of squeezed states of light. We find almost perfect squeezing for some strong pump intensities and good broad-band squeezing for low pump intensities.

CHAPTER 1

INTRODUCTION

Since the discovery of nonlinear phenomena, multiwave mixing has been one of the most important branch of quantum optics both theoretically and experimentally. It is able to treat a number of topics that involve the interaction of two or more electromagnetic waves with a nonlinear medium, topics including saturation spectroscopy, phase conjugation, resonance fluorescence, and the generation of squeezed states.

In most multiwave mixing theories, it is sufficient to treat the electromagnetic fields classically and the atoms quantum mechanically (i.e., semiclassical approximation). The first three chapters of this dissertation deal with semiclassical theories of multiwave mixing in one-photon two-level media. There are some phenomena, however, that the semiclassical approximation fails to explain. Resonance fluorescence and squeezed states of light are typical examples of these. In these cases, the weak fields must be quantized, while the strong pump fields can be treated classically.

Sargent, Holm, and Zubairy (1985) derived a theory describing quantum multiwave interactions in a nonlinear one-photon two-level medium. In their following series of papers (Quantum theory of multiwave mixing II through VIII), Holm and Sargent applied this theory to predict and explain many phenomena in quantum optics, including modulation spectroscopy, resonance fluorescence, and squeezing in such a medium. In most of this dissertation we extend the theory to describe the effects of quantum sidemode saturation in one-photon two-level media and to develop the quantum theory of multiwave mixing in two-photon three-level media.

Chapter 2 presents the simple semiclassical theory of nondegenerate four-wave mixing when the two pump frequencies differ by more than the reciprocal of the population-difference lifetime. The fringe pattern for differing frequencies leads to a walking wave. If the walking speed is sufficiently large, the pump spatial holes are washed out. Our absorption and coupling coefficients differ significantly from the original degenerate treament of Abrams and Lind, since one of the two reflection gratings is also washed out, and since two resonance Lorentzians enter instead of one. We find that the reflection coefficient is qualitatively similar to that of Abrams and Lind, but is reduced in magnitude due to incresed saturation.

Chapter 3 generalizes the spectroscopic techniques by Sargent (1978) to develop the semiclassical theory of multiwave mixing in a squeezed vacuum. A squeezed vacuum is generated by squeezed light with a bandwidth much larger than the natural linewidth of the atom. Gardiner (1986) studied the decay of two-level systems in such a vacuum. To a good approximation, he found that the Maxwell-Bloch equations are modified simply by having different in-phase and in-quadrature relaxation rates. Using a Fourier series method, we derive the nondegenerate probe absorption and coupling coefficients in a squeezed vacuum characterized by unequal in-phase and in-quadrature dipole decay times. For a highly squeezed vacuum, we find sharp resonances in the probe absorption coefficient and suppression of population pulsation contributions. We average the probe absorption and coupling coefficients over pump spatial holes and solve the coupled mode equations to find the four-wave mixing reflection coefficient. We compare the results to the case of an unsqueezed vacuum.

The remaining two chapters, which are the main portion of this dissertation, deal with quantum theories in two- and three-level media. Chapter 4 begins with a one-photon two-level medium. In two previous papers (Sargent, Holm, and Zubairy

1985; Stenholm, Holm, and Sargent 1985), a quantum theory of multiwave mixing in a two-level medium is presented. The theory assumes that the sidemode photon numbers are sufficiently small compared to the saturation photon number that a second-order perturbation treament is adequate. If this is not true such as near the laser threshold, we expect that higher order perturbation corrections are needed. This chapter extends the theory to fourth order in the weak-field interaction by using an approach similar to the quantum theory of multiwave mixing by Sargent, Holm, and Zubairy (1985).

Chapter 4 is divided into three sections. The first section extends the semiclassical theory of saturation spectroscopy by Sargent (1978) to describe the effects of sidemode saturation semiclassically. We first summarize the derivation of the general two-wave absorption coefficients allowing both probe and saturator waves to saturate the response of the medium (Sargent 1978). We show that the self-consistent equation is reduced to the algebraic equation expressed in terms of a continued fraction. We use this equation to find a degenerate solution in a closed form and a nondegenerate solution up to third order in the weak-field amplitude. In the second section we extend the theory by Sargent, Holm, and Zubairy (1985) to describe the effects of sidemode saturation fully quantum mechanically. We show that the fourth-order quantum theory reproduces the third-order semiclassical coefficient obtained by truncating a continued fraction. The final section solves the fourth-order equation of motion in steady state and studies the effects of cavities on the photon number spectrum. The results are compared to the second-order theory. We find significant differences in the sideband spectra given by the second- and fourth-order treatments, particularly as the sidemode approches the laser threshold.

Chapter 5 presents the quantum theory of multiwave mixing in a two-photon three-level medium and applies the theory to the generation of squeezed states of light.

Squeezed states of light are those for which the quantum fluctuations in one quadrature phase of the electric field are reduced below the average minimum variance permitted by the uncertainty principle. Such states have potential applications in optical communication systems and in gravity-wave detection. Due to the dependence of squeezing on the phase of the electric field, squeezed states have been predicted to occur in phase sensitive nonlinear optical processes, such as parametric amplification, second harmonic generation, and four-wave mixing. The first successful generation of squeezed states has been reported by Slusher *et al.* (1985) using nondegenerate four-wave mixing. Recently other groups have also succeeded in producing squeezed states using different types of nonlinear media.

Holm and Sargent (1987) have applied their quantum multiwave mixing theory (Sargent, Holm, and Zubairy 1985) to analyze the generation of squeezed states and compared to the experimental results of Slusher *et al.* (1985) finding reasonably good agreement. The first nondegenerate semiclassical theory of multiwave mixing in a two-photon two-level medium has given by Sargent, Ovadia, and Lu (1985) and the quantum theory of multiwave mixing in this medium has been derived in detail by Holm and Sargent (1986*a*). In this chapter we extend the quantum theory of multiwave mixing by Sargent, Holm, and Zubairy (1985) to treat squeezing in a three-level cascade model with a classical two-photon pump and a cascade of two one-photon transitions at different frequencies.

The experimental observation of the suppression of amplified spontaneous emission by the four-wave mixing process in this model has been reported by Malcuit, Gauthier, and Boyd (1985). This experiment has been interpreted using classical fields up to fourth order in all mode interactions (Boyd *et al.* 1987), while we treat a classical pump to all orders and quantized squeezed modes to first order. They also

use the one-photon rotating wave approximation for the two-photon pump and neglect the population in the intermediate level, while we include the terms dropped in these approximations. Agarwal (1986) studied this model using a weak classical two-photon pump and weak quantized sidemode fields. He showed the generation of squeezed states, but simplified his treatment by neglecting dynamic Stark shifts and the population in the intermediate level. In contrast our treatment allows for more general tuning conditions and nonzero intermediate level population as created by the potentially strong pump field in conjuction with level decays.

CHAPTER 2

SIMPLE SEMICLASSICAL THEORY OF FOUR-WAVE MIXING

In the four-wave mixing scheme for phase conjugation shown in Fig. 1, the pumps interfere in a nonlinear two-level medium inducing spatial holes in the population difference. Since these holes are out of phase with the signal and conjugate waves, the projection of the induced polarization onto these waves requires averaging over the pump spatial holes. In their initial treatment of this problem for degenerate pump and probe frequencies, Abrams and Lind (1978) supposed that the squared sinusoids representing the holes in the population denominators could be appproximated by 1/2. Later they published an erratum (Abrams and Lind 1978*b*) that carried out a more realistic average by integrating the steady-state polarization over a wavelength. The resulting reflection coefficient differs substantially in value from the simpler average. In this chapter, we use results from grating-dip spectroscopy (Sargent 1976) to justify the use of the first method in the nondegenerate case for which the two pump frequencies differ by more than the reciprocal of the population-difference lifetime ($1/T_1$). The fringe pattern for differing frequencies leads to a walking wave. If the walking speed is sufficiently large, the pump spatial holes are washed out. Our absorption and coupling coefficients still differ significantly from the original degenerate treatment of Abrams and Lind, since one of the two reflection gratings is also washed out, and since two resonance Lorentzians enter instead of one. The physics of this problem is closely related to the finite-width reflection spectrum predicted by Fu and Sargent (1979) in their treatment of signal detuning. There the reflection gratings induced by the signal with either pump are washed out if the signal and pump fre-

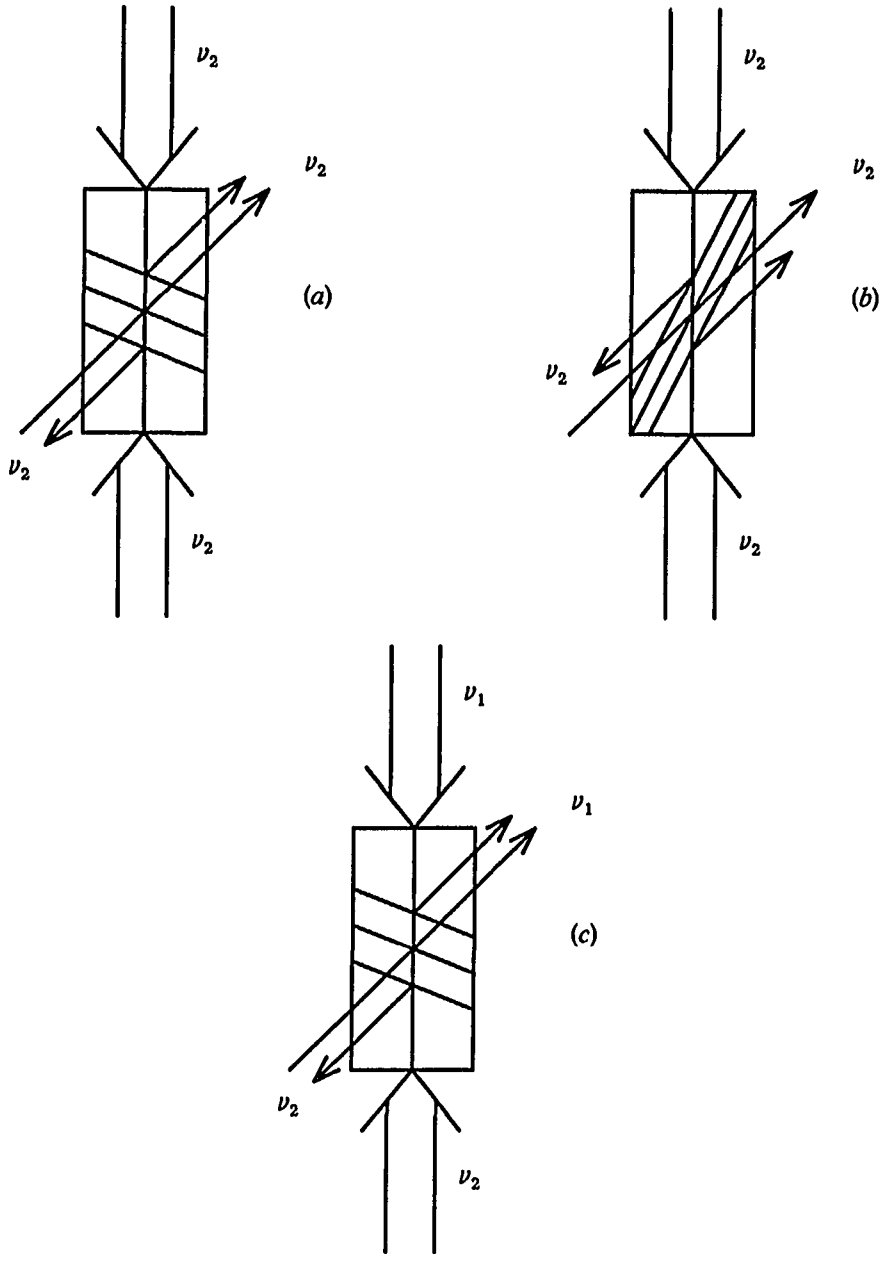

Fig. 1. (*a*) and (*b*) Four-wave mixing diagrams occurring in Abrams and Lind degenerate theory. In (*a*) the down-pump (↓) and the signal waves induce a grating. The conjugate wave is created because the up-pump (↑) scatters off this grating into the opposite direction to the signal wave. In (*b*) another grating is induced by the up-pump and the signal waves. (*c*) Phase conjugation without spatial holes. Only one grating is induced.

quencies differ by more than $1/T_1$. Agrawal (1982) has used similar arguments to justify neglecting pump spatial hole burning in two-photon phase conjugation.

2-1. Nondegenerate Phase Conjugation Without Pump Spatial Holes

We first outline the derivation of the coupled-mode absorption and coupling coefficients, and then illustrate the resulting reflection coefficient. For more detailed discussion of such derivations, see the review article (Sargent 1978). We consider an electric field given by the two-frequency expression

$$E(\mathbf{r}, t) = \frac{1}{2}\,[\mathcal{E}_1(\mathbf{r}) + \mathcal{E}_{2\downarrow}(\mathbf{r})]\, e^{-i\nu_1 t} + \frac{1}{2}\,[\mathcal{E}_{2\uparrow}(\mathbf{r}) + \mathcal{E}_3(\mathbf{r})]\, e^{-i\nu_2 t} + \text{c.c.}\,, \tag{2.1}$$

where the signal amplitude $\mathcal{E}_1(\mathbf{r}) = A_1 \exp(i\mathbf{K}_1\cdot\mathbf{r})$, the pump amplitudes $\mathcal{E}_{2\downarrow}(\mathbf{r}) = A_2 \exp(i\mathbf{K}_{2\downarrow}\cdot r)$ and $\mathcal{E}_{2\uparrow}(r) = \mathrm{A}_2 \exp(-\mathrm{i}K_{2\uparrow}\cdot\mathbf{r})$, and the conjugate amplitude $\mathcal{E}_3(\mathbf{r}) = A_3 \exp(i\mathbf{K}_3\cdot\mathbf{r})$. This induces a complex electric-dipole coherence ρ_{ab} in the medium along the lines explained in Sec. 8-2 of *Laser Physics* (Sargent, Scully, and Lamb 1974). Since the population difference D is assumed not to be able to follow the beat frequency ν_2-ν_1, it may be treated as a constant in the formal time integral for ρ_{ab}. Evaluating this integral in the rate equation approximation, we have

$$\rho_{ab} = -i(\wp/2\hbar)\,[\mathcal{D}_1[\mathcal{E}_1 + \mathcal{E}_{2\downarrow}]\, e^{-i\nu_1 t} + \mathcal{D}_2[\mathcal{E}_{2\uparrow} + \mathcal{E}_3]\, e^{-i\nu_2 t}]\, D\,, \tag{2.2}$$

where the complex denominator $\mathcal{D}_n = 1/[\gamma + i(\omega - \nu_n)]$. The population difference then obeys the rate equation

$$\dot{D} = -\frac{D-N}{T_1} - (\wp/\hbar)^2 T_2 \left[\mathcal{L}_1|\mathcal{E}_1+\mathcal{E}_{2\downarrow}|^2 + \mathcal{L}_2|\mathcal{E}_{2\uparrow}+\mathcal{E}_3|^2\right] D \,, \tag{2.3}$$

where N is the unsaturated population difference, and the dimensionless Lorentzian $\mathcal{L}_n = 1/[1+(\omega-\nu_n)^2/\gamma^2]$. In steady-state ($\dot{D}$=0), this yields to first-order in the signal and conjugate amplitudes

$$D = \frac{N}{1 + [I_{2\downarrow}+(C\mathcal{E}_1{}^*\mathcal{E}_{2\downarrow}+c.c.)]\mathcal{L}_1 + [I_{2\uparrow}+(C\mathcal{E}_3\mathcal{E}_{2\uparrow}+c.c.)]\mathcal{L}_2}$$

$$\cong \frac{N}{1+I_{2\downarrow}\mathcal{L}_1+I_{2\uparrow}\mathcal{L}_2}\left[1 - \frac{C(\mathcal{E}_1{}^*\mathcal{E}_{2\downarrow}\mathcal{L}_1 + \mathcal{E}_3\mathcal{E}_{2\uparrow}\mathcal{L}_2 + \text{c.c.})}{1 + I_{2\downarrow}\mathcal{L}_1+I_{2\uparrow}\mathcal{L}_2}\right], \tag{2.4}$$

where $C=(\wp/\hbar)^2 T_1 T_2$, and the dimensionless intensity $I_n=C|\mathcal{E}_n|^2$ (n = 2↑ or 2↓). Substituting this into Eq. (2.2), we have

$$\rho_{ab} = -i\,\frac{\wp N}{2\hbar}\left[\frac{\mathcal{D}_1[\mathcal{E}_1+\mathcal{E}_{2\downarrow}]e^{-i\omega_1 t} + \mathcal{D}_2[\mathcal{E}_{2\uparrow}+\mathcal{E}_3]\,e^{-i\omega_2 t}}{1+I_{2\downarrow}\mathcal{L}_1+I_{2\uparrow}\mathcal{L}_2}\right]$$

$$\times \left[1 - \frac{C(\mathcal{E}_1\mathcal{E}_{2\downarrow}\mathcal{L}_1 + \mathcal{E}_3\mathcal{E}_{2\uparrow}\mathcal{L}_2 + \text{c.c.})}{1 + I_{2\downarrow}\mathcal{L}_1+I_{2\uparrow}\mathcal{L}_2}\right]. \tag{2.5}$$

Projecting this onto the signal and conjugate propagation functions (e.g., $\exp(i\mathbf{K}_1\cdot\mathbf{r})$), we find the coupled mode equations

$$\frac{dA_1}{dz} = -\alpha_1 A_1 + \chi_1 A_3{}^*\, e^{2i\Delta K z} \,, \tag{2.6}$$

$$-\frac{dA_3^*}{dz} = -\alpha_3^* A_3^* + \chi_3^* A_1\, e^{-2i\Delta Kz}\,, \tag{2.7}$$

where the absorption coefficients are

$$\alpha_1 = \alpha_0\gamma\mathscr{D}_1\,\frac{1}{1+I_{2\downarrow}\mathscr{L}_1+I_{2\uparrow}\mathscr{L}_2}\left[1-\frac{I_{2\downarrow}\mathscr{L}_1}{1+I_{2\downarrow}\mathscr{L}_1+I_{2\uparrow}\mathscr{L}_2}\right], \tag{2.8}$$

$$\alpha_3 = \alpha_0\gamma\mathscr{D}_2\,\frac{1}{1+I_{2\downarrow}\mathscr{L}_1+I_{2\uparrow}\mathscr{L}_2}\left[1-\frac{I_{2\uparrow}\mathscr{L}_2}{1+I_{2\downarrow}\mathscr{L}_1+I_{2\uparrow}\mathscr{L}_2}\right], \tag{2.9}$$

the coupling coefficients are

$$\chi_1 = \alpha_0\gamma\mathscr{D}_1\,\frac{(I_{2\downarrow}I_{2\uparrow})^{1/2}\mathscr{L}_2}{(1+I_{2\downarrow}\mathscr{L}_1+I_{2\uparrow}\mathscr{L}_2)^2}\,, \tag{2.10}$$

$$\chi_3 = \alpha_0\gamma\mathscr{D}_2\,\frac{(I_{2\downarrow}I_{2\uparrow})^{1/2}\mathscr{L}_1}{(1+I_{2\downarrow}\mathscr{L}_1+I_{2\uparrow}\mathscr{L}_2)^2}\,, \tag{2.11}$$

and the phase mismatch factor

$$\Delta K = \frac{1}{2c}(\nu_2-\nu_1)(1-\cos\theta)\,, \tag{2.12}$$

where $\theta = \cos^{-1}(\mathbf{K}_1\cdot\mathbf{K}_{2\downarrow}/K_1K_{2\downarrow})$.

As shown for example by Fu and Sargent (1979), the corresponding amplitude reflection coefficient is given by

$$r = \frac{A_3^*(0)}{A_1(0)} = \chi_3^* \frac{\sinh wL}{w\cosh wL + \alpha \sinh wL} , \tag{2.13}$$

where α and w are given by

$$\alpha = (\alpha_1 + \alpha_3^* + 2i\Delta K)/2 , \tag{2.14}$$

$$w = [\alpha^2 - \chi_1 \chi_3^*]^{1/2} . \tag{2.15}$$

2-2. Comparison to Abrams and Lind Degenerate Theory

The absorption and coupling coefficients, which are calculated by Abrams and Lind (1978) averaging over spatial holes in the degenerate four-wave mixing case (see Figs. *1a* and *1b*), are given by

$$\alpha_1 = \alpha_0 \gamma \mathscr{D}_2 \frac{1 + 2I_2 \mathscr{L}_2}{(1 + 4I_2 \mathscr{L}_2)^{3/2}} , \tag{2.16}$$

$$\chi_1 = \alpha_0 \gamma \mathscr{D}_2 \frac{2I_2 \mathscr{L}_2}{(1 + 4I_2 \mathscr{L}_2)^{3/2}} . \tag{2.17}$$

Figure 2 compares the reflection coefficient $R=|r|^2$ *vs* intensity obtained with spatial holes (Abrams and Lind calculation) to those with none, each for two values of $\alpha_0 L$. In general, the reflectivity peaks slightly sooner and with about half the value for large fields without spatial holes than with. Examination of the coupling coefficients κ'*s* for the two cases suggests this behavior, in that without spatial holes, Eq.

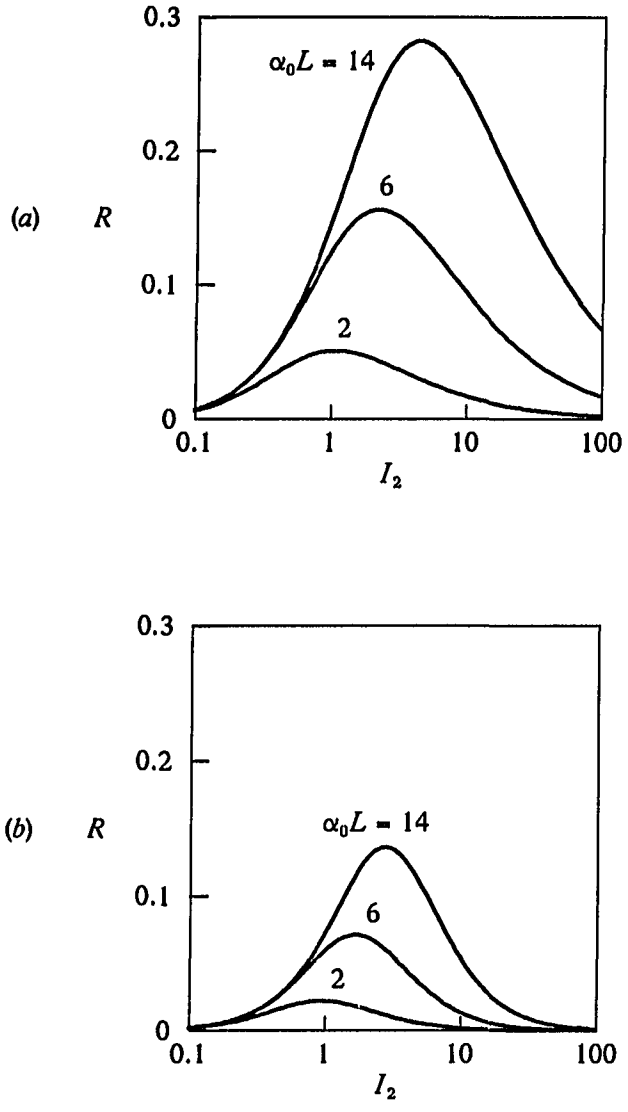

Fig. 2. Reflectivity R *vs* pump intensity I_2 (*a*) in Abrams and Lind degenerate theory and (*b*) phase conjugation without spatial holes ($I_{2\downarrow} = I_{2\uparrow}$, $\nu_1 = \nu_2$) for various values of $\alpha_0 L$. $\gamma = 1$ and $\omega = \nu_2$.

(2.11) saturates as $1/I$ for large I, whereas the Abrams-Lind formula is proportional to $I^{-1/2}$. Physically this corresponds to the fact that spatial holes mix up strong and weak saturation regions, preventing saturation from turning on as sharply. The effect is similar, although not as pronounced, as the averaging that occurs with inhomogeneous broadening, which might be called a "soft saturation." For all $\alpha_0 L$, the reflectivity without spatial holes is smaller than that with, since only one signal-pump grating is induced. When spatial holes are present, both pumps induce conjugating gratings (see Fig. 1).

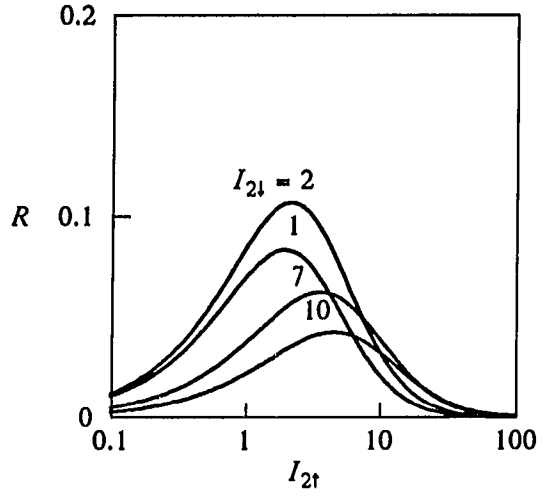

Fig. 3. Reflectivity R *vs* pump intensity $I_{2\uparrow}$ for various values of the pump intensity $I_{2\downarrow}$. $\alpha_0 L = 10$, $\nu_1 = \nu_2$, $\gamma = 1$, and $\omega = \nu_2$.

Figure 3 plots reflectivity *vs* up-pump intensity for a number of values of down-pump intensity. Initially an increase in the down-pump intensity produces higher overall reflectivity, but larger values tend to bleach the medium and reduce the reflectivity. In all cases, the large up-pump intensity region saturates substantially

more strongly than it does when spatial holes are included as expected from the discussion above.

In this chapter we have presented a simplified phase conjugation calculation in which spatial holes are assumed to average out due to the inability of a slow-response population difference to follow the moving pump fringe pattern. The large field saturation is substantially increased without spatial holes. The theory should be useful in studying the conjugation properties of media with long population difference lifetimes, such as ruby, and aspects of the present analysis should be applicable to other media having long grating decay times, such as a liquid with suspended microspheres (Smith, Ashkin, and Tomlinson 1981).

CHAPTER 3

EFFECTS OF A SQUEEZED VACUUM ON MULTIWAVE MIXING

Nonlinear phenomena can be used in two general ways, one in applications such as second-harmonic generation, lasers, phase conjugation, and optical switching. Alternatively one can use the phenomena to study the properties of the medium that generates them. The various kinds of nonlinear spectroscopy fall into the second category. Saturation spectroscopy deals typically with the *cw* absorption of waves passing through a medium to be studied. The theory is highly developed and predicts spectra of absorption versus probe-pump detuning, which reveal the dynamic Stark effect and various coherent dips (Mollow 1972; Wu, Ezekiel, Ducloy, and Mollow 1977; Sargent 1978).

A squeezed vacuum is generated by squeezed light with a bandwidth much larger than the natural linewidth of the atom. Gardiner (1986) studied the decay of two-level systems in such a vacuum. To a good approximation, he found that the Maxwell-Bloch equations are modified simply by having different in-phase and in-quadrature relaxation rates. Resonance fluorescence (Carmichael, Lane, and Walls 1987) and probe absorption (Ritsch and Zoller 1987 and 1988, An and Sargent 1988) have been studied in such a vacuum. In this chapter we extend the two-wave theory by An and Sargent (1988) to study nondegenerate three- and four-wave mixing in a squeezed vacuum.

Section 3-1 describes the interactions of an arbitrarily intense pump wave and two weak sidebands with a medium in a squeezed vacuum. This theory uses Fourier series to solve the Schrödinger equations of motion, finding the probe absorption and

coupling coefficients in such a vacuum. Section 3-2 generalizes the earlier theory of nondegenerate four-wave mixing in an unsqueezed vacuum (Fu and Sargent 1979; Boyd, Raymer, Narum, and Harter 1981) to the case of squeezed vacuums. We average the coefficients derived in section 3-1 over pump spatial holes and solve the coupled mode equations to find the four-wave mixing reflection coefficient.

3-1. Three-Wave Mixing in a Squeezed Vacuum

We consider a medium subjected to an arbitrary intense pump wave and two weak (nonsaturating) probe waves. We assume that the saturating pump wave intensity is constant throughout the interaction region and ignore transverse variations. We label the probe waves by the indices 1 and 3 and the pump wave by 2 as shown

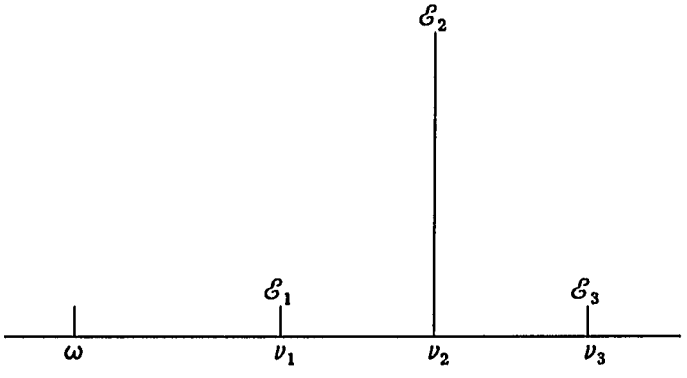

Fig. 4. Spectrum of three-wave fields. Waves with frequencies ν_1 and ν_3 are taken to be weak (nonsaturating), while the ν_2 wave is allowed to be arbitrarily intense.

in Fig. 4. Our electric field has the form

$$E(\mathbf{r},t) = \frac{1}{2}\sum_{n=1}^{3} \mathcal{E}_n(\mathbf{r})\, e^{i(\mathbf{K}_n\cdot\mathbf{r} - \nu_n t)} + \text{c.c.}\,, \tag{3.1}$$

where the mode amplitudes $\mathcal{E}_n(\mathbf{r})$ are in general complex and $\mathbf{K}_n$ are the wave propagation vectors. For simplicity we take mode functions appropriate for a unidirectional ring laser. The field (1) induces the complex polarization

$$P(\mathbf{r},t) = \frac{1}{2}\sum_{n} \mathcal{P}_n(\mathbf{r})\, e^{i(\mathbf{K}_n\cdot\mathbf{r} - \nu_n t)} + \text{c.c.}\,, \tag{3.2}$$

where $\mathcal{P}_n(\mathbf{r})$ is a complex polarization coefficient that yields index and absorption/gain characteristics for the probe and pump waves. The polarization $P(\mathbf{r},t)$ in general includes components not only at ν_1 and ν_2, but also at $\nu_1 \pm k(\nu_2-\nu_1)$, where k is an integer.

The problem reduces to determining the probe polarization $\mathcal{P}_1(\mathbf{r})$, from which the absorption coefficient is determined from the equation

$$\frac{d\mathcal{E}_1(z)}{dz} = \frac{iK}{2\epsilon}\mathcal{P}_1\,, \tag{3.3}$$

where ϵ is the permittivity of host medium. One might guess that the probe absorption coefficient is simply a probe Lorentzian multiplied by a population difference saturated by the pump wave. However an additional contribution enters due to population pulsations. Specifically the nonlinear populations respond to the superposition of

the modes to give pulsations at the beat frequency $\Delta = \nu_2 - \nu_1$. Since we suppose the probe does not saturate, the pulsations occur only at $\pm\Delta$, a point proved below. These pulsations act as modulators (or like Raman "shifters"), putting sidebands onto the medium's response to the ν_2 mode. One of these sidebands falls precisely at ν_1, yielding a contribution to the probe absorption coefficient. The other sideband influences the polarization at the frequency $\nu_3 = \nu_2 + (\nu_2 - \nu_1)$, which is the frequency of the other probe wave.

In this section we derive the complete nonsaturating probe absorption and coupling coefficients. For an unsqueezed vacuum, the population matrix with upper-to-ground-lower-level decay obeys the equations of motion

$$\dot{\rho}_{ab} = -(\gamma + i\Delta_2)\rho_{ab} + i\mathcal{V}_{ab}D \,, \tag{3.4}$$

$$\dot{D} = -\Gamma(D + N) - 2[i\mathcal{V}_{ab}\rho_{ba} + \text{c.c.}] \,, \tag{3.5}$$

where γ ($\equiv 1/T_2$) is the dipole decay constant, $\Delta_2 \equiv \omega - \nu_2$, ω is the frequency of the atomic line center, $\mathcal{V}_{ab}$ is the electric-dipole interaction energy, D is the population difference $\rho_{aa} - \rho_{bb}$, Γ is the population-difference decay constant ($\equiv 1/T_1$), and N is the unsaturated population difference per unit volume. The off-diagonal element ρ_{ba} is given by ρ_{ab}^*. We have chosen a frame rotating at the pump frequency ν_2 relative to the Schrödinger picture. In terms of ρ_{ab}, the polarization (2) is given by

$$P(\mathbf{r},t) = \wp\rho_{ab}e^{i(\mathbf{K}_2\cdot\mathbf{r} - \nu_2 t)} + \text{c.c.} \,, \tag{3.6}$$

where $\wp$ is the electric-dipole matrix element. The problem thus reduces to finding ρ_{ab}.

With a squeezed vacuum, the component of ρ_{ab} in phase with the squeezing field decays with a different rate from that in quadrature with the squeezing field. To determine the effect of this difference on ρ_{ab}, we introduce the in-phase component $U \equiv \rho_{ab} + \text{c.c.} = \rho_{ab} + \rho_{ba}$ and the in-quadrature component $V = i\rho_{ab} + \text{c.c.} = i\rho_{ab} - i\rho_{ba}$, which give $\rho_{ab} = (U - iV)/2$. On resonance and in the absence of an applied field (other than that creating the squeezed vacuum), U and V obey the equations of motion

$$\dot{U} = -\gamma_u U \ , \tag{3.7}$$

$$\dot{V} = -\gamma_v V \ . \tag{3.8}$$

Hence with this kind of decay, ρ_{ab} decays according to $\dot{\rho}_{ab} = (\dot{U} - i\dot{V})/2 = -\gamma_+\rho_{ab} - \gamma_-\rho_{ba}$, where $\gamma_\pm = (\gamma_u \pm \gamma_v)/2$. Combining these decay contributions with the dynamical contributions in Eq. (3.4), we have

$$\dot{\rho}_{ab} = -(\gamma_+ + i\Delta_2)\rho_{ab} - \gamma_-\rho_{ba} + i\mathcal{V}_{ab}D \ . \tag{3.9}$$

This reduces immediately to Eq. (3.4) if $\gamma_u = \gamma_v = \gamma$, since then $\gamma_+ = \gamma$ and $\gamma_- = 0$.

The interaction energy matrix element $\mathcal{V}_{ab}$ corresponding to Eq. (3.1) is given in the rotating-wave approximation and in the pump rotating frame as

$$\mathcal{V}_{ab} = -\frac{\wp}{2\hbar}\sum_n \mathcal{E}_{n+2}(\mathbf{r})\, e^{in[(\mathbf{K}_2-\mathbf{K}_1)\cdot\mathbf{r} - \Delta t]} \ . \tag{3.10}$$

To determine the response of the medium to this multimode field, we Fourier analyze the ρ_{ab} and the population difference D as

$$\rho_{ab} = N \sum_{m=-\infty}^{\infty} p_{m+2}\, e^{im[(\mathbf{K}_2-\mathbf{K}_1)\cdot\mathbf{r} - \Delta t]}\,, \tag{3.11}$$

$$D(\mathbf{r},t) = N \sum_{k=-\infty}^{\infty} d_k\, e^{ik[(\mathbf{K}_2-\mathbf{K}_1)\cdot\mathbf{r} - \Delta t]}\,. \tag{3.12}$$

We first calculate the Fourier coefficients p_2 and d_0 due to the pump field $\mathcal{E}_2$ acting alone. The other fields are assumed to be small enough not to saturate the medium by themselves. Substituting Eqs. (3.10), (3.11), and (3.12) into Eq. (3.9) and keeping only the e^0 contributions, we find

$$p_2 = \mathcal{D}_2[i\mathcal{V}_2 d_0 - \gamma_- p_2^*]\,, \tag{3.13}$$

where $\mathcal{D}_2$ is the $n = 2$ case of the complex denominator

$$\mathcal{D}_n = \frac{1}{\gamma_+ + i\Delta_n}\,, \tag{3.14}$$

and $\mathcal{V}_2$ is the $n = 2$ case of $\mathcal{V}_n = -\wp\mathcal{E}_n/2\hbar$. The complex conjugate of Eq. (3.13) gives p_2^* in terms of p_2. Substituting this into Eq. (3.13), we find

$$p_2 = \frac{id_0[\mathcal{V}_2(\gamma_+ - i\Delta_2) + \gamma_-\mathcal{V}_2^*]}{\gamma_u\gamma_v + \Delta_2^2}\,, \tag{3.15}$$

where $\mathcal{D}_{22}$ is the $n = m = 2$ case of

$$\mathscr{D}_{nm} = \frac{\mathscr{D}_n}{1 - \gamma_-^2 \mathscr{D}_n \mathscr{D}_m^*} . \tag{3.16}$$

This agrees with the usual result in the limit that $\gamma_u = \gamma_v = \gamma$, since then $\gamma_- \to 0$, $\gamma_+ \to \gamma$, and $\mathscr{D}_{nm} \to \mathscr{D}_n$.

We calculate the dc population difference Fourier component w_0 saturated by the pump wave $\mathscr{E}_2$ alone. Substituting Eqs. (3.10), (3.11), and (3.12) into Eq. (3.5), we have for the e^0 term

$$0 = -\Gamma(1 + d_0) - 2[i\mathscr{V}_2 p_2^* + \text{c.c.}] ,$$

yielding with Eq. (3.15)

$$d_0 = -\frac{1}{1 + I_2' \mathscr{L}_2'} , \tag{3.17}$$

where the modified pump dimensionless intensity I_2 is given by

$$I_2' = \frac{(\wp \mathscr{E}_{2r}/\hbar)^2}{\Gamma\gamma_v} + \frac{(\wp \mathscr{E}_{2i}/\hbar)^2}{\Gamma\gamma_u} , \tag{3.18}$$

and the modified dimensionless Lorentzian

$$\mathscr{L}_2' = \frac{\gamma_u \gamma_v}{\gamma_u \gamma_v + \Delta_2^2} . \tag{3.19}$$

The $\mathscr{E}_1$ contributions are ignored, since we assume $\mathscr{E}_1$ doesn't saturate.

Substituting Eqs. (3.10), (3.11), and (3.12) into Eq. (3.9) and keeping only the $e^{i\Delta t}$ terms for the probe wave ($m = -1$ term in Eq. (3.11)), we find

$$p_1 = \mathscr{D}_1[i\mathscr{V}_1 d_0 + i\mathscr{V}_2 d_{-1} - \gamma_- p_3^*] . \tag{3.20}$$

Similarly we find

$$p_3^* = -\mathscr{D}_3^*[i\mathscr{V}_3^* d_0 + i\mathscr{V}_2^* d_{-1} + \gamma_- p_1] . \tag{3.21}$$

Combining these equations, we find the probe polarization component

$$p_1 = i\mathscr{D}_{13}[(\mathscr{V}_1 + \gamma_-\mathscr{D}_3^*\mathscr{V}_3^*)d_0 + (\mathscr{V}_2 + \gamma_-\mathscr{D}_3^*\mathscr{V}_2^*)d_{-1}] . \tag{3.22}$$

Substituting Eqs. (3.10), (3.11), and (3.12) into (3.5) and equating the sum of the coefficients of $e^{i\Delta t}$ to zero, we relate the population pulsation coefficient d_{-1} to the p_n as

$$(\Gamma + i\Delta)d_{-1} = -2i[\mathscr{V}_1 p_2^* + \mathscr{V}_2 p_3^* - \mathscr{V}_2^* p_1 - \mathscr{V}_3^* p_2] .$$

Substituting Eqs. (3.15), (3.21) and (3.22) into this expression, we obtain

$$\begin{aligned}(\Gamma + i\Delta)d_{-1} = {} & -2i\mathscr{V}_1 p_2^* + 2i\mathscr{V}_3^* p_2 - 2\mathscr{V}_2\mathscr{D}_3^*(\mathscr{V}_3^* d_0 + \mathscr{V}_2^* d_{-1}) \\ & - 2(\mathscr{V}_2^* + \gamma_-\mathscr{D}_3^*\mathscr{V}_2)\mathscr{D}_{13}[(\mathscr{V}_1 + \gamma_-\mathscr{D}_3^*\mathscr{V}_3^*)d_0 + (\mathscr{V}_2 + \gamma_-\mathscr{D}_3^*\mathscr{V}_2^*)d_{-1}] ,\end{aligned}$$

which gives

$$d_{-1} = \frac{-i\mathcal{V}_1 p_2^* + i\mathcal{V}_3^* p_2 - \mathcal{V}_2\mathcal{V}_3^*\mathcal{D}_3^* d_0 - (\mathcal{V}_2^*+\gamma_-\mathcal{D}_3^*\mathcal{V}_2)\mathcal{D}_{13}(\mathcal{V}_1+\gamma_-\mathcal{D}_3^*\mathcal{V}_3^*)d_0}{(\Gamma + i\Delta)/2 + |\mathcal{V}_2|^2\mathcal{D}_3^* + (\mathcal{V}_2^* + \gamma_-\mathcal{D}_3^*\mathcal{V}_2)(\mathcal{V}_2 + \gamma_-\mathcal{D}_3^*\mathcal{V}_2^*)\mathcal{D}_{13}} . \tag{3.23}$$

Combining Eqs. (3.2), (3.6) and (3.11), we see that the probe absorption $\mathscr{P}_1$ is given by

$$\mathscr{P}_1 = 2N\wp p_1 . \tag{3.24}$$

Hence the probe absorption is given by substituting Eqs. (3.22) and (3.23) into Eq. (3.24). Making these substitutions and then substituting the result into the Beer's law, Eq. (3.3), we find the coupled mode equation

$$\frac{d\mathcal{E}_1}{dz} = -\alpha_1\mathcal{E}_1 + \chi_1\mathcal{E}_3^* , \tag{3.25}$$

where the absorption coefficient α_1 is given by

$$\alpha_1 = \frac{\alpha_0'\mathcal{D}_{13}\gamma_u\gamma_v/\gamma_+}{1+I_2'\mathscr{L}_2'}\left[1 - \frac{(\mathcal{V}_2+\gamma_-\mathcal{D}_3^*\mathcal{V}_2^*)[(\mathcal{V}_2^*+\gamma_-\mathcal{D}_3^*\mathcal{V}_2)\mathcal{D}_{13} + (\mathcal{V}_2^*+\gamma_-\mathcal{D}_2\mathcal{V}_2)\mathcal{D}_{22}^*]}{(\Gamma+i\Delta)/2 + |\mathcal{V}_2|^2\mathcal{D}_3^* + (\mathcal{V}_2+\gamma_-\mathcal{D}_3^*\mathcal{V}_2^*)(\mathcal{V}_2^*+\gamma_-\mathcal{D}_3^*\mathcal{V}_2)\mathcal{D}_{13}}\right] \tag{3.26}$$

and the coupling coefficient χ_1 is given by

$$\chi_1 = -\frac{\alpha_0'\mathscr{D}_{13}\gamma_u\gamma_v/\gamma_+}{1+I_2'\mathscr{L}_2'}\left[\gamma_-\mathscr{D}_3^* - \frac{(\mathscr{V}_2+\gamma_-\mathscr{D}_3^*\mathscr{V}_2^*)[(\mathscr{V}_2+\gamma_-\mathscr{D}_1\mathscr{V}_2^*)\mathscr{D}_{31}^* + (\mathscr{V}_2+\gamma_-\mathscr{D}_2^*\mathscr{V}_2^*)\mathscr{D}_{22}]}{(\Gamma+i\Delta)/2 + |\mathscr{V}_2|^2\mathscr{D}_3^* + (\mathscr{V}_2+\gamma_-\mathscr{D}_3^*\mathscr{V}_2^*)(\mathscr{V}_2^*+\gamma_-\mathscr{D}_3^*\mathscr{V}_2)\mathscr{D}_{13}}\right] \tag{3.27}$$

where

$$\alpha_0' = \frac{K\wp^2 N\gamma_+}{\hbar\epsilon_0\gamma_u\gamma_v}\,. \tag{3.28}$$

Substituting $\mathscr{V}_2 = -\frac{1}{2}\sqrt{I_2\Gamma\gamma_+}\,e^{-i\phi}$ into Eqs. (3.26) and (3.27), we finally have

$$\alpha_1 = \frac{\alpha_0'\mathscr{D}_{13}\gamma_u\gamma_v/\gamma_+}{1+I_2f_0}\left[1 - \frac{I_2f_1}{1+I_2f_2}\right], \tag{3.29}$$

$$\chi_1 = -\frac{\alpha_0'\mathscr{D}_{13}\gamma_u\gamma_v/\gamma_+}{1+I_2f_0}\left[\gamma_-\mathscr{D}_3^* - \frac{I_2f_3}{1+I_2f_2}\right], \tag{3.30}$$

where the complex factors f_n are given by

$$f_0 = \frac{\gamma_+^2}{\gamma_u\gamma_v + \Delta_2^2}\left[1 + \frac{\gamma_-}{\gamma_+}\cos 2\phi\right], \tag{3.31}$$

$$f_1 = \frac{\Gamma}{\Gamma+i\Delta}\frac{\gamma_+}{2}[\mathscr{D}_{13}(1+\gamma_-^2\mathscr{D}_3^{*2}) + \mathscr{D}_{22}^*(1+\gamma_-^2\mathscr{D}_3^*\mathscr{D}_2) + 2\gamma_-\mathscr{D}_3^*\mathscr{D}_{13}\cos 2\phi + \gamma_-\mathscr{D}_{22}^*(\mathscr{D}_2e^{-2i\phi} + \mathscr{D}_3^*e^{2i\phi})]\,, \tag{3.32}$$

$$f_2 = \frac{\Gamma}{\Gamma+i\Delta}\frac{\gamma_+}{2}[\mathscr{D}_3^* + \mathscr{D}_{13}(1+\gamma_-^2\mathscr{D}_3^{*2}) + 2\gamma_-\mathscr{D}_3^*\mathscr{D}_{13}\cos 2\phi]\,, \tag{3.33}$$

$$f_3 = \frac{\Gamma}{\Gamma+i\Delta}\frac{\gamma_+}{2}[\gamma_-\mathscr{D}_{22}(\mathscr{D}_2^*+\mathscr{D}_3^*) + \gamma_-\mathscr{D}_{31}^*(\mathscr{D}_1+\mathscr{D}_3^*) + (\mathscr{D}_{22}+\mathscr{D}_{31}^*)e^{-2i\phi}$$
$$+ \gamma_-^2\mathscr{D}_3^*(\mathscr{D}_2^*\mathscr{D}_{22} + \mathscr{D}_1\mathscr{D}_{31}^*)e^{2i\phi}] \,. \tag{3.34}$$

In the limit of an unsqueezed vacuum ($\gamma_- = 0$), these expressions immediately reduce to the α_1 and χ_1 of Sargent, Holm, and Zubairy (1985) and of Khitrova, Berman, and Sargent (1988), provided we make the replacement

$$\Gamma + i\Delta \to 1/T_1\mathscr{F}(\Delta) \,, \tag{3.35}$$

where T_1 is their more general population-difference decay time (here given simply by $T_1 = \Gamma^{-1}$) and $\mathscr{F}(\Delta)$ is their more general population difference dynamic factor [here given by $\mathscr{F}(\Delta) = \Gamma/(\Gamma + i\Delta)$]. In fact, we could have used the more general decay scheme of those papers and found generalizations of Eqs. (3.26) and (3.27) with this substitution.

Similarly we find

$$\frac{d\mathscr{E}_3^*}{dz} = -\alpha_3^*\mathscr{E}_3^* + \chi_3^*\mathscr{E}_1 \,, \tag{3.36}$$

where α_3 and χ_3 are given by Eqs. (3.26) and (3.27), respectively, with the subscripts 1 and 3 interchanged (note that this implies that $\Delta \to -\Delta$).

Figure 5 shows an absorption spectrum, i.e., real part of α_1 versus pump/probe beat frequency Δ for $\gamma_- = 0$ and 0.92. The pump phase differs from that of the vacuum by $\pi/2$. For a highly squeezed vacuum ($\gamma_- = 0.92$), we find a sharp Lorentzian peak near zero beat frequencies and suppresion of population pulsation contributions (Ritsch and Zoller 1987 and 1988, An and Sargent 1988). In the limit of an un-

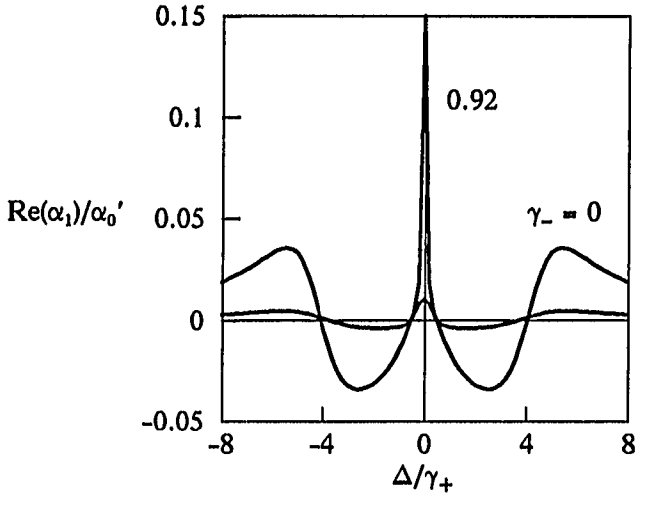

Fig. 5. Real part of α_1 versus pump/probe beat frequency $\Delta = \nu_2-\nu_1$, for $\Gamma = 2\gamma_+$, $\omega = \nu_2$, $I_2 = 9$, and $\gamma_- = 0$ (the original Mollow spectrum) and 0.92. The phase of the pump field differs from that of the vacuum by $\pi/2$. Note that our frequencies are normalized in units of γ_+, which for a highly squeezed vacuum is a much larger unit than that used by Ritsch and Zoller (1987).

squeezed vacuum ($\gamma_- = 0$), the probe absorption reduces to the original Mollow (1972) spectrum.

Figure 6 plots the real part of α_1 versus pump/probe beat frequency Δ for the pump detuning $\omega - \nu_2 = -0.2$ and -3. Comparing curves for a substantially detuned pump (e.g., -3 in Fig. 6) with and without a squeezed vacuum, we find that aside from the substantial change in the value of α_0' and some small changes near $\Delta = 0$, the probe absorption spectra are very similar. In particular, the sharp central peak is destroyed. On the other hand, the small detuning of -0.2 spoils the cancelation of the population pulsation contribution in Eq. (3.26) seen in Fig. 5 and leads to relatively large variations around the Rabi flopping frequency. This is an example of how

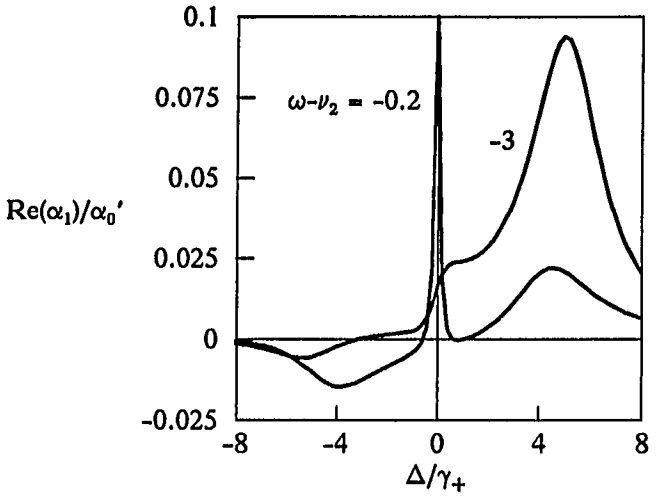

Fig. 6. Real part of α_1 versus Δ for $\omega - \nu_2 = -0.2$ and -3, $\gamma_- = 0.92$, and the other parameters are the same as in Fig. 2.

crucial the relative phases between the vacuum, pump, and atoms can be.

Figure 7 illustrates this point further by plotting the real part of α_1 versus Δ for the phase of pump field $\phi = 0$ and $2\pi/5$, and other parameters the same as in Fig. 5 for $\gamma_- = .92$. Both curves differ substantially from their counterpart in Fig. 5 and also from probe absorption in an unsqueezed vacuum. The $\phi = 0$ case is somewhat reminiscent of the AM absorption found in resonant-pump three-wave mixing and shows no central peak structure. The $\phi = 2\pi/5$ case reveals a negative peak, and $\phi = \pi/2$ gives the sharp high positive peak in Fig. 5.

Figure 8 plots the real part of χ_1 versus Δ for $\gamma_- = 0.01$ and 0.92, and $\phi = \pi/2$. For a highly squeezed vacuum, the spectrum shows similar characteristics to those in Fig. 5 (i.e., sharp resonance and suppression of population pulsation contributions). The dependence of the coupling coefficient on other parameters is also similar to that

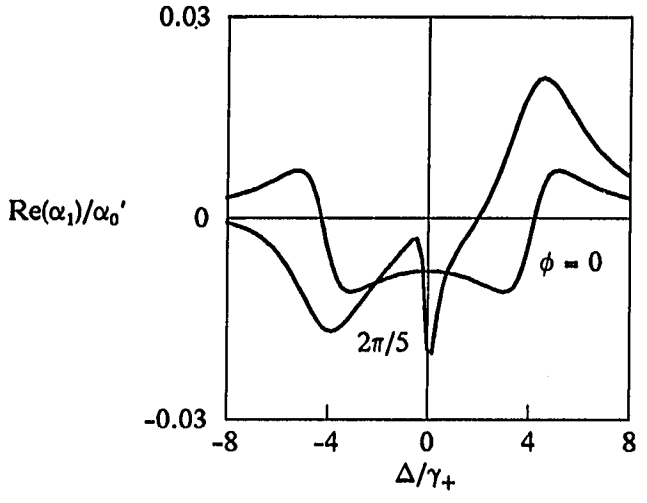

Fig. 7. Real part of α_1 versus Δ for the phase of pump field $\phi = 0$ and $2\pi/5$, $\gamma_- = 0.92$, and the other parameters are the same as in Fig. 2.

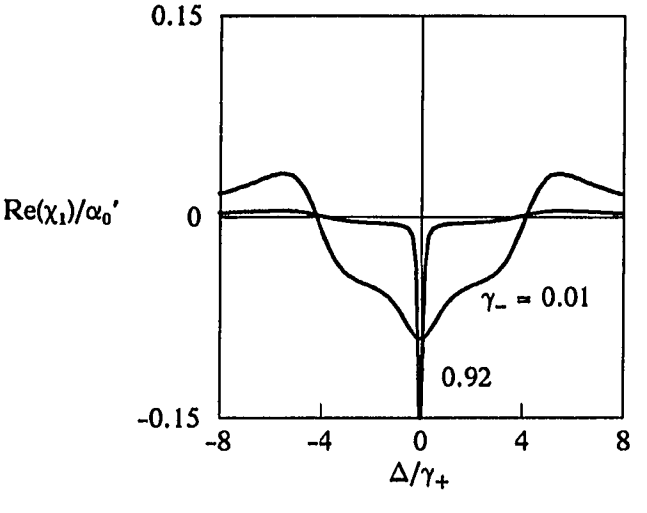

Fig. 8. Real part of χ_1 versus Δ for $\gamma_- = 0.01$ and 0.92, $\phi = \pi/2$, and the other parameters are the same as in Fig. 2.

of the probe absorption coefficient shown in Figs. 6 and 7.

3-2. Four-Wave Mixing in a Squeezed Vacuum

In this section we consider the case of four-wave mixing in which the strong pump field consists of two oppositely directed running-waves, forming a standing-wave. In this case a given pump wave interferes with the signal wave to induce a grating that scatters the other pump wave into the direction opposite that of the signal wave (see Fig. 9). This provides the source for the conjugate wave. The conjugate is phase-matched for all directions. Because of the standing-wave pump pattern in the medium, atoms in different locations in the medium experience a varying amount of saturation due to the spatial hole burning of the upper and lower population difference. We account for this by averaging the coefficients over the spatial hole burning for one wavelength.

The standing-wave pump field is given by

$$E_2 = \frac{1}{2}\,[\mathcal{E}_2\exp[i(\mathbf{K}_2\cdot\mathbf{r} - \nu_2 t)] + \mathcal{E}_2\exp[-i(\mathbf{K}_2\cdot\mathbf{r} + \nu_2 t)] + \text{c.c.}]\,. \tag{3.37}$$

We define the spatially dependent intensity

$$\mathcal{I}_{2\mathbf{r}} = 4|\mathcal{V}_2|^2 T_1 T_2 = \frac{4\wp^2|\mathcal{E}_2|^2}{\hbar^2}\cos^2(\mathbf{K}_2\cdot\mathbf{r})T_1T_2 = 4I_2\cos^2(\mathbf{K}_2\cdot\mathbf{r})\,. \tag{3.38}$$

where I_2 is the dimensionless, spatially independent intensity for each wave. For simplicity we take the wave vector $\mathbf{K}_2$ to be along the z-axis, so $\mathbf{K}_2\cdot\mathbf{r} = K_2 z = 2\pi z/\lambda_2$. We

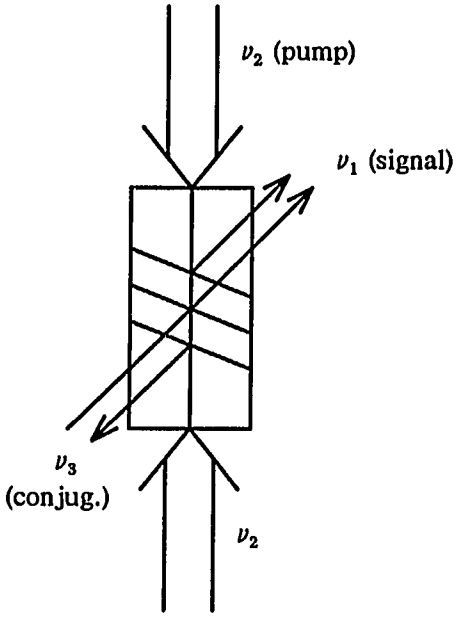

Fig. 9. Four-wave mixing diagram defining the pump, signal, and conjugate waves. There is another grating induced by the signal and the other pump wave.

substitute Eq. (3.38) for I_2 in Eqs. (3.29) and (3.30), and integrate each coefficient along the z-direction for one wavelength. For example,

$$\langle \alpha_1 \rangle = \frac{1}{\lambda_2} \int_0^{\lambda_2} dz \; \alpha_1(z) \; . \tag{3.39}$$

The α_1 and χ_1 given by Eqs. (3.29) and (3.30) have the same form as those for the unsqueezed vacuum and hence we can use the standing-wave averages calculated previously (Fu and Sargent 1979). The results are

$$\langle\alpha_1\rangle = \frac{\alpha_0'\mathscr{D}_{13}\gamma_u\gamma_v/\gamma_+}{\sqrt{1+4I_2f_0}}\left[1 - \frac{4I_2f_1}{1+4I_2f_2+\sqrt{(1+4I_2f_0)(1+4I_2f_2)}}\right], \tag{3.40}$$

$$\langle\chi_1\rangle = -\frac{\alpha_0'\mathscr{D}_{13}\gamma_u\gamma_v/\gamma_+}{\sqrt{1+4I_2f_0}}\left[\gamma_-\mathscr{D}_3^* - \frac{4I_2f_3}{1+4I_2f_2+\sqrt{(1+4I_2f_0)(1+4I_2f_2)}}\right], \tag{3.41}$$

where f_0, f_1, f_2, and f_3 are given by Eqs. (3.31) through (3.34).

Using Eqs. (3.40) and (3.41) for α_1 and χ_1 and including the phase mismatch factor, the coupled mode equations (3.25) and (3.36) are modified by

$$\frac{d\mathscr{E}_1}{dz} = -\langle\alpha_1\rangle\mathscr{E}_1 + \langle\chi_1\rangle\mathscr{E}_3^* e^{2i\Delta Kz}, \tag{3.42}$$

$$-\frac{d\mathscr{E}_3^*}{dz} = -\langle\alpha_3\rangle^*\mathscr{E}_3^* + \langle\chi_3\rangle^*\mathscr{E}_1 e^{-2i\Delta Kz}, \tag{3.43}$$

where $\Delta K = (K_3-K_1)/2$. The solutions for the coupled mode equations (3.42) and (3.43) are well-known (Fu and Sargent 1979). In particular the amplitude reflection coefficient $r = \mathscr{E}_3^*(0)/\mathscr{E}_1(0)$ is given by

$$r = \frac{\mathscr{E}_3^*(0)}{\mathscr{E}_1(0)} = \langle\chi_3\rangle^* \frac{\sinh wL}{w\cosh wL + \alpha\sinh wL}, \tag{3.44}$$

where $\alpha = (\langle\alpha_1\rangle + \langle\alpha_3\rangle^* + 2i\Delta K)/2$ and $w = [\langle\alpha\rangle^2 - \langle\chi_1\rangle\langle\chi_3\rangle^*]^{1/2}$.

Figure 10 illustrates the reflectivity $R = |r|^2$ as a function of signal detuning for $\gamma_- = 0$, 0.46, and 0.92 and $\phi = \pi/2$. We find that the reflectivity peaks in squeezed vacuums are narrower than in an unsqueezed vacuum. Figure 11 plots the reflectivity

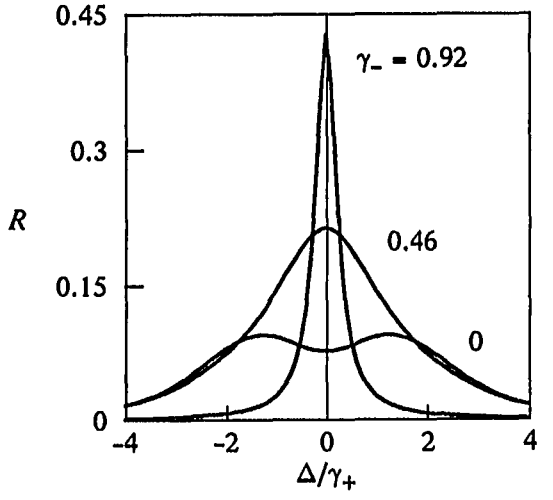

Fig. 10. Reflectivity R versus Δ for $\Gamma = 2\gamma_+$, $\omega = \nu_2$, $I_2 = 1$, $L = 4$, $\phi = \pi/2$. $\gamma_- = 0$, 0.46, and 0.92.

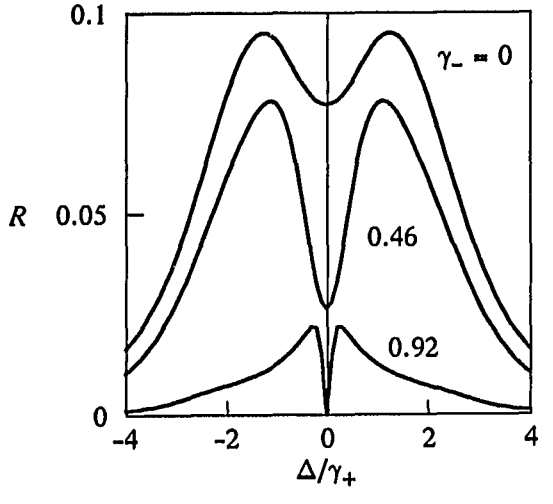

Fig. 11. Reflectivity R versus Δ for $\phi = 0$. The other parameters are the same as in Fig. 7.

R versus Δ for $\phi = 0$. The squeezed vacuum produces smaller overall reflectivity than the unsqueezed vacuum. The reflectivity dips are also found to be narrower than in an unsqueezed vacuum.

In this chapter we have derived the probe absorption and coupling coefficients in a squeezed vacuum using a standard Fourier series method. We have illustrated the sensitivity of sharp peak structures to both pump detuning and pump phase relative to the squeezed vacuum. Averaging the coefficients over pump spatial holes, we have also calculated and plotted the reflection coefficients. Near zero beat frequencies reveal sharp Lorenzian peaks in α_1, χ_1, and the reflectivity spectra. This can be traced to a common leading factor in Eqs. (3.26), (3.27), and (3.44). In fact, for small γ_ν and pump/probe detuning Δ, we find the various coefficients are proportional to the factor $\gamma_\nu(\gamma_\nu + i\Delta)$, which reveals a sharp Lorentzian with FWHM width of $2\gamma_\nu$. As such both the absorption and the reflectivity provide sensitive ways to measure the amount of squeezing in the vacuum.

CHAPTER 4

EFFECTS OF SIDEMODE SATURATION IN ONE-PHOTON TWO-LEVEL MEDIA

Most multiwave mixing theories treat the electromagnetic fields classically and the atoms quantum mechanically (semiclassical approximation). However problems like resonance fluorescence and squeezed states of light cannot be explained with a semi-classical theory. For such problems, the weak fields must be quantized, while the strong pump fields can be treated classically.

Previously Sargent, Scully, and Lamb (1970) presented a single-mode quantum theory which describes the buildup of oscillation from the vacuum and some aspects of the photon statistics. Later Sargent, Holm, and Zubairy (1985) derived a theory describing quantum multiwave interactions in a nonlinear one-photon two-level medium. The ensuing series of papers (Quantum theory of multiwave mixing II through X) apply this theory to predict and explain many quantum optical phenomena in such media.

The theory assumes that the sidemode photon numbers are sufficiently small compared to the saturation photon number that a second-order perturbation treatment is adequate. If this is not true such as near the laser threshold, we expect that higher order perturbation corrections are needed. This chapter extends the theory to fourth order in the the weak-field interaction by using an approach similar to that by Sargent, Holm, and Zubairy (1985). The results are applied to cavity problems, showing how the fourth-order theory alters the photon number spectra of the second-order theory. Because of the complexity of the fourth-order theory, we limit our

analysis to a single sidemode field, unlike the other papers in the series, all of which treat one- and two-sidemode mixing.

Section 4-1 summarizes the semiclassical theory of sidemode saturation. The self-consistent equation is reduced to the algebraic equation expressed in terms of a continued fraction (Sargent 1978). We use this equation to find a degenerate solution in a closed form and a nondegenerate solution up to third order in the weak-field amplitude. Section 4-2 extends the quantum theory of multiwave mixing by Sargent, Holm, and Zubairy (1985) to fourth order. We show that the fourth-order quantum theory yields the third-order semiclassical absorption coefficient given by truncating the continued fraction of Sec. 4-1. Section 4-3 solves the fourth-order equation of motion in steady-state and studies the effects of cavities on the photon number spectrum. The results are compared to the second-order theory.

4-1. Semiclassical Sidemode Saturation

4-1-1. Fourier Analysis and Continued Fraction

This section summarizes the treatment of two arbitrarily intense classical waves interacting with a two-level medium. A typical pump-probe setup is pictured in Fig. 12. We assume that the saturating wave intensity is constant throughout the interaction region. To distinguish between the two waves, we use the subscript 1 for the probe wave and 2 for the pump wave. Our electric field has the form

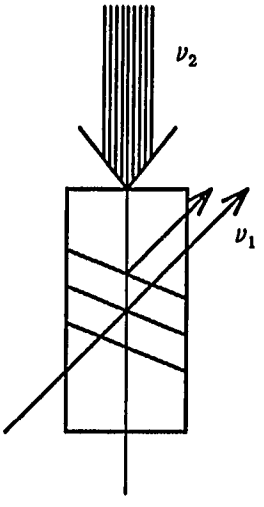

Fig. 12. Basic pump-probe saturation spectroscopy configuration.

$$E(\mathbf{r},t) = \frac{1}{2}\sum_{n=1}^{2} E_n(\mathbf{r})\, e^{i(\mathbf{K}_n\cdot\mathbf{r} - \nu_n t)} + \text{c.c.}\,, \tag{4.1}$$

where the mode amplitudes $E_n(\mathbf{r})$ are in general complex and $\mathbf{K}_n$ are the wave propagation vectors. This field induces the complex polarization

$$P(\mathbf{r},t) = \frac{1}{2}\sum_{n=1}^{2} \mathscr{P}_n(\mathbf{r})\, e^{i(\mathbf{K}_n\cdot\mathbf{r} - \nu_n t)} + \text{c.c.}\,, \tag{4.2}$$

where $\mathscr{P}_n(\mathbf{r})$ is a complex polarization coefficient that yields index and absorption/gain characteristics for the probe and saturator waves. The polarization $P(\mathbf{r},t)$ in general has other components, but we are interested only in those given by Eq. (4.2). In par-

ticular, strong wave interactions induce components not only at the frequencies ν_1 and ν_2, but at $\nu_1 \pm k(\nu_2-\nu_1)$ as well, where k is an integer.

The problem reduces to determining the probe's polarization $\mathscr{P}_1(\mathbf{r})$, from which the absorption coefficient is determined from the equation

$$\frac{dE_1}{dz} = i(K_1/2\epsilon)\mathscr{P}_1 , \tag{4.3}$$

where ϵ is the permittivity of host medium. One might guess that the probe absorption coefficient is simply a probe Lorentzian multiplied by a population difference saturated by the saturator wave. However an additional contribution enters due to population pulsations. Specifically the nonlinear populations respond to the superposition of the modes to give pulsations at the beat frequency $\Delta = \nu_2-\nu_1$.

The population matrix with upper-to-ground-lower-level decay obeys the equations of motion

$$\dot{\rho}_{ab} = -(\gamma + i\Delta_2)\rho_{ab} + i\mathscr{V}_{ab}D , \tag{4.4}$$

$$\dot{D} = -\Gamma(D + N) - 2[i\mathscr{V}_{ab}\rho_{ba} + \text{c.c.}] , \tag{4.5}$$

where γ ($\equiv 1/T_2$) is the dipole decay constant, ω is the frequency of the atomic line center, $\mathscr{V}_{ab}$ is the electric-dipole interaction energy, D is the population difference $\rho_{aa} - \rho_{bb}$, Γ is the population-difference decay constant ($\equiv 1/T_1$), and N is the unsaturated population difference per unit volume. In terms of ρ_{ab}, the polarization (2) is given by

$$P(\mathbf{r},t) = \wp\rho_{ab} e^{i(\mathbf{K}_2\cdot\mathbf{r} - \nu_2 t)} + \text{c.c.}\ , \tag{4.6}$$

where $\wp$ is the electric-dipole matrix element. The problem thus reduces as usual to finding ρ_{ab}.

The interaction energy matrix element $\mathcal{V}_{ab}$ is given in the rotating-wave approximation by

$$\mathcal{V}_{ab} = -\frac{\wp}{2\hbar} \sum_{n=1}^{2} E_n(\mathbf{r})\, e^{i(\mathbf{K}_n\cdot\mathbf{r} - \nu_n t)}\ . \tag{4.7}$$

To determine the response of the medium to this multimode field, we Fourier analyze both the polarization component ρ_{ab} of the population matrix as well as the population difference. We have

$$\rho_{ab} = N\, e^{i(\mathbf{K}_1\cdot\mathbf{r} - \nu_1 t)} \sum_{m=-\infty}^{\infty} p_{m+1}\, e^{im((\mathbf{K}_2-\mathbf{K}_1)\cdot\mathbf{r} - \Delta t)}\ , \tag{4.8}$$

$$D(\mathbf{r},t) = N \sum_{k=-\infty}^{\infty} d_k\, e^{-ik[(\mathbf{K}_2-\mathbf{K}_1)\cdot\mathbf{r} - \Delta t]}\ , \tag{4.9}$$

Substituting the Fourier expansions Eqs. (4.7) through (4.9) into the equation of motion (4.5) and identifying coefficients of common exponential frequency factors, we find the population difference component

$$d_k = \delta_{k0} - i\sqrt{T_1/T_2}\mathcal{F}(k\Delta)\sum_{n=1}^{2}(\mathcal{E}_n p_{n+k}^{*} - \mathcal{E}_n^{*} p_{n-k}) , \tag{4.10}$$

where the dimensionless "population pulsation" factor

$$\mathcal{F}(\Delta) = \frac{\Gamma}{\Gamma + i\Delta} , \tag{4.11}$$

and the dimensionless complex electric field

$$\mathcal{E}_n = \frac{\wp}{\hbar}\sqrt{T_1 T_2}E_n . \tag{4.12}$$

Similarly substituting Eqs. (4.7) through (4.9) into the equation of motion (4.4), we find the polarization component

$$p_m = -\frac{i}{2}(T_1 T_2)^{-1/2}\mathcal{D}_n \sum_k \mathcal{E}_{m+k} d_k , \tag{4.13}$$

where the complex Lorentzian denominator $\mathcal{D}_n$ is given by

$$\mathcal{D}_n = \frac{1}{\gamma + i(\omega - \nu_n)} , \tag{4.14}$$

Combining Eq. (4.10) with (4.13), we find the equation for the population difference alone

$$c_{-1,k} d_{k-1} + c_{0,k} d_k + c_{1,k} d_{k+1} = 0 , \tag{4.15}$$

where the complex coefficients

$$c_{j,k} = \frac{\gamma}{2} \sum_{n=j+1\geq 1}^{j+2\leq 2} \mathcal{E}_n \mathcal{E}_{n-j}{}^* [\mathcal{D}_{n+k}{}^* + \mathcal{D}_{n-j-k}] , \tag{4.16}$$

$$c_{0,k} = \left[1 - \frac{\delta_{k,0}}{d_0}\right] \frac{1}{\mathcal{F}(k\Delta)} + \frac{\gamma}{2} \sum_{n=1}^{2} I_n [\mathcal{D}_{n+k}{}^* + \mathcal{D}_{n-k}] , \tag{4.17}$$

where the dimensionless intensity I_n is given by

$$I_n \equiv |\mathcal{E}_n|^2 = (\wp E_n/\hbar)^2 T_1 T_2 . \tag{4.18}$$

Equation (4.15) can be written in terms of the ratios $r_k = d_k/d_{k-1}$ as

$$r_k = - \frac{c_{-1,k}}{c_{0,k} + c_{1,k} r_{k+1}} . \tag{4.19}$$

Starting with $k = 1$, we have

$$r_1 = - \frac{c_{-1,1}}{c_{0,1} + c_{1,1} r_2} , \tag{4.20}$$

and iterating Eq. (4.19) for r_2, etc., we obtain an infinite continued fraction. This fraction can always be truncated for some k due to the finite bandwidth of the medium. For the two-wave case in which the probe does not saturate, i.e., acts only once (in the sense of perturbation theory), we can find an approximate solution for r_1 dropping $c_{1,1} r_2$ in Eq. (4.20).

4-1-2. Degenerate Solution

In the degenerate case, all coefficients of Eqs. (4.16) and (4.17) are independent of k. Therefore, setting $r_{k+1} = r_k = r_1$ in Eq. (4.19), we have the quadratic equation for r_1

$$c_1 r_1^2 + c_0 r_1 + c_{-1} = 0 \ . \tag{4.21}$$

where c_1, c_0, and c_{-1} are given by

$$c_1 = \mathcal{E}_1^* \mathcal{E}_2 \mathcal{L}_2 \ , \tag{4.22}$$

$$c_{-1} = \mathcal{E}_1 \mathcal{E}_2^* \mathcal{L}_2 \ , \tag{4.23}$$

$$c_0 = 1 + (I_1 + I_2)\mathcal{L}_2 \ , \tag{4.24}$$

where the dimensionless Lorentzian $\mathcal{L}_2$ is given by

$$\mathcal{L}_2 = \frac{\gamma^2}{\gamma^2 + (\omega - \nu_2)^2} \ . \tag{4.25}$$

The solution of Eq. (4.21) is

$$r_1 = \frac{1 + (I_1 + I_2)\mathscr{L}_2}{2\mathscr{E}_1^*\mathscr{E}_2\mathscr{L}_2}\left[-1 \pm \sqrt{1 - \frac{4I_1I_2\mathscr{L}_2^2}{[1 + (I_1 + I_2)\mathscr{L}_2]^2}}\right]. \tag{4.26}$$

If we define $x \equiv 4I_1I_2\mathscr{L}_2^2/[1 + (I_1 + I_2)\mathscr{L}_2]^2$, then since $|x| < 1$ we can expand $\sqrt{1 - x}$ in Eq. (4.26) by using the Taylor series

$$\sqrt{1 - x} = 1 - \frac{1}{2}x - \frac{1}{8}x^2 - \frac{1}{16}x^3 + \cdots . \tag{4.27}$$

Substituting Eq. (4.27) into Eq. (4.26), we find r_1 up to fifth order in $\mathscr{E}_1$

$$r_1 = -\frac{\mathscr{E}_1\mathscr{E}_2^*\mathscr{L}_2}{1 + (I_1 + I_2)\mathscr{L}_2} - \frac{\mathscr{E}_1I_1\mathscr{E}_2^*I_2\mathscr{L}_2^3}{[1 + (I_1 + I_2)\mathscr{L}_2]^3} - \frac{2\mathscr{E}_1I_1^2\mathscr{E}_2^*I_2^2\mathscr{L}_2^5}{(1 + (I_1 + I_2)\mathscr{L}_2)^5}, \tag{4.28}$$

where we have chosen the (+) sign from (±) in Eq. (4.26) to recover the lowest order theory (i.e., α_1 coefficient in Eq. (4.29)). Since $I_2 \gg I_1$, we can expand the denominators in Eq. (4.28) as

$$\frac{1}{1 + (I_1 + I_2)\mathscr{L}_2} = \frac{1}{1 + I_2\mathscr{L}_2} - \frac{I_1\mathscr{L}_2}{(1 + I_2\mathscr{L}_2)^2} + \frac{I_1^2\mathscr{L}_2^2}{(1 + I_2\mathscr{L}_2)^3} + \cdots , \tag{4.29}$$

$$\frac{1}{(1 + (I_1 + I_2)\mathscr{L}_2)^3} = \frac{1}{(1 + I_2\mathscr{L}_2)^3} - \frac{3I_1\mathscr{L}_2}{(1 + I_2\mathscr{L}_2)^4} + \cdots , \tag{4.30}$$

$$\frac{1}{(1 + (I_1 + I_2)\mathscr{L}_2)^5} = \frac{1}{(1 + I_2\mathscr{L}_2)^5} + \cdots . \tag{4.31}$$

Substituting Eqs. (4.29) through (4.31) into Eq. (4.28), we finally have the semiclassical propagation equation for the probe wave up to fifth order in $\mathscr{E}_1$

$$\frac{d\mathcal{E}_1}{dz} = -\frac{\alpha_0\gamma\mathcal{D}_2}{(1 + I_2\mathcal{L}_2)}(\mathcal{E}_1 + \mathcal{E}_2 r_1)$$

$$= -\alpha_1\mathcal{E}_1 + \beta_1\mathcal{E}_1 I_1 + \gamma_1\mathcal{E}_1 I_1^2 , \tag{4.32}$$

where the coefficients α_1, β_1, and γ_1 are given by

$$\alpha_1 = \alpha_0\gamma\mathcal{D}_2 \frac{1}{(1 + I_2\mathcal{L}_2)^2} , \tag{4.33}$$

$$\beta_1 = -\alpha_0\gamma\mathcal{D}_2 \frac{I_2\mathcal{L}_2^2}{(1 + I_2\mathcal{L}_2)^4} , \tag{4.34}$$

$$\gamma_1 = \alpha_0\gamma\mathcal{D}_2 \frac{I_2\mathcal{L}_2^3 (1 - I_2\mathcal{L}_2)}{(1 + I_2\mathcal{L}_2)^6} . \tag{4.35}$$

For the central tuning (i.e., $\omega = \nu_2$), Eqs. (4.33) through (4.35) simplify to

$$\alpha_1 = \frac{\alpha_0}{(1 + I_2)^2} , \tag{4.36}$$

$$\beta_1 = -\frac{\alpha_0 I_2}{(1 + I_2)^4} , \tag{4.37}$$

$$\gamma_1 = \frac{\alpha_0 I_2 (1 - I_2)}{(1 + I_2)^6} . \tag{4.38}$$

Note that β_1 is negative for all I_2, i.e., it adds to the α_1 term rather than substracts, which has just the opposite effect from the usual saturation. The coefficient γ_1 is also negative for $I_2 > 1$.

4-1-3. Nondegenerate Solution

Dropping r_3 in Eq. (4.19) for $k = 2$, as we discussed in Sec. 4-1-1, we have

$$r_2 = -\frac{c_{-1,2}}{c_{0,2}}, \tag{4.39}$$

where

$$c_{-1,2} = \frac{\gamma}{2}\mathcal{E}_1\mathcal{E}_2^*(\mathcal{D}_3^* + \mathcal{D}_0), \tag{4.40}$$

$$c_{0,2} = \frac{1}{\mathcal{F}(2\Delta)} + \frac{\gamma}{2}I_2(\mathcal{D}_4^* + \mathcal{D}_0). \tag{4.41}$$

Substituting Eq. (4.39) into Eq. (4.20) with

$$c_{-1,1} = \frac{\gamma}{2}\mathcal{E}_1\mathcal{E}_2^*(\mathcal{D}_2^* + \mathcal{D}_1), \tag{4.42}$$

$$c_{1,1} = \frac{\gamma}{2}\mathcal{E}_1^*\mathcal{E}_2(\mathcal{D}_3^* + \mathcal{D}_0), \tag{4.43}$$

$$c_{0,1} = \frac{1}{\mathcal{F}(\Delta)} + \frac{\gamma}{2}I_2(\mathcal{D}_3^* + \mathcal{D}_1) + \frac{\gamma}{2}I_1(\mathcal{D}_2^* + \mathcal{D}_0), \tag{4.44}$$

and expanding r_1 to third order in $\mathcal{E}_1$, we find

$$\begin{aligned}\frac{d\mathcal{E}_1}{dz} &= -\alpha_0\gamma\mathcal{D}_1 d_0(\mathcal{E}_1 + \mathcal{E}_2 r_1)\\ &= -\alpha_1\mathcal{E}_1 + \beta_1\mathcal{E}_1 I_1,\end{aligned} \tag{4.45}$$

where α_1 is the usual nondegenerate probe absorption coefficient (Boyd and Sargent 1988, Sargent 1978, Mollow 1972)

$$\alpha_1 = \frac{\alpha_0 \gamma \mathscr{D}_1}{1 + I_2 \mathscr{L}_2} \left[1 - \frac{I_2 \mathscr{F}(\Delta) \frac{\gamma}{2} (\mathscr{D}_1 + \mathscr{D}_2^*)}{1 + I_2 \mathscr{F}(\Delta) \frac{\gamma}{2} (\mathscr{D}_1 + \mathscr{D}_3^*)} \right], \tag{4.46}$$

and the third-order coefficient β_1 is given by

$$\beta_1 = -\frac{\alpha_0 \gamma \mathscr{D}_1}{1 + I_2 \mathscr{L}_2} \frac{I_2 \mathscr{F}(\Delta)^2 (\gamma/2)^2 (\mathscr{D}_1 + \mathscr{D}_2^*)(\mathscr{D}_0 + \mathscr{D}_2^*)}{\left[1 + I_2 \mathscr{F}(\Delta) \frac{\gamma}{2} (\mathscr{D}_1 + \mathscr{D}_3^*) \right]^2}$$
$$+ \frac{\alpha_0 \gamma \mathscr{D}_1}{1 + I_2 \mathscr{L}_2} \frac{I_2^2 \mathscr{F}(\Delta)^2 \mathscr{F}(2\Delta) (\gamma/2)^3 (\mathscr{D}_1 + \mathscr{D}_2^*)(\mathscr{D}_0 + \mathscr{D}_3^*)^2}{\left[1 + I_2 \mathscr{F}(\Delta) \frac{\gamma}{2} (\mathscr{D}_1 + \mathscr{D}_3^*) \right]^2 \left[1 + I_2 \mathscr{F}(2\Delta) \frac{\gamma}{2} (\mathscr{D}_0 + \mathscr{D}_4^*) \right]}. \tag{4.47}$$

The propagation equation for $\mathscr{E}_1$, Eq. (4.45), can be expressed in terms of I_1 as

$$\frac{dI_1}{dz} = -\alpha_1 I_1 + \beta_1 I_1^2 + \text{c.c.} \tag{4.48}$$

In Sec. 4-2-3 we show that, in the classical limit, the fourth-order quantum theory reduces to Eq. (4.48).

4-2. Quantum Sidemode Saturation

4-2-1. Summary of the Second-Order Theory

Our Hamiltonian (in radians/second) is

$$\mathcal{H} = (\omega - \nu_2)\sigma_z + \sum_{j=1}^{2} [(\nu_j - \nu_2)a_j^\dagger a_j + (g a_j U_j \sigma^\dagger + \text{adjoint})] \,. \tag{4.49}$$

In this expression a_j is the annihilation operator for the jth field mode, $U_j = U_j(\mathbf{r})$ is the corresponding spatial mode factor, σ and σ_z are the atomic spin-flip and probability-difference operators, ω and ν_j are the atomic and field frequencies, and g is the atom-field coupling constant. As in the semiclassical theories, we take mode 2 to be arbitrarily intense, and treat it classically and undepleted. Mode 1 is a quantum field treated only to second order in amplitude, and cannot by itself saturate the atomic response. This is an important assumption and limits the applicability of the theory. The rotating-wave approximation has been made and the Hamiltonian is in an interaction picture rotating at the strong field frequency ν_2. We define an atom-field density operator ρ and obtain its time dependence from the standard density operator equation of motion

$$\dot{\rho} = -i[\mathcal{H}, \rho] + \text{relaxation processes} \,. \tag{4.50}$$

Sargent, Holm, and Zubairy (1985) carries out the calculations for a level scheme that allows for interactions between two excited states as well as for the usual situation in

laser spectroscopy for which the lower level is the ground state. In this section we restrict our calculations to the latter, which significantly simplifies our expressions. We assume the only relaxation processes are upper-to-lower level decay, described by the decay constant Γ ($=1/T_1$), and the dipole decay described by γ ($=1/T_2$). Our numerical examples consider pure spontaneous decay, for which γ is equal to $\Gamma/2$.

The two-level atom interacting with two fields involves at least four atom-field levels (i.e., $|1\rangle$, $|2\rangle$, $|4\rangle$, and $|5\rangle$ in Fig. 13). We assume all field amplitudes to vary little during atomic decay times. This allows us to solve the equations of motion of the density matix elements between the four levels in steady state, and then to obtain the the photon number probability equation up to g^2-order

$$\frac{dp_{n_1}}{dt} = -(n_1+1)[A_1 p_{n_1} - (B_1 + \nu/2Q_1)p_{n_1+1}] + n_1[A_1 p_{n_1-1} - (B_1 + \nu/2Q_1)p_{n_1}] + \text{c.c.}, \quad (4.51)$$

where Q_1 is the cavity quality for mode 1, and the coefficients A_1 and B_1 are given by

$$A_1 = \frac{g^2\mathscr{D}_1}{1+I_2\mathscr{L}_2}\left[\frac{I_2\mathscr{L}_2}{2} - \frac{I_2\mathscr{F}(\Delta)\frac{\gamma}{2}[\mathscr{D}_1 I_2\mathscr{L}_2/2 - \mathscr{D}_2^*(1+\Gamma/i\Delta)/2]}{1 + I_2\mathscr{F}(\Delta)\frac{\gamma}{2}(\mathscr{D}_1 + \mathscr{D}_3^*)}\right], \quad (4.52)$$

$$B_1 = \frac{g^2\mathscr{D}_1}{1+I_2\mathscr{L}_2}\left[1+\frac{I_2\mathscr{L}_2}{2} - \frac{I_2\mathscr{F}(\Delta)\frac{\gamma}{2}[\mathscr{D}_1(1+I_2\mathscr{L}_2/2) + \mathscr{D}_2^*(1-\Gamma/i\Delta)/2]}{1 + I_2\mathscr{F}(\Delta)\frac{\gamma}{2}(\mathscr{D}_1 + \mathscr{D}_3^*)}\right], \quad (4.53)$$

where $\Delta = \nu_2 - \nu_1$ is the beat frequency between modes one and two, the interaction energy $\mathscr{V}_2 = gU_2\sqrt{n_2+1}$, and the dimensionless intensity I_2, which is defined in Eq. (4.26), is given by

$$I_2 = 4|\mathcal{V}_2|^2 T_1 T_2 \,. \tag{4.54}$$

We are primarily interested in the build up of mode 1, which can be described by the average photon number $\langle n_1 \rangle = \Sigma_{n_1} n_1 p_{n_1}$. Using Eq. (4.51), we find the equation of motion

$$\begin{aligned}\frac{d}{dt}\langle n_1 \rangle &= -A_1(\langle n_1^2 \rangle + \langle n_1 \rangle) - (B_1 + \nu/2Q_1)\langle n_1^2 \rangle \\ &\quad + (B_1 + \nu/2Q_1)(\langle n_1^2 \rangle - \langle n_1 \rangle) + A_1(\langle n_1^2 \rangle + 2\langle n_1 \rangle + 1) + \text{c.c.} \\ &= (A_1 - B_1 - \nu/2Q_1)\langle n_1 \rangle + A_1 + \text{c.c.}\end{aligned} \tag{4.55}$$

This equation gives the time differential equation of motion for the average photon number in a cavity mode, where $B_1 - A_1$ is the complex absorption coefficient and A_1 is the source term from spontaneous emission. In free space, no build up of photon number occurs, and $d/dt\ \langle n_1 \rangle = A_1 + A_1^*$. Thus we interpret $A_1 + A_1^*$ as the spectum of resonance fluorescence, which was first obtained by Mollow (1969). The absorption coefficient $B_1 - A_1 + \text{c.c.}$ describes the absorption of a weak probe field in the presence of a strong field and was also first obtained by Mollow (1972). It is also worthwhile to note that the complex absorption coefficient $B_1 - A_1$ yields the exact semiclassical absorption coefficient α_1, Eq. (4.46), which was derived using a Fourier series method.

4-2-2. Derivation of the Fourth-Order Theory

In the second-order perturbation theory, the two-level atom interacting with two fields involves at least four atom-field levels. The fourth-order perturbation theory, however, requires at least eight atom-field levels as depicted in Fig. 13. To derive the sidemode photon number probability equation of motion, we need the density matrix elements between the eight levels in Fig. 13. The states depicted in Fig. 13 have been numerically labeled as shown for notational simplicity. For example ρ_{51} is equal to $\langle an_1n_2|\rho|bn_1+1\,n_2\rangle$. In the derivation we treat mode 2 classically and inevitably neglect the difference between n_2 and $n_2 \pm 1$. Hence the probability of finding n_1 photons in mode 1 is given by the trace

$$p_{n_1} = \rho_{55} + \rho_{11}\Big|_{n_1 \to n_1 - 1} . \tag{4.56}$$

The photon number probability equation of motion for mode 1 is given by the corresponding time derivative. Using the density operator equation of motion, Eq. (4.50), we find

$$\dot{\rho}_{55} = -\Gamma\rho_{55} - [i\mathcal{V}_1\rho_{15} + i\mathcal{V}_2\rho_{25} + \text{c.c.}] , \tag{4.57}$$

$$\dot{\rho}_{11} = \Gamma\rho_{55}|_{n_1 \to n_1+1} + [i\mathcal{V}_1\rho_{15} + i\mathcal{V}_2\rho_{14} + \text{c.c.}] , \tag{4.58}$$

where the interaction energy $\mathcal{V}_1$ for mode 1 is given by

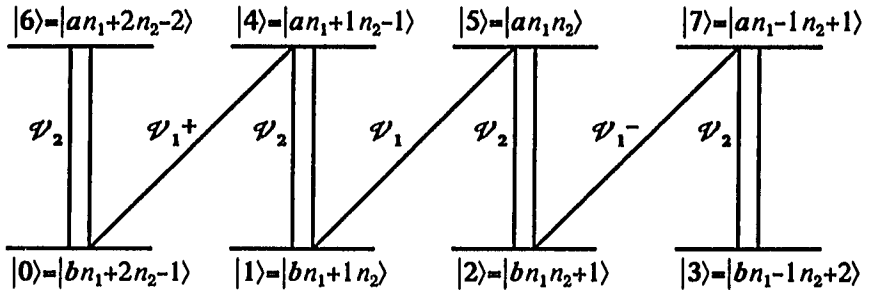

Fig. 13. Eight-level atom-field energy-level diagram.

$$\mathcal{V}_1 = gU_1\sqrt{n_1 + 1}\,, \tag{4.59}$$

and the interaction energy $\mathcal{V}_2$ for mode 2 is given by

$$\mathcal{V}_2 = gU_2\sqrt{n_2} \cong gU_2\sqrt{n_2 \pm 1}\,, \tag{4.60}$$

where we neglect the difference between n_2 and $n_2 \pm 1$, i.e., we treat the strong mode classically. Taking the time derivative of Eq. (4.56) and substituting Eqs. (4.57) and (4.58), we find the sidemode photon number probability equation of motion

$$\dot{p}_{n_1} = i\mathcal{V}_1^*\rho_{51} - i(\mathcal{V}_1^*\rho_{51})\Big|_{n_1 \to n_1 - 1} + \text{c.c.} \tag{4.61}$$

The problem thus reduces to finding ρ_{51}.

The first step to solve the problem is to expand the density matrix in a power series in g

$$\rho = \rho^{(0)} + \rho^{(1)} + \rho^{(2)} + \rho^{(3)} + \cdots , \tag{4.62}$$

where $\rho^{(n)}$ denotes the g^n-order term in the expansion of ρ. We assume that (ρ_{55}, ρ_{22}), $(\rho_{54}, \rho_{21}, \rho_{24})$, and $(\rho_{50}, \rho_{56}, \rho_{20}, \rho_{26})$ are given by the lowest order in g

$$(\rho_{55}, \rho_{22}) = (\rho_{55}^{(0)}, \rho_{22}^{(0)}) , \tag{4.63}$$

$$(\rho_{54}, \rho_{21}, \rho_{24}) = (\rho_{54}^{(1)}, \rho_{21}^{(1)}, \rho_{24}^{(1)}) , \tag{4.64}$$

$$(\rho_{50}, \rho_{56}, \rho_{20}, \rho_{26}) = (\rho_{50}^{(2)}, \rho_{56}^{(2)}, \rho_{20}^{(2)}, \rho_{26}^{(2)}) . \tag{4.65}$$

Moreover we assume that (ρ_{44}, ρ_{11}), $(\rho_{46}, \rho_{10}, \rho_{16})$, $(\rho_{75}, \rho_{32}, \rho_{35})$, and $(\rho_{71}, \rho_{74}, \rho_{31}, \rho_{34})$ are given by

$$(\rho_{44}, \rho_{11}) = (\rho_{55}^{(0)}, \rho_{22}^{(0)}) \Big|_{n_1 \to n_1+1} , \tag{4.66}$$

$$(\rho_{46}, \rho_{10}, \rho_{16}) = (\rho_{54}^{(1)}, \rho_{21}^{(1)}, \rho_{24}^{(1)}) \Big|_{n_1 \to n_1+1} , \tag{4.67}$$

$$(\rho_{75},\ \rho_{32},\ \rho_{35}) = (\rho_{54}^{(1)},\ \rho_{21}^{(1)},\ \rho_{24}^{(1)})\Big|_{n_1 \to n_1 - 1}\ , \tag{4.68}$$

$$(\rho_{71},\ \rho_{74},\ \rho_{31},\ \rho_{34}) = (\rho_{50}^{(2)},\ \rho_{56}^{(2)},\ \rho_{20}^{(2)},\ \rho_{26}^{(2)})\Big|_{n_1 \to n_1 - 1}\ . \tag{4.69}$$

We know from the second-order theory that $\rho_{55}^{(0)}$ and $\rho_{22}^{(0)}$ are given by

$$\rho_{55}^{(0)} = \frac{f_a}{1 + I_2\mathscr{L}_2} p_{n_1}\ , \tag{4.70}$$

$$\rho_{22}^{(0)} = \frac{f_b}{1 + I_2\mathscr{L}_2} p_{n_1}\ , \tag{4.71}$$

where $p_{n_1} \equiv \rho_{n_1 n_1}$ is the probability of n_1 photons and the probability factors f_a and f_b for the upper and lower levels, respectively, are given by

$$f_a = \frac{1}{2} I_2\mathscr{L}_2\ , \tag{4.72}$$

$$f_b = 1 + \frac{1}{2} I_2\mathscr{L}_2\ . \tag{4.73}$$

To find the dipole elements ρ_{52} and ρ_{41}, we write the the density matrix equations for ρ_{52} and ρ_{41}

$$\dot{\rho}_{52} = -(\gamma + i\Delta_2)\rho_{52} + i\mathscr{V}_2(\rho_{55} - \rho_{22}) + i\mathscr{V}_1^{*}\rho_{57} - i\mathscr{V}_1\rho_{12}\ , \tag{4.74}$$

$$\dot{\rho}_{41} = -(\gamma + i\Delta_2)\rho_{41} + i\mathscr{V}_2(\rho_{44} - \rho_{11}) + i\mathscr{V}_1^{*}\rho_{57} - i\mathscr{V}_1\rho_{12}\ , \tag{4.75}$$

where

$$\mathcal{V}_1^{\pm} = \mathcal{V}_1\Big|_{n_1 \to n_1 \pm 1} . \tag{4.76}$$

Using Eqs. (4.63), (4.64), (4.70), and (4.71), the steady state solutions to Eqs. (4.74) and (4.75) are given by

$$\begin{aligned}\rho_{52} &= i\mathcal{V}_2\mathcal{D}_2 \frac{f_a - f_b}{1 + I_2\mathcal{L}_2} p_{n_1} + i\mathcal{D}_2(\mathcal{V}_1^{-}\rho_{57}^{(1)} - \mathcal{V}_1\rho_{12}^{(1)}) \\ &= \rho_{52}^{(0)} + \rho_{52}^{(2)} ,\end{aligned} \tag{4.77}$$

$$\begin{aligned}\rho_{41} &= i\mathcal{V}_2\mathcal{D}_2 \frac{f_a - f_b}{1 + I_2\mathcal{L}_2} p_{n_1+1} + i\mathcal{D}_2(\mathcal{V}_1\rho_{45}^{(1)} - \mathcal{V}_1^{+}\rho_{01}^{(1)}) \\ &= \rho_{41}^{(0)} + \rho_{41}^{(2)} .\end{aligned} \tag{4.78}$$

The full equations of motion for the density matrix element between the eight levels are then reduced to the equations of motion of two sets, (ρ_{50}, ρ_{56}, ρ_{20}, ρ_{26}) and (ρ_{51}, ρ_{54}, ρ_{21}, ρ_{24}). The detailed derivation of the equations of motion and the steady state solutions of the equations are given in Appendix.

After finding the dipole element ρ_{51} up to g^3-order

$$\rho_{51} = \rho_{51}^{(1)} + \rho_{51}^{(3)} , \tag{4.79}$$

and substituting Eq. (4.79) into Eq. (4.61), we obtain the photon number probability equation up to g^4-order

$$\frac{dp_{n_1}}{dt} = -(n_1+1)\,[\,-q_0 n_1 p_{n_1-1} + \{\,A_1 - [r_0 n_1 + r_1(n_1+1) + r_2(n_1+2)]\,\}p_{n_1}$$
$$+ \{\,-B_1 - \nu/2Q_1 - [s_0 n_1 + s_1(n_1+1) + s_2(n_1+2)]\,\}p_{n_1+1} - t_2(n_1+2)p_{n_1+2}\,]$$
$$+ (\text{same with } n_1 \text{ replaced by } n_1\text{-}1) + \text{c.c.}\,, \qquad (4.80)$$

where the g^2-order coefficients A_1 and B_1 are given by Eqs. (4.52) and (4.53), and the g^4-order coefficients q_0, r_0, r_1, r_2, s_0, s_1, s_2, and t_2 are given by Eqs. (*A.28*) through (*A.35*) in Appendix. The average photon number rate equation is

$$\frac{d}{dt}\langle n_1\rangle = H_1\langle n_1^2\rangle + (A_1 - B_1 - \nu/2Q_1 + G_1)\langle n_1\rangle + (A_1 + F_1) + \text{c.c.}\,, \qquad (4.81)$$

where the fourth-order coefficients H_1, G_1, and F_1 are given by

$$H_1 = -(q_0 + r_0 + r_1 + r_2 + s_0 + s_1 + s_2 + t_2)\,, \qquad (4.82)$$

$$G_1 = -(3q_0 + r_0 + 2r_1 + 3r_2 - s_0 + s_2 - t_2)\,, \qquad (4.83)$$

$$F_1 = -(2q_0 + r_1 + 2r_2)\,. \qquad (4.84)$$

It is useful to define the dimensionless coefficients H_1', G_1', and F_1' as

$$H_1' \equiv \frac{H_1}{4g^4T_1T_2^2}\,,\ G_1' \equiv \frac{G_1}{4g^4T_1T_2^2}\,,\ \text{and}\ F_1' \equiv \frac{F_1}{4g^4T_1T_2^2}\,. \qquad (4.85)$$

Figure 14 plots the coefficient $H' \equiv H_1' + H_1'^*$ versus pump/probe beat frequency Δ for $T_2 = 2T_1$ and $I_2 = 50$ (or $\Omega \equiv$ Rabi frequency $= 5$). The spectrum shows fast changes from the negative to positive peaks near the Rabi side bands. Figures 15 and

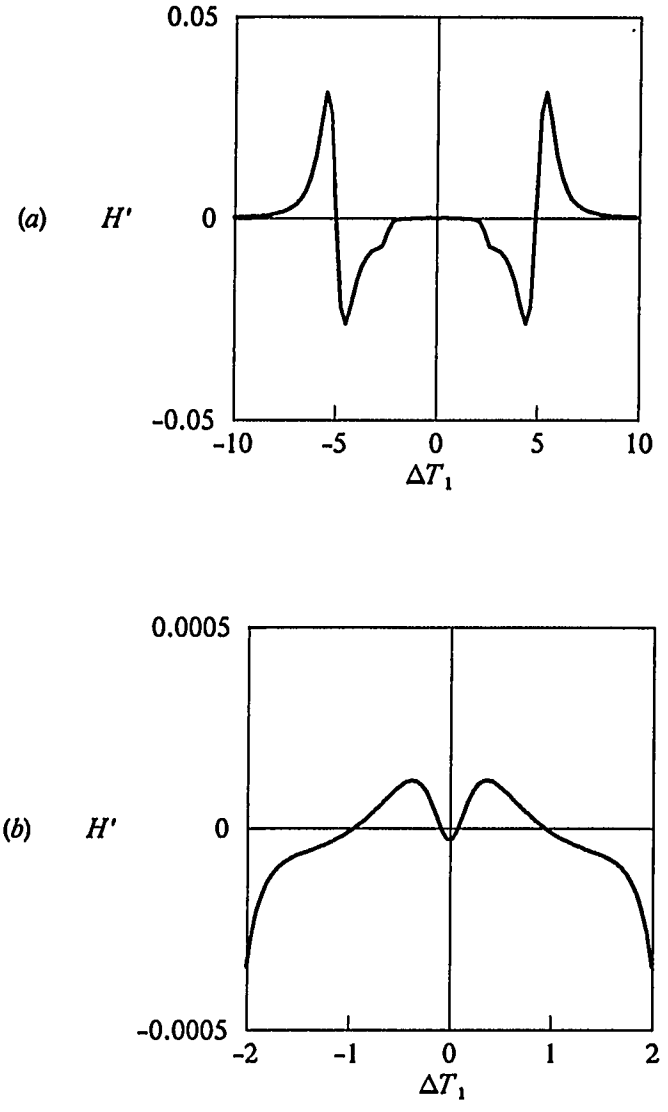

Fig. 14. (*a*) and (*b*) H' versus ΔT_1 for $T_2 = 2T_1$ and $I_2 = 50$.

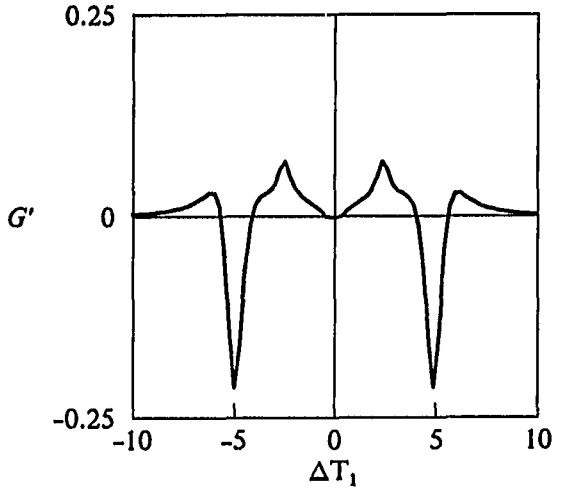

Fig. 15. G' versus ΔT_1. Same parameters as in Fig. 14.

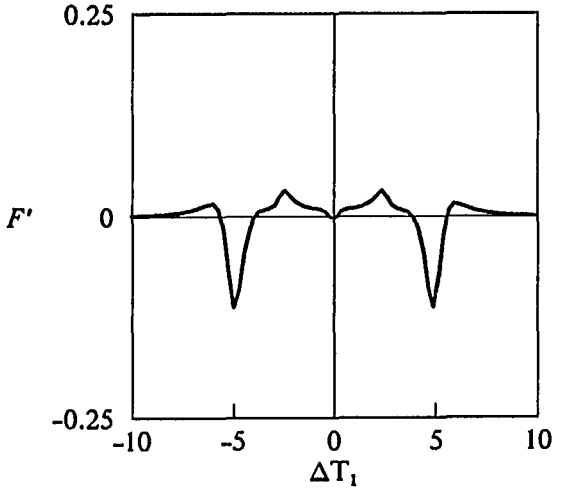

Fig. 16. F' versus ΔT_1. Same parameters as in Fig. 14.

16 plot the coefficients $G' \equiv G_1' + G_1'^*$ and $F' \equiv F_1' + F_1'^*$ versus Δ, respectively, for the same parameters as in Fig. 12. We notice that both G and F have small positive peaks at $\Delta = \Omega/2$, as well as the main negative peaks at $\Delta = \Omega$. We show in Sec. 4-3-2 that these small peaks also influence the photon number spectra.

4-2-3. Reduction to the Semiclassical Theory

We first define the renormalized photon number n_1' as

$$n_1' \equiv (4g^2T_1T_2)n_1 \ . \tag{4.86}$$

Then, in the classical limit where $\langle n_1 \rangle \gg 1$, the average renormalized photon number reduces to the classical dimensionless intensity, i.e.,

$$\langle n_1' \rangle = I_1 \ . \tag{4.87}$$

The photon number rate equation, Eq. (4.81), is expressed in terms of $\langle n_1' \rangle$ as

$$\frac{d}{dt}\langle n_1' \rangle = H_1'' \langle n_1'^2 \rangle + (A_1 - B_1 - v/Q_1 + G_1'') \langle n_1' \rangle + (A_1 + F_1'') + \text{c.c.} \ , \tag{4.88}$$

where H_1'', G_1'', and F_1'' are defined as

$$H_1'' = \frac{H_1}{4g^2T_1T_2} \ , \ G_1'' = \frac{G_1}{4g^2T_1T_2} \ , \text{ and } F_1'' = \frac{F_1}{4g^2T_1T_2} \ , \tag{4.89}$$

In the classical limit, we can neglect, in Eq. (4.88), the constant term $A_1 + F_1''$ compared to terms with $\langle n_1' \rangle$ and $\langle n_1'^2 \rangle$, and G_1'' compared to $A_1 - B_1$. Futhermore, in this limit, we have (Sargent, Scully, and Lamb 1970)

$$\langle n_1'^2 \rangle \cong \langle n_1' \rangle^2 . \tag{4.90}$$

Hence, Eq. (4.88) reduces to

$$\frac{d}{dt}\langle n_1' \rangle = H_1''\langle n_1' \rangle^2 + (A_1 - B_1 - \nu/Q_1)\langle n_1' \rangle + \text{c.c.} . \tag{4.91}$$

We note that letting $z = ct$, Eq. (4.91) has the same form as Eq. (4.48), except for the cavity factor ν/Q_1, with $\langle n_1' \rangle$ related to I_1 by Eq. (4.87). Therefore we expect the coefficients $B_1 - A_1$ and H_1'' of Eq. (4.91) to be equal to α_1 and β_1 of Eq. (4.48).

From the result of the second-order quantum theory (see Sec. 4-2-1), we already know that $B_1 - A_1$ is equal to α_1. To prove that H_1'' is equal to β_1, we have added all the coefficients given by Eqs. (4.37) through (4.44). With a considerable amount of algebra, we find that the result simplifies to

$$\begin{aligned} H_1'' = &-\frac{1}{4}g^2\Gamma\gamma\mathscr{D}_1 d_0 \frac{(i\Delta)^2 4|\mathscr{V}_2|^2(\mathscr{D}_1 + \mathscr{D}_2^*)(\mathscr{D}_0 + \mathscr{D}_2^*)}{[\mathscr{D}_1\mathscr{D}_3^* N(\Delta)]^2} \\ &+ \frac{1}{4}g^2\Gamma\gamma\mathscr{D}_1 d_0 \frac{(i\Delta)^3 16|\mathscr{V}_2|^4(\mathscr{D}_1 + \mathscr{D}_2^*)(\mathscr{D}_0 + \mathscr{D}_3^*)^2}{[\mathscr{D}_1\mathscr{D}_3^* N(\Delta)]^2[\mathscr{D}_0\mathscr{D}_4^* N(2\Delta)]} , \end{aligned} \tag{4.92}$$

where $N(\Delta)$ and $N(2\Delta)$, which are defined by Eqs. (*A.23*) and (*A.28*), can be expressed as

$$N(\Delta) = \frac{i\Delta}{\mathscr{D}_1\mathscr{D}_3^*}\frac{\Gamma}{\mathscr{F}(\Delta)}\left[1 + I_2\mathscr{F}(\Delta)\frac{\gamma}{2}(\mathscr{D}_1 + \mathscr{D}_3^*)\right], \tag{4.93}$$

$$N(2\Delta) = \frac{i2\Delta}{\mathscr{D}_0\mathscr{D}_4^*}\frac{\Gamma}{\mathscr{F}(2\Delta)}\left[1 + I_2\mathscr{F}(2\Delta)\frac{\gamma}{2}(\mathscr{D}_0 + \mathscr{D}_4^*)\right]. \tag{4.94}$$

Substituting Eqs. (4.93) and (4.94) into Eq. (4.92) and using the relation $g^2 = \alpha_0\gamma$ (see Eq. (4.96)), we finally find that Eq. (4.92) becomes exactly equal to Eq. (4.47). Note that H'' is negative at $\Delta = 0$ (see Fig. 14(*b*)), as discussed in Sec. 4-1-2.

4-3. Effects of Cavities on the Photon Number Spectrum

4-3-1. Second-Order Theory

In this section we consider the experimental situation shown in Fig. 1 of Holm, Sargent, and Stenholm (1985). An atomic beam passes through a high-finesse Fabry-Perot cavity and is irradiated perpendicularly (or at a substantial angle) by an intense laser field. The fluorescent emission selected by a cavity mode frequency is then measured by an external detector. This is essentially the configuration used in the experiment of Hartig, Rasmussen, Schieder, and Walther (1976). Note that the cavity mode separation must be larger compared to the overall width of the resonance fluorescence spectrum. When the emission takes place in a cavity, the photon number $\langle n_1 \rangle$ increases until a steady state occurs. Using Eq. (4.55) we solve for the steady-state value

$$\langle n_1 \rangle = \frac{A}{\nu/Q_1 - (A - B)} \equiv \langle n_{10} \rangle \ , \tag{4.95}$$

where $A \equiv A_1 + A_1^*$ and $B \equiv B_1 + B_1^*$. In the limit $\nu/Q_1 \gg B - A$, corresponding to a poor cavity, Eq. (4.95) simplifies to become $\langle n_1 \rangle = Q_1 A/\nu$, and we recover the free-space expression for the spectrum. Note that we are now defining the spectrum to be given by $\langle n_1 \rangle$ as a function of $\nu_2 - \nu_1$, where ν_1 is given by a cavity resonance. This is consistent with other quantum mechanical definitions of the spectrum. For further discussion see the review paper by Cresser (1983). When ν/Q_1 and $A - B$ become comparable (near sidemode laser threshold), however, the spectrum is altered appreciably.

$(B - A)\langle n_1 \rangle$ is the number of absorptions/second of the mode 1 and $(\nu/Q_1)\langle n_1 \rangle$ is the cavity loss rate of mode 1. The absorption rate depends upon the such quantities as the atomic number density, the dipole matrix element between levels a and b, and the pump mode intensity I_2. It is well known that this absorption can go negative, giving gain. The cavity loss rate depends upon many factors, such as diffraction effects, mirror reflectivity, and nonsaturable absorptions. To uniformly relate these two quantities we define α_0 as the value of the mode 1 absorption when the strong field intensity I_2 is zero and when $\omega = \nu_1$, i.e., the unsaturated centrally tuned absorption rate:

$$\alpha_0 = (B - A)\big|_{I_2=0,\nu_1=\omega} = \frac{g^2}{\gamma} \ . \tag{4.96}$$

The coefficients A_1 and B_1 can all be expressed in terms of this quantity. We define the coefficients A_1' and B_1' as

$$A_1' = \frac{A_1}{\alpha_0} \text{ and } B_1' = \frac{B_1}{\alpha_0} . \tag{4.97}$$

These quantities are the dimensionless magnitudes of A_1 and B_1 in units of the unsaturated resonant absorption coefficient. We also define the parameter β as the ratio of the cavity loss rate to α_0:

$$\beta = \frac{\nu/Q_1}{\alpha_0} . \tag{4.98}$$

Equation (4.95) can then be expressed as

$$\langle n_{10} \rangle = \frac{A'}{\beta + (B'-A')} . \tag{4.99}$$

We now investigate how the scattered spectrum, given by Eq. (4.99), depends upon β. Since we are interested in how the shape of the spectrum changes, we multiply Eq. (4.99) by β to normalize our results. The limit $\beta \to \infty$ then recovers the free space answer. Figure 17 shows the spectrum of $I_2 = 50$ (corresponding to a Rabi flopping frequency of 5Γ) for $\beta = 1.0$, 0.1, and 0.05. It can be seen that as β decreases (cavity finesse increases), the sidebands increase in size, become somewhat sharper, and move slightly toward line center relative to the free space case. On the other hand, the central peak remains unchanged. As β decreases further, the sideband intensities continue to increase to infinity. At this point (the threshold for sidemode lasing), the denominator of Eq. (4.99) is zero and our linear theory has broken down. To obtain the spectrum in this case it is necessary to include saturation of the sidemode in the theory. Because this theory neglects this, β must not be allowed to come too close to $A'-B'$. This saturation problem does not occur in the semiclassical theory, since the

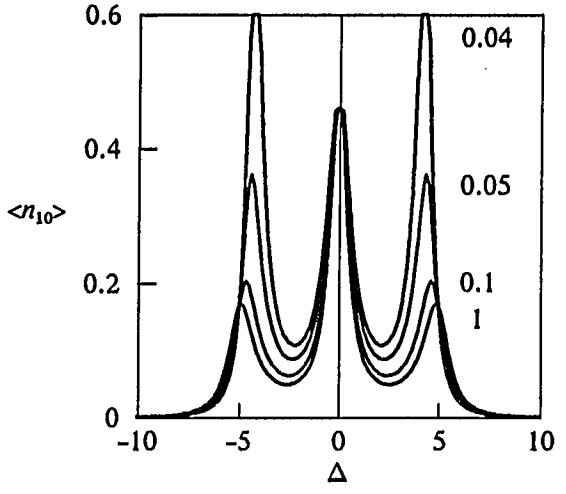

Fig. 17. The spectrum of $\langle n_{10} \rangle$ given by Eq. (4.99) versus ΔT_1 for $\beta = 1.0$, 0.1, 0.05, and 0.04. $T_2 = 2T_1$ and $I_2 = 50$.

cavity modes are below threshold. In a quantum field theory, such as Scully-Lamb (1967), saturation is important just below as well as above threshold.

4-3-2. Fourth-Order Theory

If we neglect intensity-intensity correlations $\langle a_1^\dagger a_1 a_1^\dagger a_1 \rangle \cong \langle a_1^\dagger a_1 \rangle \langle a_1^\dagger a_1 \rangle$, i.e., $\langle n_1^2 \rangle \cong \langle n_1 \rangle^2$, then the photon number rate equation, Eq. (4.81) becomes in the steady-state

$$H\langle n_1 \rangle^2 + (A - B - \nu/Q_1 + G)\langle n_1 \rangle + (A + F) = 0 , \tag{4.100}$$

where $H = H_1 + H_1^*$, $G = G_1 + G_1^*$, and $F = F_1 + F_1^*$. The solution of Eq. (4.100) is

$$\langle n_1 \rangle = \frac{1}{2H} \left\{ (B + \nu/Q_1 - A - G) \pm (B + \nu/Q_1 - A - G) \sqrt{1 - \frac{4H\,(A + F)}{(B + \nu/Q_1 - A - G)^2}} \right\} \quad (4.101)$$

Since the fourth-order coefficients H, G, and F are much less than the second order coefficients A and F in magnitude, we can expand the solution as power series up to second order in g

$$\langle n_1 \rangle = \frac{A}{\nu/Q_1 + (B - A)} + \frac{F}{\nu/Q_1 + (B - A)} + \frac{A}{\nu/Q_1 + (B - A)} \frac{G}{\nu/Q_1 + (B - A)} + \left[\frac{A}{\nu/Q_1 + (B - A)} \right]^2 \frac{H}{\nu/Q_1 + (B - A)} , \quad (4.102)$$

where we choose (-) sign from (±) in Eq. (4.101) to recover the second-order theory, i.e., the first term in Eq. (4.102). Similarly to Eq. (4.99), Eq. (4.102) can be expressed in terms of dimensionless coefficients as

$$\begin{aligned} \langle n_1 \rangle &= \langle n_{10} \rangle + \frac{4\alpha}{\beta + (B' - A')} [F' + \langle n_{10} \rangle G' + \langle n_{10} \rangle^2 H'] \\ &\equiv \langle n_{10} \rangle + \langle \delta n_1 \rangle , \end{aligned} \quad (4.103)$$

where $H' \equiv H_1' + H_1'^*$, $G' \equiv G_1' + G_1'^*$, $F' \equiv F_1' + F_1'^*$, $\langle n_{10} \rangle$ is defined in Eqs. (4.95) and (4.99), and $\langle \delta n_1 \rangle$ is the higher order correction term of $\langle n_1 \rangle$. The dimensionless parameter α in Eq. (4.103) is defined as

$$\alpha \equiv g^2 T_1 T_2 = \alpha_0 T_1 . \quad (4.104)$$

Note that the dimensionless coefficients H_1', G_1', and F_1' defined in Eq. (4.85) are related to H_1'', G_1'', and F_1'' defined in Eq. (4.89) by

$$H_1' = \frac{H_1''}{\alpha_0}, \; G_1' = \frac{G_1''}{\alpha_0}, \text{ and } F_1' = \frac{F_1''}{\alpha_0}. \tag{4.105}$$

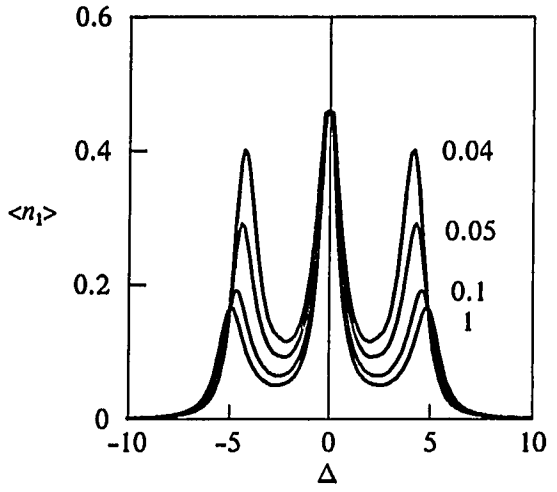

Fig. 18. The spectrum of $\langle n_1 \rangle$ given by Eq. (4.103) for $\alpha = 0.01$. Other parameters are the same as in Fig. 17.

Figure 18 plots the spectrum of $\langle n_1 \rangle$ given by Eq. (4.103) for $\alpha = 0.01$. Compared to the second-order theory, Fig. 17, we see that the sideband peaks do not diverge, even when β decreases to 0.05. In Fig. 19, we increase α to 0.05. We find that the sideband peaks converge faster than the case of $\alpha = 0.01$. Futhermore, we notice that the secondary sideband peaks grow at $\Delta = \Omega/2$, as we have mentioned in Sec. 4-3-2.

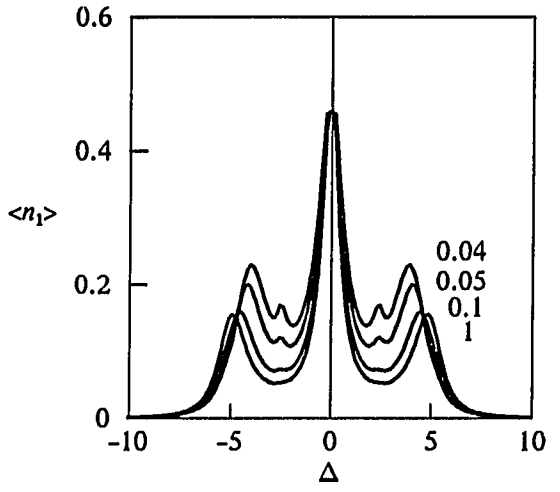

Fig. 19. The spectrum of $\langle n_1 \rangle$ given by Eq. (4.103) for $\alpha = 0.05$. Other parameters are the same as in Fig. 17.

In this chapter we have studied the effects of sidemode saturation on the two-wave mixing both semiclassically and quantum mechanically. The degenerate semiclassical theory shows that the third-order semiclassical sidemode absorption contribution have the same sign as the probe absorption coefficient, which has just the opposite effect from the usual saturation. We have derived explicit formulas for the fourth-order quantum coefficients. The results are much more complicated than the corresponding semiclassical case, but reduce to it in the appropriate limit. We have applied the results to cavity problems. We find that the sidemode fluorescence spectra do not diverge even near the sidemode laser threshold. Futhermore we notice that the secondary sideband peaks grow at $\Delta = \Omega/2$. This problem is important for the study of optical instabilities, but unfortunately is very complicated. Even extending the fourth-order theory to the two sidemode case, e.g., for three- and four-wave mixing, seems to be prohibitively difficult.

CHAPTER 5
QUANTUM MULTIWAVE MIXING IN TWO-PHOTON THREE-LEVEL MEDIA

Squeezed states of light are those for which the quantum fluctuations in one quadrature phase of the electric field are reduced below the average minimum variance permitted by the uncertainty principle. Such states have potential applications in optical communication systems and gravity-wave detection. Due to the dependence of squeezing on the phase of the electric field, squeezed states have been predicted to occur in phase sensitive nonlinear optical processes, such as parametric amplification, second harmonic generation, and four-wave mixing. The first successful generation of squeezed states has been reported by Slusher *et al.* (1985). using nondegenerate four-wave mixing. Recently other groups (Shelby *et al.* 1985, Maeda *et al.* 1987, and Wu *et al.* 1986) have also succeeded in producing squeezed states using different types of nonlinear media.

Previously Sargent, Holm, and Zubiary (1985) have derived a theory describing quantum multiwave interactions in a nonlinear one-photon two-level medium, in which the levels are connected by an electric dipole. Later they have applied this theory to analyze the generation of squeezed states and compared to the experimental results of Slusher *et al.* finding reasonably good agreement (Holm and Sargent 1987). The first nondegenerate semiclassical theory of multiwave mixing in a two-photon two-level medium has been given by Sargent, Ovadia, and Lu (1985). The quantum theory of multiwave mixing in such a medium has been derived in detail by Holm and Sargent (1986*a*). Recently Capron, Holm, and Sargent (1987) have applied the quantum theory

of multiwave mixing for the two-photon two-level model to the generation of squeezed states of light.

In this chapter we extend the quantum theory of multiwave mixing by Holm and Sargent to treat squeezing in a three-level cascade model with a classical two-photon pump at frequency ν_2 and a cascade of two one-photon transitions at frequencies ν_1 and ν_3 (see Fig. 20). The preliminary result was presented in a letter (An and Sargent 1988*a*). The model differs from those studied by Savage and Walls (1986), for which all field frequencies are identical.

The experimental observation of the suppression of amplified spontaneous emission by the four-wave mixing process in this model has been reported by Malcuit, Gauthier, and Boyd (1985). This experiment has been interpreted by Boyd *et al.* (1987) using classical fields up to fourth order in all mode interactions, while we treat a classical pump to all orders and quantized squeezed modes to first order. They also make the one-photon rotating wave approximation for the two-photon pump and neglects the population in the intermediate level, while we include the terms dropped in these approximations. Agarwal (1986) studied this model using a weak classical two-photon pump and weak quantized sidemode fields. He showed the generation of squeezed states, but simplified his treatment along the lines of Malcuit, Gauthier, Boyd (1985) by neglecting dynamic Stark shifts and the population in the intermediate level. In contrast our treatment allows for more general tuning conditions and nonzero intermediate level population as created by the potentially strong pump field in conjuction with level decays.

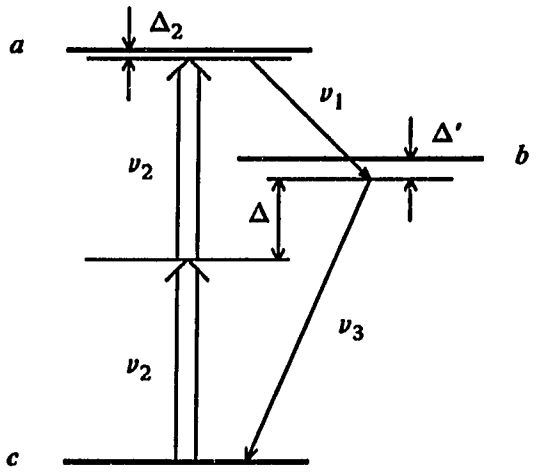

Fig. 20. The three-level cascade model with a two-photon pump.

The two-photon three-level model is shown in Fig. 20. The upper level a and ground level c have the same parity, but the intermediate level b has an opposite one. Therefore the transitions $a \leftrightarrow b$ and $b \leftrightarrow c$ are dipole allowed with frequencies ν_1 and ν_3 respectively, whereas the transition $c \leftrightarrow a$ requires two pump photons with the frequency ν_2. We assume that the one-photon pump detuning $\omega_{bc} - \nu_2$ is sufficiently large that the dipole transition $c \leftrightarrow b$ with pump frequency ν_2 is negligible. The pump frequency ν_2 is approximately one-half the atomic resonance frequency $\omega_{ac} \equiv \omega_a - \omega_c$. The sidemode frequencies ν_1 and ν_3 are assumed to satisfy the conservation condition $\nu_1 + \nu_3 = 2\nu_2$, which gives the relation between the sidemode detuning Δ' and the beat frequency $\Delta \equiv \nu_2 - \nu_1$ as $\Delta' = (\omega_{bc}-\nu_2) - \Delta$. We assume that the upper level a decays at the rate Γ_a $(= \Gamma_1 + \Gamma_2)$ to the lower levels b and c. Here Γ_1 and Γ_3 are the decay constants for the $a \rightarrow b$ and $b \rightarrow c$ transitions, and Γ_2 allows for nonradiative decay of level a to level c.

Section 5-1 summarizes the basic theory of semiclassical single-mode interation. In Section 5-2 we use the results of Section 5-1 to develop the theory of quantum sidemode interactions. Section 5-3 applies the theory to the generation of squeezed states of light.

5-1. Semiclassical Single-Mode Interaction

In this section we consider the single-mode case and derive the steady state semiclassical population matrix elements with the population difference decay time T_1. In an interaction picture rotating at the two-photon frequency $2\nu_2$, the equation of motion for the population matrix elements are given by

$$\dot{\rho}_{aa} = -(\Gamma_2 + \Gamma_1)\rho_{aa} - [i\mathcal{V}_2\rho_{ca} + \text{c.c.}] \tag{5.1}$$

$$\dot{\rho}_{cc} = \Gamma_2\rho_{aa} + \Gamma_3\rho_{bb} + [i\mathcal{V}_2\rho_{ca} + \text{c.c.}] \tag{5.2}$$

$$\dot{\rho}_{bb} = \Gamma_1\rho_{aa} - \Gamma_3\rho_{bb} \tag{5.3}$$

$$\dot{\rho}_{ac} = -[\gamma_2 + i(\omega_{ac} + \omega_s I_2 - 2\nu_2)]\rho_{ac} + i\mathcal{V}_2(\rho_{aa} - \rho_{cc}) , \tag{5.4}$$

where $\gamma_2 \equiv 1/T_2$ is the two-photon coherent decay rate between levels a and c, ω_s is the Stark shift parameter, $\mathcal{V}_2 \equiv -k_{ac}\mathcal{E}_2^2/2$ is the effective two photon interaction energy with the two-photon coefficient k_{ac} (Sargent, Ovadia, and Lu 1985; Holm and Sargent 1986*a*), and the two-photon dimensionless intensity I_2 is defined by

$$I_2 = 2|\mathcal{V}_2|\sqrt{T_1T_2} . \tag{5.5}$$

Using Eqs. (5.1) and (5.2) with the steady state solution of Eq. (5.3)

$$\rho_{cc} = (\Gamma_1/\Gamma_3)\rho_{aa} \ , \tag{5.6}$$

we find the equation of motion for the population difference $D = \rho_{aa} - \rho_{cc}$

$$\dot{D} = -2\Gamma_a\rho_{aa} - 2(i\mathcal{V}_2\rho_{ca} + \text{c.c.}) \ , \tag{5.7}$$

where $\Gamma_a = \Gamma_2 + \Gamma_1$. Combining Eq. (5.6) and the trace condition

$$\rho_{aa} + \rho_{bb} + \rho_{cc} = 1 \ , \tag{5.8}$$

we have

$$\rho_{aa} = \frac{\Gamma_3}{\Gamma_1 + 2\Gamma_3}(D + 1) \ . \tag{5.9}$$

Substituting Eq. (5.9) into (5.7), we have

$$\dot{D} = -(D + 1)/T_1 - 2(i\mathcal{V}_2\rho_{ca} + \text{c.c.}) \ , \tag{5.10}$$

where the population difference decay time T_1 is given by

$$T_1 = \frac{1}{\Gamma_a}\left[1 + \frac{\Gamma_1}{2\Gamma_3}\right] . \tag{5.11}$$

The steady-state solution to the dipole equation (5.4) is

$$\rho_{ac} = i\mathcal{V}_2\mathcal{D}_2(\Delta_2)D \ , \tag{5.12}$$

where $\Delta_2 \equiv \omega_{ac} + \omega_s I_2 - 2\nu_2$ is the pump field detuning as shown in Fig. 20 and the the complex Lorentzian denominator

$$\mathcal{D}_2(\Delta_2) = \frac{1}{\gamma_2 + i\Delta_2} \ . \tag{5.13}$$

Substituting Eq. (5.12) into (5.10), we have

$$\dot{D} = -(D + 1)/T_1 - 2RD \ , \tag{5.14}$$

where the rate constant

$$R = I_2^2\mathcal{L}_2(\Delta_2)/2T_1 \ , \tag{5.15}$$

and the dimensionless Lorentzian

$$\mathcal{L}_2(\Delta_2) = \frac{\gamma_2^2}{\gamma_2^2 + \Delta_2^2} \ . \tag{5.16}$$

Solving Eq. (5.14) in steady-state, we find

$$D = \rho_{aa} - \rho_{cc} = \frac{-1}{1 + I_2^2\mathcal{L}_2} \ . \tag{5.17}$$

Finally, using Eqs. (5.6), (5.8), and (5.17), we have

$$\rho_{kk} = \frac{f_k}{1 + I_2^2 \mathscr{L}_2} , \tag{5.18}$$

where $k = a, b, c$, and the probability factors f_k's are given by

$$f_a = \frac{\Gamma_3}{\Gamma_1 + 2\Gamma_3} I_2^2 \mathscr{L}_2 , \tag{5.19}$$

$$f_b = \frac{\Gamma_1}{\Gamma_1 + 2\Gamma_3} I_2^2 \mathscr{L}_2 , \tag{5.20}$$

$$f_c = 1 + f_a . \tag{5.21}$$

The assumptions and method used to obtain Eqs. (5.18) - (5.21) are again employed in the next section when the quantum-mechanical model is introduced, and we frequently refer to these results.

5-2. Quantum Sidemode Interactions

The total Hamiltonian $\mathscr{H}$ consists of three parts, the atom, the field, and the interaction:

$$\mathscr{H} = \mathscr{H}_{atom} + \mathscr{H}_{field} + \mathscr{H}_{int} . \tag{5.22}$$

The atom Hamiltonian is given by

$$\mathcal{H}_{atom} = \begin{bmatrix} \omega_a & 0 & 0 \\ 0 & \omega_b & 0 \\ 0 & 0 & \omega_c \end{bmatrix} . \tag{5.23}$$

The field Hamiltonian is

$$\mathcal{H}_{field} = \sum_{j=1}^{3} \nu_j a_j^\dagger a_j , \tag{5.24}$$

and the interaction Hamiltonian is

$$\mathcal{H}_{int} = \sum_{j} g_j a_j U_j \sigma_j^\dagger , \tag{5.25}$$

where a_1 and a_3 are the annihilation operators for the field modes 1 and 3, a_2 is the effective two-photon annihilation operator for the field mode 2, $U_j = U_j(\mathbf{r})$ is the spatial mode factor for the *jth* field mode, g_j is the atom-field (*jth*) coupling constant, and the matrices $\sigma_1^\dagger$, $\sigma_2^\dagger$, and $\sigma_3^\dagger$ are defined by

$$\sigma_1^\dagger = \begin{bmatrix} 0 & 1 & 0 \\ 0 & 0 & 0 \\ 0 & 0 & 0 \end{bmatrix} , \sigma_2^\dagger = \begin{bmatrix} 0 & 0 & 1 \\ 0 & 0 & 0 \\ 0 & 0 & 0 \end{bmatrix} , \sigma_3^\dagger = \begin{bmatrix} 0 & 0 & 0 \\ 0 & 0 & 1 \\ 0 & 0 & 0 \end{bmatrix} . \tag{5.26}$$

We take mode 2 (two-photon pump field) to be classical, undepleted, and arbitrarily intense. Modes 1 and 3 are sidemode quantum fields treated only to second order in amplitude and cannot by themselves saturate the atomic response. The three-level atom interacting with one strong and two weak field modes involves at least five

atom-field levels as shown in Fig. 21. We define an atom-field density operator $\rho_{a\text{-}f}$ and calculate the reduced electric field density operator ρ that describes the time dependence of the two quantized fields by taking the trace of $\rho_{a\text{-}f}$ over the atomic states. The states depicted in Fig. 21 have been numerically labeled for notational simplicity. For example, ρ_{53} is equal to $\langle an_1n_2n_3|\rho_{a\text{-}f}|bn_1{+}1\,n_2n_3\rangle$.

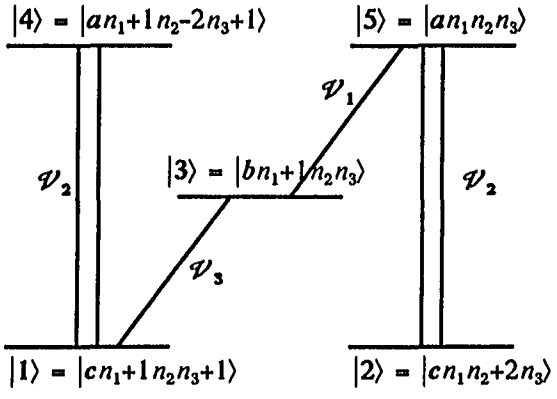

Fig. 21. Five-level atom-field energy-level diagram.

The probability of finding n_1 and n_3 photons in mode 1 and 3 is given by the trace

$$p_{n_1,n_3} = \langle n_1n_3|\rho|n_1n_3\rangle$$
$$= \rho_{55} + \rho_{33}|_{n_1\to n_1-1} + \rho_{11}|_{n_{1,3}\to n_{1,3}-1} \cdot \qquad (5.27)$$

The photon rate equation for mode 1 and 3 is given by the corresponding time derivative. To find $\dot{\rho}_{55}$, $\dot{\rho}_{33}$, and $\dot{\rho}_{11}$ and the density matrix elements coupling to them, we use the basic equation

$$\dot{\rho}_{a\text{-}f} = -i[\mathcal{H}, \rho_{a\text{-}f}] + \text{relaxation terms} \tag{5.28}$$

with the Hamiltonian given by Eq. (5.22). We have

$$\dot{\rho}_{55} = -(\Gamma_2 + \Gamma_1)\rho_{55} - [i\mathcal{V}_2\rho_{25} + i\mathcal{V}_1\rho_{35} + \text{c.c.}] , \tag{5.29}$$

$$\dot{\rho}_{33} = \Gamma_1\rho_{55}|_{n_1\to n_1+1} - \Gamma_3\rho_{33} - [i\mathcal{V}_1^*\rho_{53} + i\mathcal{V}_3\rho_{13} + \text{c.c.}] , \tag{5.30}$$

$$\dot{\rho}_{11} = \Gamma_2\rho_{44} + \Gamma_3\rho_{33}|_{n_3\to n_3+1} - [i\mathcal{V}_3^*\rho_{31} + i\mathcal{V}_2^*\rho_{41} + \text{c.c.}] , \tag{5.31}$$

where the one-photon interaction energies $\mathcal{V}_1$ and $\mathcal{V}_3$ are given by

$$\mathcal{V}_1 = g_1U_1\sqrt{n_1 + 1} , \mathcal{V}_3 = g_3U_3\sqrt{n_3 + 1} , \tag{5.32}$$

and the effective two-photon interaction energy $\mathcal{V}_2$ is

$$\mathcal{V}_2 = g_2U_2\sqrt{n_2} \cong -k_{ac}\mathcal{E}_2^2/2 , \tag{5.33}$$

where we neglect the difference between n_2 and n_2+1, i.e., we treat the strong mode classically.

Taking the time derivative of Eq. (5.27) and substituting Eqs. (5.29) - (5.31), we find the photon number equation of motion for the sidemode fields

$$\dot{p}_{n_1,n_3} = i\mathcal{V}_1^*\rho_{53} - i(\mathcal{V}_1^*\rho_{53})\Big|_{n_1\to n_1-1} + i(\mathcal{V}_3^*\rho_{31})\Big|_{n_1\to n_1-1} - i(\mathcal{V}_3^*\rho_{31})\Big|_{n_{1,3}\to n_{1,3}-1} + \text{c.c.} \quad (5.34)$$

This equation shows that all we need to find is the dipole elements ρ_{53} and ρ_{31}. Using Eq. (5.28), we find the equation of motion for ρ_{53}, ρ_{31}, and the density matrix elements coupling to them

$$\dot{\rho}_{53} = -[\gamma_1 + i(\omega_{ab} - \nu_1)]\rho_{53} - i[\mathcal{V}_2\rho_{23} + \mathcal{V}_1\rho_{33} - \mathcal{V}_1\rho_{55}] + i\mathcal{V}_3^*\rho_{51} , \quad (5.35)$$

$$\dot{\rho}_{31} = -[\gamma_3 + i(\omega_{bc} - \nu_3)]\rho_{53} - i[\mathcal{V}_3\rho_{11} - \mathcal{V}_3\rho_{33} - \mathcal{V}_2\rho_{34}] - i\mathcal{V}_1^*\rho_{51} , \quad (5.36)$$

$$\dot{\rho}_{43} = -[\gamma_1 + i(\omega_{ab} - \nu_1)]\rho_{43} - i[\mathcal{V}_2\rho_{13} - \mathcal{V}_3^*\rho_{41}] + i\mathcal{V}_1\rho_{45} , \quad (5.37)$$

$$\dot{\rho}_{32} = -[\gamma_3 + i(\omega_{bc} - \nu_1)]\rho_{32} - i[\mathcal{V}_1^*\rho_{52} - \mathcal{V}_2\rho_{35}] - i\mathcal{V}_3\rho_{12} , \quad (5.38)$$

where we used the conservation condition $\nu_1 + \nu_3 = 2\nu_2$ in Eqs. (5.36) and (38). To solve Eqs. (5.35) - (5.38), we note that the weak sidemode fields assumption means that $\mathcal{V}_1$ can only appear to second order. This means that the density matrix elements ρ_{55}, ρ_{33}, ρ_{11}, ρ_{52}, and ρ_{41}, which are multiplied by the weak sidemode interaction potentials, can be factored into the corresponding semiclasscal value determined by the $\mathcal{V}_2$ interaction alone, multiplied by the corresponding photon number probability

$$\rho_{55} = \rho_{aa}\rho_{0000} , \quad (5.39)$$

$$\rho_{33} = \rho_{bb}\rho_{1010} , \quad (5.40)$$

$$\rho_{11} = \rho_{cc}\rho_{1111} , \quad (5.41)$$

$$\rho_{52} = i\mathcal{V}_2\mathcal{D}_2(\rho_{aa} - \rho_{cc})\rho_{0000} , \quad (5.42)$$

$$\rho_{41} = i\mathcal{V}_2\mathcal{D}_2(\rho_{aa} - \rho_{cc})\rho_{1111} , \quad (5.43)$$

where ρ_{aa}, ρ_{bb}, and ρ_{cc} are given by Eq. (5.18) and the photon number probabilities ρ_{0000}, ρ_{1010}, and ρ_{1111} are defined as

$$\rho_{0000} = \langle n_1 n_3|\rho|n_1 n_3\rangle = p_{n_1,n_3} , \tag{5.44}$$

$$\rho_{1010} = \langle n_1+1\, n_3|\rho|n_1+1\, n_3\rangle , \tag{5.45}$$

$$\rho_{1111} = \langle n_1+1\, n_3+1|\rho|n_1+1\, n_3+1\rangle . \tag{5.46}$$

Similarly the density matrix elements ρ_{54}, ρ_{21}, and ρ_{51}, which are also multiplied by the weak sidemode interaction potentials in Eqs. (5.35) through (5.38), are given by

$$\rho_{54} = \rho_{aa}\rho_{0011} , \tag{5.47}$$

$$\rho_{21} = \rho_{cc}\rho_{0011} , \tag{5.48}$$

$$\rho_{51} = i\mathcal{V}_2\mathcal{D}_2(\rho_{aa} - \rho_{cc})\rho_{0011} , \tag{5.49}$$

where ρ_{0011} is defined by

$$\rho_{0011} = \langle n_1 n_3|\rho|n_1+1\, n_3+1\rangle . \tag{5.50}$$

To find the density matrix element ρ_{53} and ρ_{31}, we solve Eqs. (5.35) through (5.38) in steady state. Combining Eqs. (5.35) and Eq. (5.38) and solving for ρ_{53} in steady state, we have

$$\rho_{53} = \frac{-i\mathcal{D}_1\,[\mathcal{V}_1(-f_a-\mathcal{D}_3^*\mathcal{D}_2^*|\mathcal{V}_2|^2)\rho_{0000} + \mathcal{V}_1 f_b\rho_{1010} + i\mathcal{V}_3^*\mathcal{V}_2(f_c\mathcal{D}_3^*+\mathcal{D}_2)\rho_{0011}]}{(1 + \mathcal{D}_1\mathcal{D}_3^*|\mathcal{V}_2|^2)\,(1 + I_2^2\mathcal{L}_2)} , \tag{5.51}$$

where we used Eqs. (5.39) through (5.43) and Eqs. (5.47) through (5.49). The complex

Lorentzians for mode 1 and 3 are defined by

$$\mathscr{D}_k = \frac{1}{\gamma_k + i\Delta_k}, \tag{5.52}$$

where γ_1 and γ_3 are the dipole decay constants for $a \leftrightarrow b$ and $b \leftrightarrow c$ transitions, $\Delta_1 = \Delta_2 - \Delta'$, and $\Delta_3 = \Delta'$. Similarly the matrix element ρ_{31} is found from the steady state solutions of Eqs. (5.36) and (5.37)

$$\rho_{31} = \frac{-i\mathscr{D}_3 \left[\mathscr{V}_3(f_c - \mathscr{D}_1^*\mathscr{D}_2^*|\mathscr{V}_2|^2)\rho_{1111} - \mathscr{V}_3 f_b \rho_{1010} + i\mathscr{V}_1^*\mathscr{V}_2(f_a\mathscr{D}_1^* - \mathscr{D}_2)\rho_{0011}\right]}{(1 + \mathscr{D}_1^*\mathscr{D}_3|\mathscr{V}_2|^2)\,(1 + I_2^2\mathscr{L}_2)}. \tag{5.53}$$

Substituting Eqs. (5.51) and (5.53) into Eq. (5.34) and using Eq. (5.32), we find the equation of motion

$$\begin{aligned}
\langle n_1 n_3|\dot{\rho}|n_1 n_3\rangle = &- A_1(n_1+1)\langle n_1 n_3|\rho|n_1 n_3\rangle - A_1 n_1\langle n_1-1\, n_3|\rho|n_1-1\, n_3\rangle \\
&- A_3(n_3+1)\langle n_1 n_3|\rho|n_1 n_3\rangle - A_3 n_3\langle n_1 n_3-1|\rho|n_1 n_3-1\rangle \\
&+ B_1(n_1+1)\langle n_1+1\, n_3|\rho|n_1+1\, n_3\rangle - B_1 n_1\langle n_1 n_3|\rho|n_1 n_3\rangle \\
&+ B_3(n_3+1)\langle n_1 n_3+1|\rho|n_1 n_3+1\rangle - B_3 n_3\langle n_1 n_3|\rho|n_1 n_3\rangle \\
&- C_3\sqrt{n_1(n_3+1)}\langle n_1-1\, n_3|\rho|n_1 n_3+1\rangle - C_3\sqrt{n_1 n_3}\langle n_1-1\, n_3-1|\rho|n_1 n_3\rangle \\
&- D_1\sqrt{(n_1+1)(n_3+1)}\langle n_1 n_3|\rho|n_1+1\, n_3+1\rangle - D_1\sqrt{n_1(n_3+1)}\langle n_1-1\, n_3|\rho|n_1 n_3+1\rangle
\end{aligned} \tag{5.54}$$

where the coefficients A_1, B_1, A_3, B_3, C_3, and D_1 are given by

$$A_1 = \frac{g_1^2\mathcal{D}_1}{1 + I_2^2\mathcal{L}_2}\,\frac{f_a + I_2^2\mathcal{D}_3^*\mathcal{D}_2^*/4T_1T_2}{1 + I_2^2\mathcal{D}_1\mathcal{D}_3^*/4T_1T_2}\,, \tag{5.55}$$

$$B_1 = \frac{g_1^2\mathcal{D}_1}{1 + I_2^2\mathcal{L}_2}\,\frac{f_b}{1 + I_2^2\mathcal{D}_1\mathcal{D}_3^*/4T_1T_2}\,, \tag{5.56}$$

$$A_3 = \frac{g_3^2\mathcal{D}_3}{1 + I_2^2\mathcal{L}_2}\,\frac{f_b}{1 + I_2^2\mathcal{D}_1^*\mathcal{D}_3/4T_1T_2}\,, \tag{5.57}$$

$$B_3 = \frac{g_3^2\mathcal{D}_3}{1 + I_2^2\mathcal{L}_2}\,\frac{f_c - I_2^2\mathcal{D}_1^*\mathcal{D}_2^*/4T_1T_2}{1 + I_2^2\mathcal{D}_1^*\mathcal{D}_3/4T_1T_2}\,, \tag{5.58}$$

$$C_3 = \frac{ig_3^2\mathcal{D}_3}{1 + I_2^2\mathcal{L}_2}\,U_1^*U_3^*\mathcal{V}_2\,\frac{-f_a\mathcal{D}_1^* + \mathcal{D}_2}{1 + I_2^2\mathcal{D}_1^*\mathcal{D}_3/4T_1T_2}\,, \tag{5.59}$$

$$D_1 = \frac{ig_1^2\mathcal{D}_1}{1 + I_2^2\mathcal{L}_2}\,U_1^*U_3^*\mathcal{V}_2\,\frac{f_c\mathcal{D}_3^* + \mathcal{D}_2}{1 + I_2^2\mathcal{D}_1\mathcal{D}_3^*/4T_1T_2}\,. \tag{5.60}$$

We can write an operator equation that yields Eq. (5.60) by noting the properties of creation and annihilation operator for mode k

$$a_k^\dagger|n_k\rangle = \sqrt{n_k+1}\,|n_k+1\rangle \quad \text{and} \quad a_k|n_k\rangle = \sqrt{n_k}\,|n_k-1\rangle\,. \tag{5.61}$$

Using Equation (5.61) we finally find the the equation of motion for ρ, the reduced density operator for the sidemode fields, in terms of the creation and annihilation operators of the sidemodes:

$$\dot{\rho} = -A_1(\rho a_1 a_1^\dagger - a_1^\dagger \rho a_1) - (B_1 + \nu/2Q)(a_1^\dagger a_1 \rho - a_1 \rho a_1^\dagger)$$
$$- A_3(\rho a_3 a_3^\dagger - a_3^\dagger \rho a_3) - (B_3 + \nu/2Q)(a_3^\dagger a_3 \rho - a_3 \rho a_3^\dagger)$$
$$+ C_3(a_3^\dagger a_1^\dagger \rho - a_1^\dagger \rho a_3^\dagger) + D_1(\rho a_3^\dagger a_1^\dagger - a_1^\dagger \rho a_3^\dagger)$$
$$+ \text{adjoint} , \tag{5.62}$$

where ν/Q is the rate of cavity losses for mode 1 and 3.

The equations of motion for the number operator $a_k^\dagger a_k$ for mode k and combination tone operator $a_1 a_3$ are easily obtained from Equation (5.62)

$$\frac{d}{dt}\langle a_1^\dagger a_1\rangle = \langle a_1^\dagger a_1 \dot{\rho}\rangle = (A_1 - B_1 - \nu/2Q)\langle a_1^\dagger a_1\rangle - D_1^*\langle a_1 a_3\rangle + A_1 + \text{c.c.} , \tag{5.63}$$

$$\frac{d}{dt}\langle a_3^\dagger a_3\rangle = \langle a_3^\dagger a_3 \dot{\rho}\rangle = (A_1 - B_1 - \nu/2Q)\langle a_3^\dagger a_3\rangle + C_3^*\langle a_1 a_3\rangle + A_3 + \text{c.c.} , \tag{5.64}$$

$$\frac{d}{dt}\langle a_1 a_3\rangle = \langle a_1 a_3 \dot{\rho}\rangle = (A_1 + A_3 - B_1 - B_3 - \nu/Q)\langle a_1 a_3\rangle - D_1\langle a_3^\dagger a_3\rangle + C_3\langle a_1^\dagger a_1\rangle + C_3 . \tag{5.65}$$

In free space, no build up of photon number occurs, and $d\langle n_k\rangle/dt = A_k + A_k^*$. Thus we interpret the inhomogeneous term $A_k + A_k^*$ of Eqs. (5.63) and (5.64) as the spectrum of resonance fluorescence for mode k. Figure 22 plots the centrally tuned spectrum of $A_1 + A_1^*$ for $I_2 = 0.5$ and 20. For the strong pump field of $I_2 = 20$, we note that the resonance fluorescence spectrum has only two peaks, both of which are at the Rabi frequencies, compared to the three peaks (two side peaks and one central peak) spectrum of the one-photon two-level case (Holm, Sargent, and Stenholm 1985). The difference $A_k - B_k$ is the semiclassical complex gain/absorption coefficient for mode k. Similarly the inhomogeneous term C_3 of Eq. (5.65) is the source contribution for the quantum combination tone $\langle a_1 a_3\rangle$, which is responsible for squeezing (Holm and Sargent 1987; Holm, Sargent, and Capron 1986). The real part of C_3 has two peaks at the Rabi frequencies for strong pump fields as shown in Fig. 23, but unlike for A_1 one

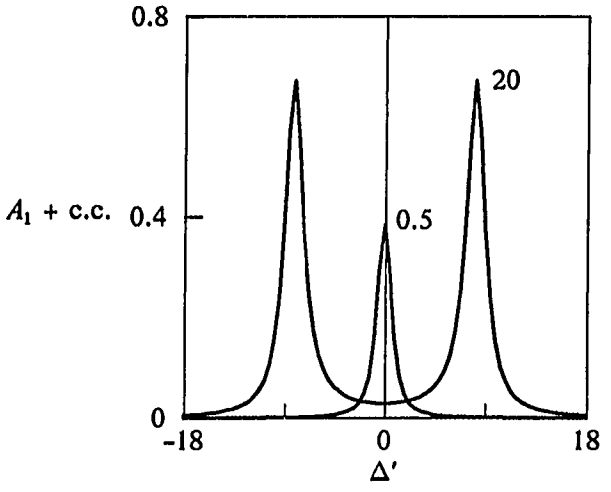

Fig. 22. The free space resonance fluorescence spectrum A_1 + c.c. versus Δ' for $I_2 = 0.5$ and 20, $\Delta_2 = 0$, $C = 1$, $\Gamma_a = 1$, $\Gamma_1 = \Gamma_3 = 1$, and $\gamma_1 = \gamma_3 = \gamma_2 = 1$. All frequencies are in units of γ_2.

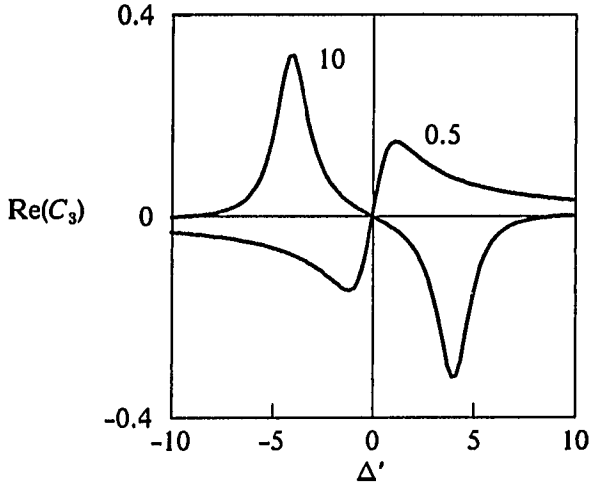

Fig. 23. Real part of C_3 for $I_2 = 0.5$ and 10. The other parameters are the same as in Fig. 22.

peak is negative.

5-3. Application to Squeezing

The squeezed light results from a linear combination of the sidemode annihilation and creation operators a_1 and $a_3^\dagger$. A possible experimental configuration in a cavity is depicted in the paper by Holm and Sargent (1987). The squeezed light may be measurable by means of a homodyne detection scheme (Slusher *et al.* 1985). This homodyne detection permits the direct measurement of the variance for any relative phase shift θ of the local oscillator. The amplitude d of the squeezed field is

$$d = 2^{-1/2}(a_1 e^{i\theta} + a_3^\dagger e^{-i\theta}) \ . \tag{5.66}$$

We define two Hermitian operators $d_{1,2} = (d \pm d^\dagger)/2$ and calculate the spectrum of their variances as discussed by Holm and Sargent (1987). The expression for the minimum variance outside the cavity is given by

$$\Delta d_1^2 = \frac{1}{4} + \frac{1}{4}\frac{\nu}{Q}(\mathcal{S}_{12} + \mathcal{S}_{34} - 2|\mathcal{S}_{13}|) \ , \tag{5.67}$$

where the spectral quantities $\mathcal{S}_{12}$, $\mathcal{S}_{13}$, and $\mathcal{S}_{34}$ are given by Eqs. (38) through (40) of the paper by Holm and Sargent (1987) letting $C_1 = D_3 = 0$ and using the coefficients given by Eqs. (5.55) through (5.60) of this chapter

$$\mathcal{J}_{12} = \frac{(\alpha_3 - i\omega)(\alpha_3^* + i\omega)A_1 + |D_1|^2 A_3 - (\alpha_3^* + i\omega)D_1^* C_3 + \text{c.c.}}{|(\alpha_1 + i\omega)(\alpha_3^* + i\omega) + D_1 C_3^*|^2}, \tag{5.68}$$

$$\mathcal{J}_{13} = \frac{(\alpha_3^* + i\omega)C_3(A_1 + A_1^*) - (\alpha_1^* - i\omega)D_1(A_3 + A_3^*) + (\alpha_1^* - i\omega)(\alpha_3^* + i\omega)C_3 - D_1|C_3|^2}{|(\alpha_1 + i\omega)(\alpha_3^* + i\omega) + D_1 C_3^*|^2}, \tag{5.69}$$

$$\mathcal{J}_{34} = \mathcal{J}_{12} \text{ (interchange 1 and 3)}, \tag{5.70}$$

where the absorption coefficients $\alpha_k = B_k - A_k + \nu/2Q$.

Substituting Eqs. (5.68) through (5.70) into Eq. (5.67) and letting $\omega = 0$, we calculate the squeezing variance Δd_1^2 as a function of the pump intensity I_2, the pump detuning Δ_2, the sidemode detuning Δ', and the cooperativity parameter $C = Ng^2Q/\gamma_2\nu$ (Holm and Sargent 1987), where we take $g_1 = g_2 = g$. Figure 24 shows the minimum variance Δd_1^2 given by Eq. (5.67) versus the sidemode detuning Δ' for $I_2 = 0.5$ and 150, $C = 100$, and $\Delta_2 = 0$. We notice that for the low intensity case there are two large regions with squeezing on either side of a small unsqueezed region around $\Delta' = 0$. For pump intensities small enough to be treated by fourth-order perturbation theory, four-wave mixing is the dominate nonlinearity, since spontaneous emission processes first show up in sixth-order perturbation theory. A lack of spontaneous emission aids in the generation of good squeezing. On the other hand for strong pump intensities, we obtain even better squeezing, namely for Δ' values within the Rabi sidebands. This is due to the Rabi splitting of the upper level *a* accompanied by vanishing splitting of level *b*, which as Fig. 22 shows leads to negligible spontaneous emission for this tuning region.

Figure 25 plots the minimum variance versus the pump intensity in the center of this region ($\Delta' = 0$) for various values of the cooperativity parameter C. We see

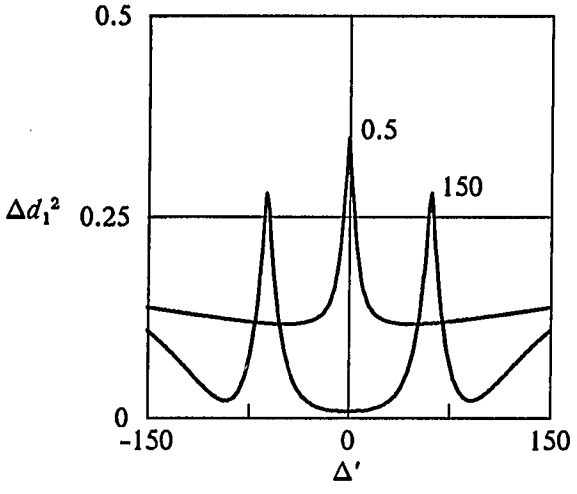

Fig. 24. Variance Δd_1^2 versus $\Delta' = (\omega_{bc}-\nu_2) - \Delta$ for $I_2 = 0.5$ and 150, $C = 100$, and the other parameters are the same as in Fig. 22.]

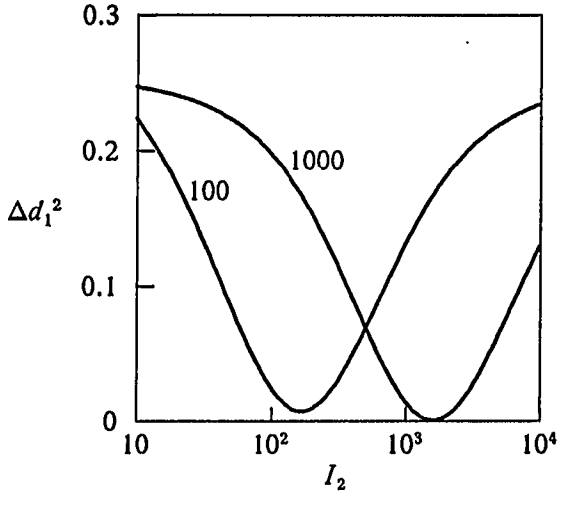

Fig. 25. Variance Δd_1^2 versus I_2 for $C = 100$ and 1000, $\Delta' = 0$, and the other parameters are the same as in Fig. 22.

that as C increases, squeezing is significantly enhanced for certain strong-pump intensities. In fact, we can get almost perfect squeezing by choosing suitable values of the cooperativity parameter and pump intensity (e.g., $\Delta d_1^2 \cong 10^{-2}$ for $C = 100$ and $I_2 \cong 150$, and $\Delta d_1^2 \cong 10^{-3}$ for $C = 1000$ and $I_2 \cong 1500$).

In this chapter we have treated quantum multiwave interactions in a two-photon three-level cascade model. We have derived the explicit formula for the resonance fluorescence spectrum and have shown that the spectrum has only two peaks, compared to the three peaks spectum of the one-photon two-level case. We have applied our theory to the generation of squeezed states of light and have shown that the two-photon three-level cascade model predicts broad-band squeezing for low pump intensities and excellent squeezing for strong pump intensities in the vicinity of small sidemode detunings.

SUMMARY

This dissertation has developed theories of multiwave mixing in one-photon two-level and two-photon three-level media both semiclassiclly and quantum mechanically.

Chapter 2 has presented a simplified phase conjugation calculation in which spatial holes are assumed to average out due to the inability of a slow-response population difference to follow the moving pump fringe pattern. We find that the large field saturation is substantially increased without spatial holes. The reflection coefficient is qualitatively similar to that of Abrams and Lind, but is reduced in magnitude due to incresed saturation. The theory should be useful in studying the conjugation properties of media with long population difference lifetimes, such as ruby, and aspects of the present analysis should be applicable to other media having long grating decay times.

Chapter 3 has derived the probe absorption and coupling coefficients in a squeezed vacuum using a standard Fourier series method. We have illustrated the sensitivity of sharp peak structures to both pump detuning and pump phase relative to the squeezed vacuum. Averaging the coefficients over pump spatial holes, we have also calculated and plotted the four-wave mixing reflection coefficients. Reflectivity peaks and dips are found to be narrower than in an unsqueezed vacuum. In fact, for small γ_ν and pump/probe detuning Δ, we find the various coefficients are proportional to the factor $\gamma_\nu(\gamma_\nu + i\Delta)$, which reveals a sharp Lorentzian with FWHM width of $2\gamma_\nu$. As such both the absorption and the reflectivity provide sensitive ways to measure the amount of squeezing in the vacuum.

Chapter 4 has studied the effects of sidemode saturation on the two-wave mixing both semiclassically and quantum mechanically. The degenerate semiclassical theory shows that the third-order semiclassical sidemode absorption contribution have the same sign as the probe absorption coefficient, which has just the opposite effect from the usual saturation. We have derived explicit formulas for the fourth-order quantum coefficients. The results are much more complicated than the corresponding semiclassical case, but reduce to it in the appropriate limit. We have applied the results to cavity problems. We find that the sidemode fluorescence spectra do not diverge even near the sidemode laser threshold. Furthermore we notice that the secondary sideband peaks grow at $\Delta = \Omega/2$. This problem is important for the study of optical instabilities, but unfortunately is very complicated. Even extending the fourth-order theory to the two sidemode case, e.g., for three- and four-wave mixing, seems to be prohibitively difficult.

The final chapter has treated quantum multiwave interactions in a two-photon three-level cascade model. We have derived the explicit formula for the resonance fluorescence spectrum and have shown that the spectrum has only two peaks, compared to the three peaks spectum of the one-photon two-level case. We have applied our theory to the generation of squeezed states of light and have shown that the two-photon three-level cascade model predicts broad-band squeezing for low pump intensities and excellent squeezing for strong pump intensities in the vicinity of small sidemode detunings. Both cases avoid regions of significant spontaneous emission.

APPENDIX

In this Appendix we derive the equations of motion for (ρ_{50}, ρ_{56}, ρ_{20}, ρ_{26}) and (ρ_{51}, ρ_{54}, ρ_{21}, ρ_{24}) of chapter 4, and obtain the steady state solutions to the equations. The equations of motion for (ρ_{51}, ρ_{54}, ρ_{21}, ρ_{24}) is given by

$$\dot{\rho}_{51} = -(\gamma+i\Delta_1)\rho_{51} - i\mathcal{V}_2\rho_{21} + i\mathcal{V}_2\rho_{54} + i\mathcal{V}_1(\rho_{55} - \rho_{11}) , \tag{A.1}$$

$$\dot{\rho}_{54} = -(\Gamma+i\Delta)\rho_{54} - i\mathcal{V}_2\rho_{24} - i\mathcal{V}_1\rho_{14} + i\mathcal{V}_2^{*}\rho_{51} + i\mathcal{V}_1^{+*}\rho_{50} , \tag{A.2}$$

$$\dot{\rho}_{21} = \Gamma\rho_{54} - i\Delta\rho_{21} - i\mathcal{V}_2^{*}\rho_{51} - i\mathcal{V}_1^{-*}\rho_{71} + i\mathcal{V}_2\rho_{24} + i\mathcal{V}_1\rho_{25} , \tag{A.3}$$

$$\dot{\rho}_{24} = -(\gamma-i\Delta_3)\rho_{24} - i\mathcal{V}_2^{*}\rho_{54} - i\mathcal{V}_1^{-*}\rho_{74} + i\mathcal{V}_2^{*}\rho_{21} + i\mathcal{V}_1^{+*}\rho_{20} . \tag{A.4}$$

The equation for the steady state to Eqs. (*A.1*) through (*A.4*) can be written in terms of the vecter and matrix as

$$\mathbf{H}(\Delta)\mathbf{X} = \mathbf{U} , \tag{A.5}$$

where

$$\mathbf{X} = \begin{bmatrix} \rho_{51} \\ \rho_{54} \\ \rho_{21} \\ \rho_{24} \end{bmatrix} , \tag{A.6}$$

$$\mathbf{H}(\Delta) = \begin{bmatrix} -(\gamma+i\Delta_1) & i\mathscr{V}_2 & -i\mathscr{V}_2 & 0 \\ i\mathscr{V}_2^* & -(\Gamma+i\Delta) & 0 & -i\mathscr{V}_2 \\ -i\mathscr{V}_2^* & \Gamma & -i\Delta & i\mathscr{V}_2 \\ 0 & -i\mathscr{V}_2^* & i\mathscr{V}_2^* & -(\gamma-i\Delta_3) \end{bmatrix} , \tag{A.7}$$

and

$$\mathbf{U} = \begin{bmatrix} -i\mathscr{V}_1(\rho_{55} - \rho_{11}) \\ i\mathscr{V}_1\rho_{14} - i\mathscr{V}_1{}^{+*}\rho_{50} \\ i\mathscr{V}_1{}^{-*}\rho_{71} - i\mathscr{V}_1\rho_{25} \\ i\mathscr{V}_1{}^{-*}\rho_{74} - i\mathscr{V}_1{}^{+*}\rho_{20} \end{bmatrix} . \tag{A.8}$$

Note that $\Delta_1 = \Delta_1(\Delta)$ and $\Delta_3 = \Delta_3(\Delta)$ in Eq. (*A.7*) are defined as

$$\Delta_1 = \omega - (\nu_2 - \Delta) = \Delta_2 + \Delta , \tag{A.9}$$

$$\Delta_3 = \omega - (\nu_2 + \Delta) = \Delta_2 - \Delta . \tag{A.10}$$

The solution to Eq. (*A.5*) can be written in terms of the inverse

$$\mathbf{H}^{-1}(\Delta) = \frac{1}{N(\Delta)}\mathbf{M}(\Delta) , \tag{A.11}$$

as

$$\mathbf{X} = \frac{1}{N(\Delta)}\mathbf{M}(\Delta)\mathbf{U} , \tag{A.12}$$

where $N(\Delta)$ is the determinant of the matrix $\mathbf{H}(\Delta)$ and $\mathbf{M}(\Delta)$ is a 4×4 matrix. In particular, the dipole element ρ_{51} is given by

$$\rho_{51} = \frac{1}{N(\Delta)} [M_{11}(\Delta)U_1 + M_{12}(\Delta)U_2 + M_{13}(\Delta)U_3 + M_{14}(\Delta)U_4] . \qquad (A.13)$$

By direct calculation we find

$$N(\Delta) = i\Delta \{ 2|\mathcal{V}_2|^2[(\gamma+i\Delta_1) + (\gamma-i\Delta_3)] + (\gamma+i\Delta_1)(\gamma-i\Delta_3)(\Gamma+i\Delta) \} , \qquad (A.14)$$

and

$$M_{11}(\Delta) = -i\Delta[2|\mathcal{V}_2|^2 + (\Gamma+i\Delta)(\gamma-i\Delta_3)] , \qquad (A.15)$$

$$M_{12}(\Delta) = i\mathcal{V}_2(\Gamma-i\Delta)(\gamma-i\Delta_3) , \qquad (A.16)$$

$$M_{13}(\Delta) = i\mathcal{V}_2(\Gamma+i\Delta)(\gamma-i\Delta_3) , \qquad (A.17)$$

$$M_{14}(\Delta) = -i2\Delta\mathcal{V}_2^2 . \qquad (A.18)$$

To express the vecter **U** in terms of the g^0 and g^1-order density matrix elemets, we need to find the equations of motion for (ρ_{50}, ρ_{56}, ρ_{20}, ρ_{26})

$$\dot{\rho}_{50} = -(\gamma+i\Delta_0)\rho_{50} - i\mathcal{V}_2\rho_{20} - i\mathcal{V}_1\rho_{10} + i\mathcal{V}_1^+\rho_{54} + i\mathcal{V}_2\rho_{56} , \qquad (A.19)$$

$$\dot{\rho}_{56} = -(\Gamma+i2\Delta)\rho_{56} - i\mathcal{V}_2\rho_{26} - i\mathcal{V}_1\rho_{16} + i\mathcal{V}_2^*\rho_{50} , \qquad (A.20)$$

$$\dot{\rho}_{20} = \Gamma\rho_{56} - i2\Delta\rho_{20} - i\mathcal{V}_2^*\rho_{50} + i\mathcal{V}_2\rho_{26} + i\mathcal{V}_1^+\rho_{24} , \qquad (A.21)$$

$$\dot{\rho}_{26} = -(\gamma-i\Delta_4)\rho_{26} - i\mathcal{V}_2^*\rho_{56} + i\mathcal{V}_2^*\rho_{20} . \qquad (A.22)$$

Similarly to Eq. (*A.5*), the equation for the steady state solution can be written as

$$\mathbf{H}(2\Delta)\mathbf{Y} = \mathbf{V} , \tag{A.23}$$

where

$$\mathbf{Y} = \begin{bmatrix} \rho_{50} \\ \rho_{56} \\ \rho_{20} \\ \rho_{26} \end{bmatrix} , \tag{A.24}$$

$$\mathbf{H}(2\Delta) \equiv \mathbf{H}(\Delta)\Big|_{\Delta \to 2\Delta} , \tag{A.25}$$

and

$$\mathbf{V} = \begin{bmatrix} i\mathcal{V}_1\rho_{10} - i\mathcal{V}_1^{+}\rho_{54} \\ i\mathcal{V}_1\rho_{16} \\ -i\mathcal{V}_1^{+}\rho_{24} \\ 0 \end{bmatrix} . \tag{A.26}$$

The solution is given by

$$\mathbf{Y} = \frac{1}{N(2\Delta)}\mathbf{M}(2\Delta)\mathbf{V} , \tag{A.27}$$

where $N(2\Delta)$ is defined by

$$N(2\Delta) = N(\Delta)\Big|_{\Delta\to 2\Delta} . \tag{A.28}$$

and $\mathbf{M}(2\Delta)$ is defined similarly.

Substituting Eq. (*A.27*) into Eq. (*A.13*) to find the dipole matrix element ρ_{51} up to g^3-order and using Eq. (4.61), we finally have Eq. (4.80). The g^4-order coefficients are given by

$$\begin{aligned}
q_0 = {} & g^4\Pi(\Delta)\,\frac{\mathscr{D}_2^*}{\mathscr{D}_1\mathscr{D}_3^*}\,\frac{1}{\mathscr{D}(\Delta)\mathscr{D}_3^*}\,|\mathscr{V}_2|^2\,\{\,-if_a\Delta\mathscr{D}_1 - \mathscr{D}_2^*|\mathscr{V}_2|^2\,(\mathscr{D}_1+\mathscr{D}_3^*)\,\} \\
& + ig^4\Pi(2\Delta)\,\frac{1}{\mathscr{D}_1\mathscr{D}_3^*}\,\frac{1}{\mathscr{D}(\Delta)\mathscr{D}_3^*}\,|\mathscr{V}_2|^2\,\{\,-if_a\Delta\mathscr{D}_1 - \mathscr{D}_2^*|\mathscr{V}_2|^2\,(\mathscr{D}_1+\mathscr{D}_3^*)\,\} \\
& \qquad \times 2\Delta\left\{2|\mathscr{V}_2|^2 + \frac{1}{\mathscr{D}(2\Delta)\mathscr{D}_4^*}\right\} \\
& - ig^4\Pi(2\Delta)\,\frac{1}{\mathscr{D}(\Delta)\mathscr{D}_3^*}\,|\mathscr{V}_2|^4\left\{-f_a 2\Delta - i\frac{\mathscr{D}_2^*}{\mathscr{D}_1\mathscr{D}(\Delta)}\right\}\frac{1}{\mathscr{D}(2\Delta)\mathscr{D}_4^*} \\
& + g^4\Pi(2\Delta)\,\frac{2\Delta}{\mathscr{D}_1\mathscr{D}_3^*}\,|\mathscr{V}_2|^2\,\{\,-if_a\Delta\mathscr{D}_1 - \mathscr{D}_2^*|\mathscr{V}_2|^2\,(\mathscr{D}_1+\mathscr{D}_3^*)\,\}\,|\mathscr{V}_2|^2\,\frac{2\Delta}{\mathscr{D}_4^*} \\
& - g^4\Pi(2\Delta)\,2\Delta\,|\mathscr{V}_2|^4\left\{-f_a 2\Delta - i\frac{\mathscr{D}_2^*}{\mathscr{D}_1\mathscr{D}(\Delta)}\right\}|\mathscr{V}_2|^2\left[\frac{1}{\mathscr{D}_0}+\frac{1}{\mathscr{D}_4^*}\right]
\end{aligned} \tag{A.29}$$

$$\begin{aligned}
r_0 = {} & g^4\Pi(\Delta)\,\frac{\mathscr{D}_2^*}{\mathscr{D}_1\mathscr{D}_3^*}\,\frac{1}{\mathscr{D}(\Delta)\mathscr{D}_3^*}\,|\mathscr{V}_2|^2\,\{\,if_b\Delta\mathscr{D}_1 + \mathscr{D}_2^*\,[\,|\mathscr{V}_2|^2\,(\mathscr{D}_1+\mathscr{D}_3^*) + i\Delta\,]\,\} \\
& - ig^4\Pi(2\Delta)\,\frac{1}{\mathscr{D}_1\mathscr{D}_3^*}\,\frac{1}{\mathscr{D}(\Delta)\mathscr{D}_3^*}\,|\mathscr{V}_2|^2\,\{\,if_a\Delta\mathscr{D}_1 - \mathscr{D}_2^*\,[\,|\mathscr{V}_2|^2\,(\mathscr{D}_1+\mathscr{D}_3^*) + 1/\mathscr{D}(\Delta)\,]\,\} \\
& \times 2\Delta\left\{2|\mathscr{V}_2|^2 + \frac{1}{\mathscr{D}(2\Delta)\mathscr{D}_4^*}\right\} \\
& + ig^4\Pi(2\Delta)\,\frac{1}{\mathscr{D}_1\mathscr{D}_3^*}\,\frac{1}{\mathscr{D}(\Delta)\mathscr{D}_3^*}\,|\mathscr{V}_2|^2\,\{\,if_b\Delta\mathscr{D}_1 + \mathscr{D}_2^*\,[\,|\mathscr{V}_2|^2\,(\mathscr{D}_1+\mathscr{D}_3^*) + i\Delta\,]\,\}
\end{aligned}$$

$$\times\, 2\Delta\left\{2|\mathcal{V}_2|^2 + \frac{1}{\mathcal{D}(2\Delta)\mathcal{D}_4^*}\right\}$$

$$+\, ig^4\Pi(2\Delta)\ \frac{1}{\mathcal{D}(\Delta)\mathcal{D}_3^*}\,|\mathcal{V}_2|^4\left\{-f_a 2\Delta - i\frac{\mathcal{D}_2^*}{\mathcal{D}_1\mathcal{D}(\Delta)}\right\}\frac{1}{\mathcal{D}(2\Delta)^*\mathcal{D}_4^*}$$

$$-\, ig^4\Pi(2\Delta)\ \frac{1}{\mathcal{D}(\Delta)\mathcal{D}_3^*}\,|\mathcal{V}_2|^4\left\{f_b 2\Delta + i\frac{\mathcal{D}_2^*}{\mathcal{D}_1\mathcal{D}(\Delta)^*}\right\}\frac{1}{\mathcal{D}(2\Delta)\mathcal{D}_4^*}$$

$$-\, g^4\Pi(2\Delta)\ \frac{2\Delta}{\mathcal{D}_1\mathcal{D}_3^*}\ |\mathcal{V}_2|^2\ \{\, if_a\Delta\mathcal{D}_1 - \mathcal{D}_2^*\ [\ |\mathcal{V}_2|^2\ (\mathcal{D}_1+\mathcal{D}_3^*) + 1/\mathcal{D}(\Delta)\ ]\ \}\ |\mathcal{V}_2|^2\,\frac{2\Delta}{\mathcal{D}_4^*}$$

$$+\, g^4\Pi(2\Delta)\ \frac{2\Delta}{\mathcal{D}_1\mathcal{D}_3^*}\ |\mathcal{V}_2|^2\ \{\, if_b\Delta\mathcal{D}_1 + \mathcal{D}_2^*\ [\ |\mathcal{V}_2|^2\ (\mathcal{D}_1+\mathcal{D}_3^*) + i\Delta\ ]\ \}\ |\mathcal{V}_2|^2\,\frac{2\Delta}{\mathcal{D}_4^*}$$

$$+\, g^4\Pi(2\Delta)\ 2\Delta\ \ |\mathcal{V}_2|^4\left\{-f_a 2\Delta - i\frac{\mathcal{D}_2^*}{\mathcal{D}_1\mathcal{D}(\Delta)}\right\}\left\{|\mathcal{V}_2|^2\left[\frac{1}{\mathcal{D}_0}+\frac{1}{\mathcal{D}_4^*}\right] + i\frac{2\Delta}{\mathcal{D}_0\mathcal{D}_4^*}\right\}$$

$$-\, g^4\Pi(2\Delta)\ 2\Delta\ \ |\mathcal{V}_2|^4\left\{f_b 2\Delta + i\frac{\mathcal{D}_2^*}{\mathcal{D}_1\mathcal{D}(\Delta)^*}\right\}|\mathcal{V}_2|^2\left[\frac{1}{\mathcal{D}_0}+\frac{1}{\mathcal{D}_4^*}\right] \qquad (A.30)$$

$$r_1 = -\, g^4\Pi(\Delta)\ \frac{\mathcal{D}_2^*}{\mathcal{D}_1\mathcal{D}_3^*}\ \ \frac{1}{\mathcal{D}(\Delta)^*\mathcal{D}_3^*}\ |\mathcal{V}_2|^2\ \{\, -if_a\Delta\mathcal{D}_1 - \mathcal{D}_2^*|\mathcal{V}_2|^2\ (\mathcal{D}_1+\mathcal{D}_3^*)\ \}$$

$$-\, g^4\Pi(\Delta)\ \frac{\mathcal{D}_2^*}{\mathcal{D}_1\mathcal{D}_3^*}\ \ \frac{1}{\mathcal{D}(\Delta)\mathcal{D}_3^*}\ |\mathcal{V}_2|^2\ \{\, if_a\Delta\mathcal{D}_1 - \mathcal{D}_2^*\ [\ |\mathcal{V}_2|^2\ (\mathcal{D}_1+\mathcal{D}_3^*) + 1/\mathcal{D}(\Delta)\ ]\ \} \qquad (A.31)$$

$$r_2 = -\, ig^4\Pi(2\Delta)\ \frac{1}{\mathcal{D}_1\mathcal{D}_3^*}\ \ \frac{1}{\mathcal{D}(\Delta)^*\mathcal{D}_3^*}\ |\mathcal{V}_2|^2\ \{\, -if_a\Delta\mathcal{D}_1 - \mathcal{D}_2^*|\mathcal{V}_2|^2\ (\mathcal{D}_1+\mathcal{D}_3^*)\ \}$$

$$\times\, 2\Delta\left\{2|\mathcal{V}_2|^2 + \frac{1}{\mathcal{D}(2\Delta)\mathcal{D}_4^*}\right\}$$

$$+\, ig^4\Pi(2\Delta)\ \frac{1}{\mathcal{D}(\Delta)^*\mathcal{D}_3^*}\,|\mathcal{V}_2|^4\left\{-f_a 2\Delta - i\frac{\mathcal{D}_2^*}{\mathcal{D}_1\mathcal{D}(\Delta)}\right\}\frac{1}{\mathcal{D}(2\Delta)\mathcal{D}_4^*}$$

$$+\, g^4\Pi(2\Delta)\ \frac{2\Delta}{\mathcal{D}_1\mathcal{D}_3^*}\ |\mathcal{V}_2|^2\ \{\, -if_a\Delta\mathcal{D}_1 - \mathcal{D}_2^*|\mathcal{V}_2|^2\ (\mathcal{D}_1+\mathcal{D}_3^*)\ \}\ |\mathcal{V}_2|^2\,\frac{2\Delta}{\mathcal{D}_4^*}$$

$$+ g^4\Pi(2\Delta)\ |\mathcal{V}_2|^4 \left\{-f_a 2\Delta - i\frac{\mathcal{D}_2^*}{\mathcal{D}_1\mathcal{D}(\Delta)}\right\}\left\{|\mathcal{V}_2|^2\left[\frac{1}{\mathcal{D}_0}+\frac{1}{\mathcal{D}_4^*}\right] + \frac{\Gamma+i2\Delta}{\mathcal{D}_0\mathcal{D}_4^*}\right\} \qquad (A.32)$$

$$s_0 = -\, ig^4\Pi(2\Delta)\ \frac{1}{\mathcal{D}_1\mathcal{D}_3^*}\ \frac{1}{\mathcal{D}(\Delta)\mathcal{D}_3^*}\ |\mathcal{V}_2|^2\ \{\ -if_b\Delta\mathcal{D}_1 + \mathcal{D}_2^*\ [\ |\mathcal{V}_2|^2\ (\mathcal{D}_1+\mathcal{D}_3^*) + \Gamma\ ]\ \}$$

$$\times\ 2\Delta\left\{2|\mathcal{V}_2|^2 + \frac{1}{\mathcal{D}(2\Delta)\mathcal{D}_4^*}\right\}$$

$$+\, ig^4\Pi(2\Delta)\ \frac{1}{\mathcal{D}(\Delta)\mathcal{D}_3^*}\ |\mathcal{V}_2|^4\left\{f_b 2\Delta + i\frac{\mathcal{D}_2^*}{\mathcal{D}_1\mathcal{D}(\Delta)^*}\right\}\frac{1}{\mathcal{D}(2\Delta)^*\mathcal{D}_4^*}$$

$$-\, g^4\Pi(2\Delta)\ \frac{2\Delta}{\mathcal{D}_1\mathcal{D}_3^*}\ |\mathcal{V}_2|^2\ \{\ -if_b\Delta\mathcal{D}_1 + \mathcal{D}_2^*\ [\ |\mathcal{V}_2|^2\ (\mathcal{D}_1+\mathcal{D}_3^*) + \Gamma\ ]\ \}\ |\mathcal{V}_2|^2\ \frac{2\Delta}{\mathcal{D}_4^*}$$

$$+\, g^4\Pi(2\Delta)\ \frac{2\Delta}{\mathcal{D}_1\mathcal{D}_3^*}\ |\mathcal{V}_2|^4\left\{f_b 2\Delta + i\frac{\mathcal{D}_2^*}{\mathcal{D}_1\mathcal{D}(\Delta)^*}\right\}\left\{|\mathcal{V}_2|^2\left[\frac{1}{\mathcal{D}_0}+\frac{1}{\mathcal{D}_4^*}\right] + i\frac{2\Delta}{\mathcal{D}_0\mathcal{D}_4^*}\right\} \qquad (A.33)$$

$$s_1 = -\, g^4\Pi(\Delta)\ \frac{\mathcal{D}_2^*}{\mathcal{D}_1\mathcal{D}_3^*}\ \frac{1}{\mathcal{D}(\Delta)^*\mathcal{D}_3^*}\ |\mathcal{V}_2|^2\ \{\ if_b\Delta\mathcal{D}_1 + \mathcal{D}_2^*\ [\ |\mathcal{V}_2|^2\ (\mathcal{D}_1+\mathcal{D}_3^*) + i\Delta\ ]\ \}$$

$$-\, g^4\Pi(\Delta)\ \frac{\mathcal{D}_2^*}{\mathcal{D}_1\mathcal{D}_3^*}\ \frac{1}{\mathcal{D}(\Delta)\mathcal{D}_3^*}\ |\mathcal{V}_2|^2\ \{\ -if_b\Delta\mathcal{D}_1 + \mathcal{D}_2^*\ [\ |\mathcal{V}_2|^2\ (\mathcal{D}_1+\mathcal{D}_3^*) + \Gamma\ ]\ \} \qquad (A.34)$$

$$s_2 = g^4\Pi(\Delta)\ \frac{\mathcal{D}_2^*}{\mathcal{D}_1\mathcal{D}_3^*}\ \frac{1}{\mathcal{D}(\Delta)^*\mathcal{D}_3^*}\ |\mathcal{V}_2|^2\ \{\ if_a\Delta\mathcal{D}_1 - \mathcal{D}_2^*\ [\ |\mathcal{V}_2|^2\ (\mathcal{D}_1+\mathcal{D}_3^*) + 1/\mathcal{D}(\Delta)\ ]\ \}$$

$$+\, ig^4\Pi(2\Delta)\ \frac{1}{\mathcal{D}_1\mathcal{D}_3^*}\ \frac{1}{\mathcal{D}(\Delta)^*\mathcal{D}_3^*}\ |\mathcal{V}_2|^2\ \{\ if_a\Delta\mathcal{D}_1 - \mathcal{D}_2^*\ [\ |\mathcal{V}_2|^2\ (\mathcal{D}_1+\mathcal{D}_3^*) + 1/\mathcal{D}(\Delta)\ ]\ \}$$

$$\times\ 2\Delta\left\{2|\mathcal{V}_2|^2 + \frac{1}{\mathcal{D}(2\Delta)\mathcal{D}_4^*}\right\}$$

$$-\, ig^4\Pi(2\Delta)\ \frac{1}{\mathcal{D}_1\mathcal{D}_3^*}\ \frac{1}{\mathcal{D}(\Delta)^*\mathcal{D}_3^*}\ |\mathcal{V}_2|^2\ \{\ if_b\Delta\mathcal{D}_1 + \mathcal{D}_2^*\ [\ |\mathcal{V}_2|^2\ (\mathcal{D}_1+\mathcal{D}_3^*) + i\Delta\ ]\ \}$$

$$\times\ 2\Delta\left\{2|\mathcal{V}_2|^2 + \frac{1}{\mathcal{D}(2\Delta)\mathcal{D}_4^*}\right\}$$

$$
\begin{aligned}
&- ig^4\Pi(2\Delta)\ \frac{1}{\mathscr{D}(\Delta)^*\mathscr{D}_3^*}\,|\mathscr{V}_2|^4\left\{-f_a 2\Delta - i\frac{\mathscr{D}_2^*}{\mathscr{D}_1\mathscr{D}(\Delta)}\right\}\frac{1}{\mathscr{D}(2\Delta)^*\mathscr{D}_4^*}\\
&+ ig^4\Pi(2\Delta)\ \frac{1}{\mathscr{D}(\Delta)^*\mathscr{D}_3^*}\,|\mathscr{V}_2|^4\left\{f_b 2\Delta + i\frac{\mathscr{D}_2^*}{\mathscr{D}_1\mathscr{D}(\Delta)^*}\right\}\frac{1}{\mathscr{D}(2\Delta)\mathscr{D}_4^*}\\
&- g^4\Pi(2\Delta)\ \frac{2\Delta}{\mathscr{D}_1\mathscr{D}_3^*}\ |\mathscr{V}_2|^4\left\{-f_a 2\Delta - i\frac{\mathscr{D}_2^*}{\mathscr{D}_1\mathscr{D}(\Delta)}\right\}|\mathscr{V}_2|^2\frac{2\Delta}{\mathscr{D}_4^*}\\
&+ g^4\Pi(2\Delta)\ \frac{2\Delta}{\mathscr{D}_1\mathscr{D}_3^*}\ |\mathscr{V}_2|^2\{\,if_b\Delta\mathscr{D}_1 + \mathscr{D}_2^*[\,|\mathscr{V}_2|^2(\mathscr{D}_1+\mathscr{D}_3^*) + i\Delta\,]\,\}\,|\mathscr{V}_2|^2\frac{2\Delta}{\mathscr{D}_4^*}\\
&- g^4\Pi(2\Delta)\,2\Delta\ |\mathscr{V}_2|^4\left\{-f_a 2\Delta - i\frac{\mathscr{D}_2^*}{\mathscr{D}_1\mathscr{D}(\Delta)}\right\}\left\{|\mathscr{V}_2|^2\left[\frac{1}{\mathscr{D}_0}+\frac{1}{\mathscr{D}_4^*}\right] + \frac{\Gamma}{\mathscr{D}_0\mathscr{D}_4^*}\right\}\\
&+ g^4\Pi(2\Delta)\,2\Delta\ |\mathscr{V}_2|^4\left\{f_b 2\Delta + i\frac{\mathscr{D}_2^*}{\mathscr{D}_1\mathscr{D}(\Delta)^*}\right\}\left\{|\mathscr{V}_2|^2\left[\frac{1}{\mathscr{D}_0}+\frac{1}{\mathscr{D}_4^*}\right] + \frac{\Gamma+i2\Delta}{\mathscr{D}_0\mathscr{D}_4^*}\right\}
\end{aligned}
\tag{A.35}
$$

$$
\begin{aligned}
t_2 = {}& g^4\Pi(\Delta)\ \frac{\mathscr{D}_2^*}{\mathscr{D}_1\mathscr{D}_3^*}\ \frac{1}{\mathscr{D}(\Delta)^*\mathscr{D}_3^*}\,|\mathscr{V}_2|^2\{\,-if_b\Delta\mathscr{D}_1 + \mathscr{D}_2^*[\,|\mathscr{V}_2|^2(\mathscr{D}_1+\mathscr{D}_3^*) + \Gamma\,]\,\}\\
&+ ig^4\Pi(2\Delta)\ \frac{1}{\mathscr{D}_1\mathscr{D}_3^*}\ \frac{1}{\mathscr{D}(\Delta)^*\mathscr{D}_3^*}\,|\mathscr{V}_2|^2\{\,-if_b\Delta\mathscr{D}_1 + \mathscr{D}_2^*[\,|\mathscr{V}_2|^2(\mathscr{D}_1+\mathscr{D}_3^*) + \Gamma\,]\,\}\\
&\times 2\Delta\left\{2|\mathscr{V}_2|^2 + \frac{1}{\mathscr{D}(2\Delta)\mathscr{D}_4^*}\right\}\\
&- ig^4\Pi(2\Delta)\ \frac{1}{\mathscr{D}_1\mathscr{D}_3^*}\ \frac{1}{\mathscr{D}(\Delta)^*\mathscr{D}_3^*}\,|\mathscr{V}_2|^4\left\{f_b 2\Delta + i\frac{\mathscr{D}_2^*}{\mathscr{D}_1\mathscr{D}(\Delta)^*}\right\}\frac{1}{\mathscr{D}(2\Delta)^*\mathscr{D}_4^*}\\
&- g^4\Pi(2\Delta)\ \frac{2\Delta}{\mathscr{D}_1\mathscr{D}_3^*}\ |\mathscr{V}_2|^2\{\,-if_b\Delta\mathscr{D}_1 + \mathscr{D}_2^*[\,|\mathscr{V}_2|^2(\mathscr{D}_1+\mathscr{D}_3^*) + \Gamma\,]\,\}\,|\mathscr{V}_2|^2\frac{2\Delta}{\mathscr{D}_4^*}\\
&- g^4\Pi(2\Delta)\,2\Delta\ |\mathscr{V}_2|^4\left\{f_b 2\Delta + i\frac{\mathscr{D}_2^*}{\mathscr{D}_1\mathscr{D}(\Delta)^*}\right\}\left\{|\mathscr{V}_2|^2\left[\frac{1}{\mathscr{D}_0}+\frac{1}{\mathscr{D}_4^*}\right] + \frac{\Gamma}{\mathscr{D}_0\mathscr{D}_4^*}\right\}
\end{aligned}
\tag{A.36}
$$

where

$$
\mathscr{D}(\Delta) = \frac{1}{\Gamma + i\Delta}\,, \tag{A.37}
$$

$$\Pi(\Delta) = \frac{1}{(1 + I_2 \mathscr{L}_2)\, N(\Delta)^2}\,, \tag{A.38}$$

$$\Pi(2\Delta) = \frac{1}{(1 + I_2 \mathscr{L}_2)\, N(\Delta)^2\, N(2\Delta)}\,, \tag{A.39}$$

and from Eq. (4.54) we can express $|\mathscr{V}_2|^2$ in terms of I_2 as

$$|\mathscr{V}_2|^2 = I_2/4T_1T_2\,. \tag{A.40}$$

REFERENCES

Abrams, R. L., and Lind, R. C., Opt. Lett. **2**, 94 (1978*a*).

Abrams, R. L., and Lind, R. C., Opt. Lett. **3**, 205 (1978*b*).

Agrawal, G. P., Opt. Comm. **42**, 366 (1982).

Agarwal, G. S., Phys. Rev. Lett. **57**, 827 (1986).

An, S., and Sargent, M. III, Opt. Lett. **13**, 473 (1988*a*).

An, S., and Sargent, M. III, Opt. Comm. **67**, 373 (1988*b*).

An, S., and Sargent, M. III, submitted to Phys. Rev. A

Boyd, R. W., Raymer, M. G., Narum, P., and Harter, D. J., Phys. Rev. *A*24, 411 (1981).

Boyd, R. W., Malcuit, M. S., Gauthier, D. J., and Rzażewski, K., Phys. Rev. A35, 1648 (1987).

Boyd, R. W., and Sargent, M. III, J. Opt. Soc. Am. *B*5, 99 (1988).

Capron, B. A., Holm, D. A., and Sargent, M. III, Phys. Rev. *A*35, 3388 (1987).

Carmichael, H. J., Lane, A. S., and Walls, D. F., Phys. Rev. Lett. **58**, 2539 (1987); J. of Mod. Opt. **34**, 821 (1987).

Cresser, J. D., Phys. Rep. **94**, 48 (1983).

Fu, T., and Sargent, M. III, Opt. Lett. **4**, 366 (1979).

Gardiner, C. W., Phys. Rev. Lett. **56**, 1917 (1986).

Hartig, W., Rasmussen, W., Schieder, R., and Walther, H., Z. Phys. *A*278, 205 (1976).

Holm, D. A., An, S., and Sargent, M. III, Opt. Comm. **60**, 328 (1986).

Holm, D. A., and Sargent, M. III, Phys. Rev. *A*33, 1073 (1986*a*).

Holm, D. A., and Sargent, M. III, J. Opt. Soc. Am. *B*3, 732 (1986*b*).

Holm, D. A., and Sargent, M. III, Phys. Rev. *A*33, 4001 (1986*c*).

Holm, D. A., and Sargent, M. III, Phys. Rev. *A*35, 2150 (1987). Note: in Eq. (39), the term $+\chi_1\chi_3$ should be multiplied by $C_1^*+C_3^*$.

Holm, D. A., Sargent, M. III, and Capron, B. A., Opt. Lett. **11**, 443 (1986).

Holm, D. A., Sargent, M. III, and Hoffer, L. M., Phys. Rev. *A*32, 963 (1985).

Holm, D. A., Sargent, M. III, and Stenholm, S., J. Opt. Soc. Am. *B*2, 1456 (1985).

Khitrova, G., Berman, P. R., and Sargent, M. III, J. Opt. Soc. *B*5, 160 (1988).

Maeda, M., Kumar, P., and Shapiro, J. H., Opt. Lett. **12**, 161 (1987).

Malcuit, M. S., Gauthier, D. J., and Boyd, R. W., Phys. Rev. Lett. **55**, 1086 (1985).

Mollow, B. R., Phys. Rev. **188**, 1969 (1969).

Mollow, B. R., Phys. Rev. *A*5, 2217 (1972).

Ritsch, H., and Zoller, P., Opt. Comm. **64**, 523 (1987); Opt. Comm. **66**, 333 (1988), Erratum.

Sargent, M. III, Appl. Phys. **9**, 127 (1976).

Sargent, M. III, Phys. Rep. **43**, 223 (1978).

Sargent, M. III, Holm, D. A., and Zubairy, M. S., Phys. Rev. *A*31, 3112 (1985).

Sargent, M. III, Ovadia, S., and Lu, M. H., Phys. Rev. *A*32, 1596 (1985).

Sargent, M. III, Scully, M. O., and Lamb, W. E. Jr., Appl. Opt. **9**, 2423 (1970).

Sargent, M. III, Scully, M. O., and Lamb, W. E. Jr., *Laser Physics* (Addison-Wesley, Reading, Mass., 1974).

Savage, C. M., and Walls, D. F., Phys. Rev. *A*33, 3282 (1986).

Scully, M. O., and Lamb, W. E. Jr., Phy. Rev. **159**, 208 (1967).

Shelby, R. M., Levenson, M. D., Perlmutter, S. H., DeVoe, R. V., and Walls, D. F., Phy. Rev. Lett. **57**, 691 (1986).

Slusher, R. E., Hollberg, L. W., Yurke, B., Mertz, J. C., and Valley, J. F., Phys. Rev. Lett. **55**, 2409 (1985).

Smith, P. W., Ashkin, A., and Tomlinson, W. J., Opt. Lett. **6**, 284 (1981).

Stenholm, S., Holm, D. A., and Sargent, M. III, Phys. Rev. *A*31, 3124 (1985).

Wu, F. Y., Ezekiel, S., Ducloy, M., and Mollow, B. R., Phys. Rev. Lett. **38**, 1077 (1977).

Wu, L. A., Kimble, H. J., Hall, J. L., and Wu, H., Phys. Rev. Lett. **57**, 2520 (1986).